Sa

11 2 7-1

КОЛЛОИДНЫЙ ЖУРНАЛ

(13)

COLLOID JOURNAL

(KOLLOIDNY ZHURNAL)

POSTMASTER:
IF NOT [illegible] NOTIFY
WITHDRAWN
Chemical Abstracts
OHIO STATE UNIV., COLUMBUS 10, O.
AND POSTAGE WILL BE SENT
REC'D. MAR 3 1958 C. A. LIBRARY
ABSTRACTOR:
PLEASE RETURN PROMPTLY TO
CHEMICAL ABSTRACTS
OHIO STATE UNIV., COLUMBUS 10, O.

IN ENGLISH TRANSLATION

VOL. 19

NO. 1

CONSULTANTS BUREAU, INC.

227 WEST 17TH STREET, NEW YORK 11, N. Y.

an agency for the interpretation of international knowledge

CUSTOM TRANSLATION

TRANSLATIONS BY SCIENTISTS

OUR RATES PER THOUSAND WORDS, FOR TRANSLATION ON AN INDIVIDUAL ORDER BASIS, ARE AS FOLLOWS:

$20 . . . **RUSSIAN,** GERMAN, ITALIAN, FRENCH, SPANISH.

$25 . . . BULGARIAN, CZECH, DUTCH, POLISH, PORTUGUESE, ROUMANIAN, SCANDINAVIAN, UKRAINIAN.

$30 . . . CHINESE, GREEK, HUNGARIAN, JAPANESE, SERBO-CROATIAN, TURKISH.

Whatever the field, whatever the language, Consultants Bureau's expert *scientist-translators* provide accurate, currently informed translation of the original material into precise, fluent English. Ten years of experience in scientific translation allow us to guarantee satisfaction to the scientist, and to the scientific librarian. All diagrammatic and tabular material is included, at no extra charge. Material to be translated is located without charge, whenever necessary. Material translated within 30 days of receipt of original.

CONSULTANTS BUREAU, INC.
227 WEST 17th STREET, NEW YORK 11, N. Y. — U.S.A.
Telephone: ALgonquin 5-0713 • Cable Address: CONBUREAU, NEW YORK

COLLOID JOURNAL

(KOLLOIDNY ZHURNAL)

Journal of Theoretical and Applied Physics and

Chemistry of Colloids

Volume XIX

(Number 1, January-February, 1957)

Editor

A. V. Dumansky

Editorial Board

P. N. Antipov-Karataev, B. V. Deryagin, B. A. Dogadkin (Deputy Editor), A. V. Dumansky,
V. A. Kargin, S. M. Lipatov, P. A. Rebinder, I. P. Serdobolsky (Secretary), M. P. Volarovich

Publication of the Academy of Sciences of the USSR

IN ENGLISH TRANSLATION

Copyright, 1957

CONSULTANTS BUREAU, INC.
227 West 17th Street
New York 11, N. Y.

Printed in the United States

Annual Subscription	$ 80.00
Single issue.	20.00

Note: The sale of photostatic copies of any portion of this copyright translation is expressly prohibited by the copyright owners. A complete copy of any paper in this issue may be purchased from the publisher for $ 7.50.

SIGNIFICANCE OF ABBREVIATIONS MOST FREQUENTLY ENCOUNTERED IN SOVIET PERIODICALS

FIAN	Phys. Inst. Acad. Sci. USSR.
GDI	Water Power Inst.
GITI	State Sci.-Tech. Press
GITTL	State Tech. and Theor. Lit. Press
GONTI	State United Sci.-Tech. Press
Gosenergoizdat	State Power Press
Goskhimizdat	State Chem. Press
GOST	All-Union State Standard
GTTI	State Tech. and Theor. Lit. Press
IL	Foreign Lit. Press
ISN (Izd. Sov. Nauk)	Soviet Science Press
Izd. AN SSSR	Acad. Sci. USSR Press
Izd. MGU	Moscow State Univ. Press
LEIIZhT	Leningrad Power Inst. of Railroad Engineering
LET	Leningrad Elec. Engr. School
LETI	Leningrad Electrotechnical Inst.
LETIIZhT	Leningrad Electrical Engineering Research Inst. of Railroad Engr.
Mashgiz	State Sci.-Tech. Press for Machine Construction Lit.
MEP	Ministry of Electrical Industry
MES	Ministry of Electrical Power Plants
MESEP	Ministry of Electrical Power Plants and the Electrical Industry
MGU	Moscow State Univ.
MKhTI	Moscow Inst. Chem. Tech.
MOPI	Moscow Regional Pedagogical Inst.
MSP	Ministry of Industrial Construction
NII ZVUKSZAPIOI	Scientific Research Inst. of Sound Recording
NIKFI	Sci. Inst. of Modern Motion Picture Photography
ONTI	United Sci.-Tech. Press
OTI	Division of Technical Information
OTN	Div. Tech. Sci.
Stroiizdat	Construction Press
TOE	Association of Power Engineers
TsKTI	Central Research Inst. for Boilers and Turbines
TsNIEL	Central Scientific Research Elec. Engr. Lab.
TsNIEL-MES	Central Scientific Research Elec. Engr. Lab.—Ministry of Electric Power Plants
TsVTI	Central Office of Economic Information
UF	Ural Branch
VIESKh	All-Union Inst. of Rural Elec. Power Stations
VNIIM	All-Union Scientific Research Inst. of Meteorology
VNIIZhDT	All-Union Scientific Research Inst. of Railroad Engineering
VTI	All-Union Thermotech. Inst.
VZEI	All-Union Power Correspondence Inst.

Note: Abbreviations not on this list and not explained in the translation have been transliterated, no further information about their significance being available to us. — Publisher.

CALCULATION OF THE LIMITING SHEAR STRESS (YIELD VALUE) OF DISPERSE SYSTEMS IN EXPERIMENTS WITH THE CONE PLASTOMETER

N. N. Agranat and M. P. Volarovich

The yield value θ is an important rheological parameter of plastic disperse systems, the determination of which is necessary for characterization of the structuromechanical properties of such systems. There are several methods for determination of θ in disperse systems [1-11]; the relative accuracy obtained in determinations by each of these is of the order of several percent. A greater accuracy in determination of θ is difficult to obtain because, like any other yield value, it depends to some extent on the experimental conditions, such as the time during which the force acts [12], etc. Until recently, however, few investigations have dealt with comparative tests of different methods for determination of θ [3,13,14]. It was therefore important to determine θ simultaneously by different methods in some definite disperse systems, such as lubricant greases, and to compare the results.

We have determined θ for several greases with the use of six different instruments: the RV-4 rotational viscosimeter [1], a vertically moving plate [7] and cylinder [5,6], Tolstoi's cone instrument [9], Simonyan's capillary type instrument [10], and Rebinder's cone plastimeter [8]. Fairly good agreement was found between the values of θ measured by all these methods. However, the values of θ calculated from the results of measurements with the cone plastometer by Rebinder's approximate formula [8] were 1.5-2.5 times as large as the values obtained by other methods. This was also found in other investigations [15]. We advanced the view, jointly with M. F. Shirokov, that the reason for the discrepancy was the fact that in derivation of the formula only the shearing stress acting along the cone surface was taken into account, and extension of plastic deformations into the volume near the cone was ignored; this last effect has been established experimentally by means of X-ray transmission [16]. In this investigation the cone has been considered as an axially symmetrical punch pressed into the plane boundary of the plastic medium. Examples of the solution of such problems by the construction of a network of slippage lines for complete plasticity conditions are contained in publications by Sokolovsky [17] and Ishlinsky [18]. Hencky [19] and Puchkov [18] have shown that problems of this type can be solved to a sufficient degree of accuracy by construction of slippage lines for the corresponding plane problem. We have applied this method to the cone, the basis adopted being the fact that at limiting equilibrium of the system the pressure P acting on the punch from the side of the plastic medium becomes equal to the external acting force G, i.e., P = G.

The pressure force P was determined by two methods. First, Puchkov's approximate method [18] was used. In this case the total pressure force of the plastic medium on the cone can be represented by the formula:

$$P = p_A F + \frac{p_O - p_A}{h} V, \tag{1}$$

where p_O and p_A are the pressures at points O and A (Fig. 1), the point A being very close to the apex of the cone; F is the cross section of the cone at the surface of the plastic medium; V is the volume of the immersed portion of the cone; h is the maximum immersion depth.

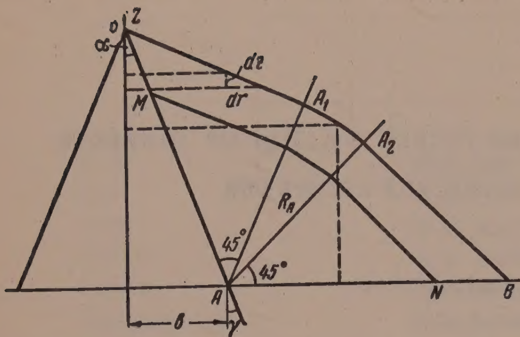

Fig. 1. Slippage lines for the plane problem (conical punch).

The pressure p_A and p_O were calculated from the formula

$$p_M = \sigma_S\left(1 + \gamma_M + \frac{1}{2}\ln\frac{r_N}{r_M} - \frac{1}{2}\int\limits_M^N \frac{dz}{r}\right), \quad (2)$$

where σ_S is the maximum normal stress, equal to the flow limit in extension; γ_M is the angle formed by the tangent to the cone at the given point and the negative direction of the z axis (Fig. 1); M and N are points at the cone surface and the surface of the plastic medium respectively, belonging to the given slippage line; r, z, and ψ are cylindrical coordinates [8]. By the Mises conditions, in this case $\sigma_S = 2\tau_{max}$, where τ_{max} is the flow limit in shear, i.e., $\tau_{max} = \theta$. Therefore Equation (2) may be written as follows:

$$p_M = \theta\left(2 + 2\gamma_M + \ln\frac{r_N}{r_M} - \int\limits_M^N \frac{dz}{r}\right). \quad (3)$$

According to Fig. 1, for the slippage line OA_1A_2B

$$p_0 = \theta\left(2 + 2\alpha + \ln\frac{r_B}{r_0} - \int\limits_0^B \frac{dz}{r}\right) \quad (4)$$

here r_0 is the radius of curvature of the cone apex (in practice r_0 is never 0), and α is half the vertical angle of the cone. The pressure at the rounded apex may be neglected, as projection of it on a very small area gives a negligible value.

From Fig. 1 we have

$$\int\limits_0^B \frac{dz}{r} = \int\limits_0^{A_1} \frac{dz}{r} + \int\limits_{A_1}^{A_2} \frac{dz}{r} + \int\limits_{A_2}^{B} \frac{dz}{r}. \quad (5)$$

Putting for each of the regions z = f (r), we have

$$\int\limits_0^B \frac{dz}{r} = -\left[\operatorname{tg}\left(\frac{\pi}{4} - \alpha\right)\ln\frac{r_{A_1}}{r_0} + \ln\frac{r_B}{r_{A_2}} + \int\limits_{A_1}^{A_2} \frac{r-b}{r\sqrt{R_A^2 - (r-b)^2}}\,dr\right]. \quad (6)$$

Substituting Equations (6) and (3) into Equation (4) and calculating $p_A = \theta\,(2 + 2\alpha)$, we find, in accordance

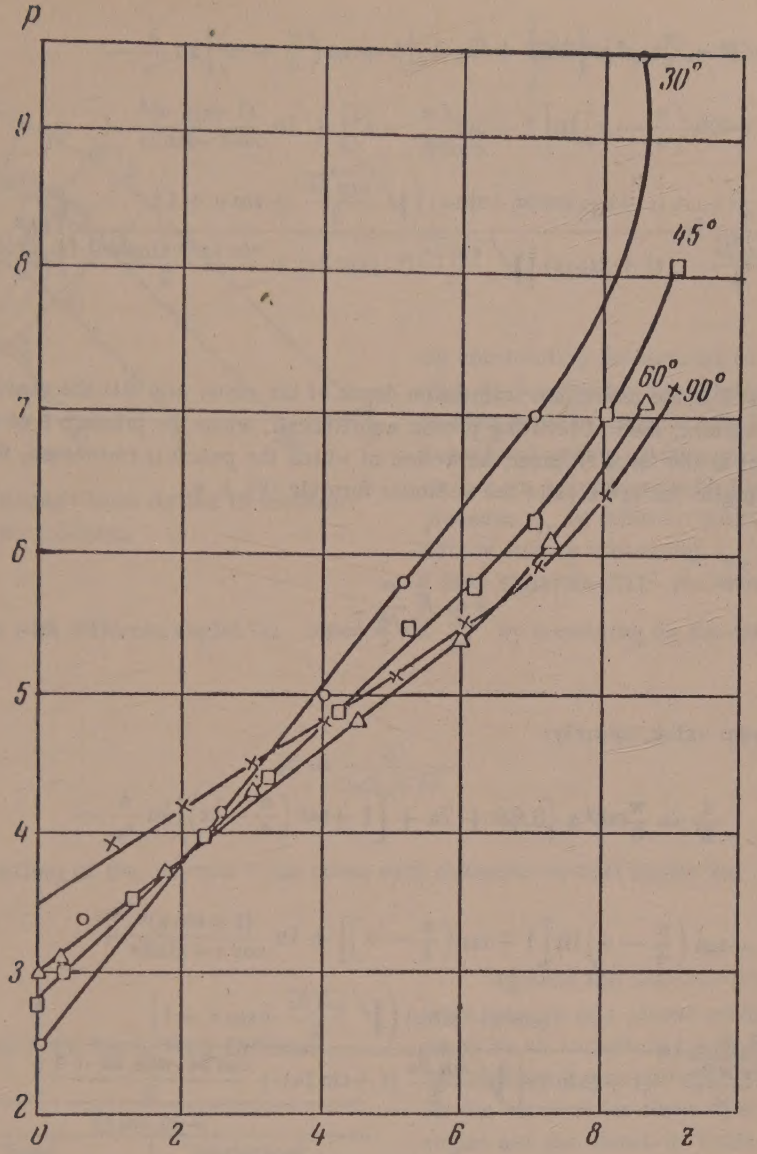

Fig. 2. Pressure distribution over the surface of a conical punch for cones of different vertical angles.

with Equation (1), the total pressure P of the plastic medium on the punch, after first expressing all the quantities in the formula in terms of α and $\underline{h}$

$$P = \frac{\pi}{3}\tan^2\alpha\left\{6.69 + 7\alpha + \left[1 + \tan\left(\frac{\pi}{4} - \alpha\right)\right]\ln\frac{h}{r_0} - \right.$$
$$-\tan\left(\frac{\pi}{4} - \alpha\right)\ln\left[1 + \tan\left(\frac{\pi}{4} - \alpha\right)\right] + \ln\frac{(1+\sin\alpha)^2}{\cos\alpha + \sin 2\alpha} +$$
$$\left. + \frac{\sin\alpha}{\sqrt{\frac{\cos 2\alpha}{2}}}\ln\frac{(\cos\alpha + \sin\alpha)\left(\sqrt{\frac{\cos 2\alpha}{2}} + \sin\alpha + 1\right)}{(1 + 2\sin\alpha)\left[\sqrt{\frac{\cos 2\alpha}{2}}(1 + \sin 2\alpha) + \frac{\cos 2\alpha + \sin 2\alpha + 1}{2}\right]}\right\}\theta h^2. \tag{7}$$

It was found that if $\underline{h}$ is the maximum immersion depth of the cone, and θ is the yield value, equal to the flow limit of the system, then at limiting plastic equilibrium, when the pressure P of the medium on the punch becomes equal to the force G under the action of which the punch is immersed, the relationship between these values remains the same as in the Rebinder formula [8], i. e.,

$$\theta = K\frac{P}{h^2}. \tag{8}$$

However, K has a different value, namely:

$$\frac{1}{K} = \frac{\pi}{3}\tan^2\alpha\left\{6.69 + 7\alpha + \left[1 + \tan\left(\frac{\pi}{4} - \alpha\right)\right]\ln\frac{h}{r_0} - \right.$$
$$-\tan\left(\frac{\pi}{4} - \alpha\right)\ln\left[1 + \tan\left(\frac{\pi}{4} - \alpha\right)\right] + \ln\frac{(1+\sin\alpha)^2}{\cos\alpha + \sin 2\alpha} +$$
$$\left. + \frac{\sin\alpha}{\sqrt{\frac{\cos 2\alpha}{2}}}\ln\frac{(\cos\alpha + \sin\alpha)\left(\sqrt{\frac{\cos 2\alpha}{2}} + \sin\alpha + 1\right)}{(1 + 2\sin\alpha)\left[\sqrt{\frac{\cos 2\alpha}{2}}(1 + \sin 2\alpha) + \frac{\cos 2\alpha + \sin 2\alpha + 1}{2}\right]}\right\}. \tag{9}$$

Formula (1), put forward by V. V. Puchkov, gives somewhat low values of P (and therefore low values of K), as the relationship between p_M and z_M can be regarded as linear only over a restricted region, and linearity is disturbed as the vertex is approached (Fig. 2). Formula (9) contains the term, $\ln h/r_0$, where r_0 is the radius of curvature of the cone vertex. This means that K depends not only on the cone angle 2α, but also on the ratio h/r_0.

There is also a graphical method for calculation of the total pressure P of a plastic medium on a punch [17]. It is easy to show that

$$P = \int_0^b 2\pi\, p_m r_m\, dr_m. \tag{10}$$

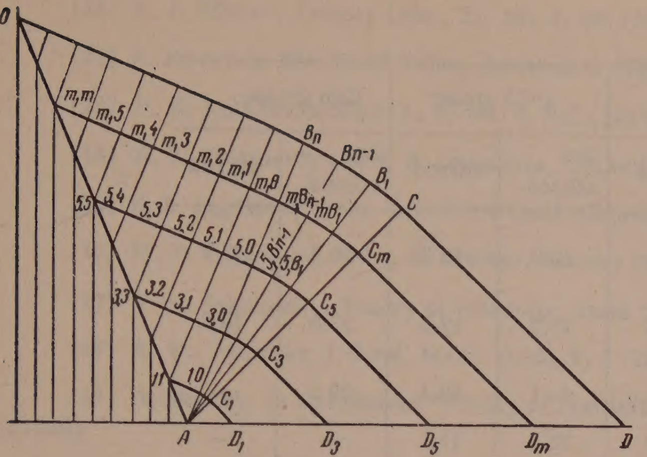

Fig. 3. Network of slippage lines for the immersion of a cone into a plastic medium.

This integral can be replaced by a sum

$$P = \int_0^b 2\pi\, p_m r_m\, dr_m = 2\pi\theta\Sigma\overline{pr}\,\Delta r, \tag{11}$$

where

$$\overline{pr} = \frac{1}{2\theta}(p_{i-1} r_{i-1} + p_i r_i).$$

By constructing the network of slippage lines (Fig. 3) (for greater calculation accuracy the drawing must be considerably larger than the actual dimensions of the punch) it is possible to find, in accordance with Equation (2), the pressures p_m at different points of the cone surface and by measuring r_m, to calculate P from Equation (11). We found the values of P for conical punches with different angles 2α. Since $\theta = K \frac{P}{h^2}$ by measuring on the diagram the immersion depth h, the equation

$$K = \frac{h^2}{2\pi\Sigma\,\overline{pr}\,\Delta r} \tag{14}$$

was used to find the values of the constant K for cones with different vertical angles 2α. These values are given in Table 1.

TABLE 1

Values of the Constant K for Cones With Different Vertical Angles 2α

2α	Value of K	
	found graphically	analytical solution
30°	0.949	0.959
45°	0.416	0.416
60°	0.217	0.214

Agranat and Shirokov [21] determined the total pressure of a plastic medium on a conical punch by an analytical method. A formula for the constant K was derived. The values so found for the constant for cones with different vertical angles are also shown in Table 1.

It is seen from Table 1 that the graphical method gives values close to those found by the analytical method.

We determined experimental values of the yield stress θ for a number of greases by means of a number of instruments of different types, including the cone plastometer, for which the value of θ was calculated from experimental data with the use of values of K calculated by the analytical (and also the graphical) method. The experimental results are given in Table 2.

It is seen from Table 2 that the values obtained for θ with the cone plastometer coincide with the values found by means of other types of instruments. Rebinder and Segalova [22] showed that, for systems with yield values of the order of 1 g/cm² and less, in calculations with the aid of Formula (8) the expression $K = \frac{1}{\pi}\cot\alpha\cos^2\alpha$ may be used. This also gives good agreement with yield values found by other methods. We did not test such systems.

TABLE 2

Yield Values (g/cm^2) of Greases, Determined by Different Methods

Method of determination	Synthetic solidol grease		1-13 grease		Gun grease	
	not stirred	stirred	not stirred	stirred	not stirred	stirred
Cone plastometer	11.7	5.1	22.9	12.3	30.7	17.9
RV-4 rotational viscosimeter	10.5	5.8	21.2	12.5	27.0	19.8
Tangential plate displacement	—	—	24.1	10.4	29.5	—
Axial cylinder displacement	11.7	6.0	25.1	11.1	—	—
D. M. Tolstoi's cone instrument	—	5.1	23.3	10.8	35.0	17.5
A. A. Simonyan's capillary type instrument	—	—	—	10.5	28.0	—

SUMMARY

1. P. A. Rebinder's cone plastometer must be regarded as the most convenient instrument for measurement of θ, as it is possible to measure yield values over a wide range of θ and to repeat the experiments many times, with good agreement between the results. The instrument is simple to construct and operate.

2. The values of the constants K given in Table 1 should be used for measurements on systems with yield values greater than 1 g /cm^2 by means of the cone plastometer.

3. If, in addition to θ, it is also necessary to determine the plastic viscosity of a disperse system, the rotational viscosimeter should be used.

The Moscow Peat Institute
The S. Ordzhonikidze Institute of Aviation, Moscow
Chair of Physics

Received August 8, 1956

LITERATURE CITED

[1] M. P. Volarovich, Tran. Inst. Mineral Raw Materials, No. 66, 1 (1934).

[2] P. A. Rebinder, Trans. Conf. on Viscosity of Liquids and Colloid Solutions, 1, 361 (1941); 2, 173 (1944).

[3] M. P. Volarovich, Colloid J., 16, No. 3, 227 (1954).

[4] M. P. Volarovich and N. N. Kulakov, Bull. Acad. Sci. USSR, No. 10, 1331 (1935).

[5] D. M. Tolstoi, J. Phys. Chem., 5,28 (1934).

[6] M. P. Volarovich, Trans. Polygraphic Inst. State United Press, No. 5 (1937); M. P. Volarovich and D. M. Tolstoi, Colloid J., 6, No. 5, 409 (1940).

[7] P. A. Rebinder and S. Ya. Veiler, Proc. Acad. Sci. USSR, 49, No. 5, 354 (1945).

[8] P. A. Rebinder and B. Ya. Yampolsky, Colloid J., 10, No. 6, 466 (1948); P. A. Rebinder and N. N. Semenenko, Proc. Acad. Sci. USSR, 64, No. 6, 835 (1949).

[9] D. M. Tolstoi, Proc. Acad. Sci. USSR, 77, No. 5, 847 (1951).

[10] A. A. Simonyan, Peat Ind., No. 10, 24 (1953).

[11] K. I. Klimov, Factory Labs., 21, No. 4, 491 (1955).

[12] R. Houwink, The Yield Value, Amsterdam (1938).

[13] N. N. Kulakov, Colloid J., 3, No. 3, 217 (1937).

[14] N. P. Volarovich and E. P. Loshakova, Colloid J., 8, No. 3, 127 (1946).

[15] E. E. Segalova, Trans. All-Union Conf. Colloid Chem., Kiev (1950).

[16] M. P. Volarovich and S. N. Markov, Factory Labs., 17, No. 12, 1461 (1951).

[17] V. V. Sokolovsky, Theory of Plasticity, State Tech. Press (1950).

[18] A. Yu. Ishlinsky, J. Appl. Math. Mech. 8, 3 (1944).

[19] G. Hencky, in Symposium "Theory of Plasticity" edited by Yu. N. Rabotnov, Leningrad – Moscow (1948).

[20] A. A. Ilyushin, Plasticity, State Tech. Press (1948).

[21] N. N. Agranat and M. F. Shirokov, Colloid J., 19, 9 (1957).

[22] P. A. Rebinder and E. E. Segalova, Colloid J., 10, No. 3 (1948).

THEORY OF THE CONE IMMERSION METHOD FOR DETERMINATION OF THE YIELD VALUES OF DISPERSE SYSTEMS

N. N. Agranat and M. F. Shirokov

A widely used method for determination of the yield values of disperse systems, proposed by Rebinder [1], is based on the immersion of a cone into a viscoplastic medium under the action of a constant force. The method depends on the relationship

$$\theta = K\frac{G}{h^2}, \tag{1}$$

where θ is the yield value; G is the force causing immersion of the cone; h is the maximum depth of immersion; K is a constant which, according to [1], should be calculated from the formula

$$K = \frac{1}{\pi}\cos^2\alpha\cot\alpha, \tag{2}$$

where α is half the vertical cone angle.

It has been found, however, that values of θ for disperse systems calculated from Formulas (1) and (2) from experimental data on the immersion of a cone are 1.5-2.5 times as large as the values of θ found by other methods [2, 3]. It is likely that the reason for this is that in derivation of Formulas (1) and (2) the spread of plastic deformation into the volume around the cone was not taken into consideration. In fact the medium around the cone is in a state of elasticoplastic deformation. Therefore the cone can be regarded as an axially symmetrical punch pressed into the plane surface of a plastic medium. The general theory leads to the following expression for the pressure p_M at a given point M in the surface [4]

$$p_M = \sigma_S\left(1 + \gamma_M + \frac{1}{2}\int\limits_M^N \frac{dr - dx}{r}\right), \tag{3}$$

where σ_S is the maximum normal stress; γ_M is the angle between the tangent to the cone surface and the negative direction of the X axis; r, x, φ are cylindrical coordinates of the point on the slippage line joining the points M and N in the surface and in the medium, lying in the meridianal plane (Fig. 1).

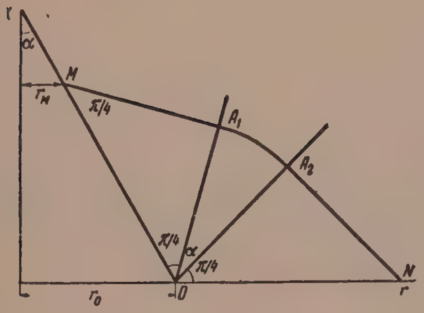

Fig. 1. Slippage line for the penetration of a conical punch into a plastic medium.

Methods for construction of the slippage lines have already been developed [5-7]. The force P which acts from the direction of the medium upon the surface of the punch in contact with it in the direction of the X axis is given by the expression

$$P = \int p_M n_x df,$$

where n_x is the vector component of the normal $\overline{n}$, external relative to the medium, to an element df of the cone surface area. It is evident that $n_x\, df = -2\pi r_M dr_M$.

Consequently,

$$G = P = +\int_0^{r_0} p_M \, 2\pi r_M \, dr_M. \tag{4}$$

Substituting into this the value of p_M from Equation (3), and remembering that for a cone $\gamma = \alpha$, we have:

$$G = \sigma_S \int_0^{r_0} \left(1 + \alpha + \frac{1}{2} \int_{r_M}^{r_N} \frac{dr - dx}{r}\right) 2\pi r_M \, dr_M$$

or

$$G = \sigma_S \int_0^{r_0} \left(1 + \alpha + \frac{1}{2} \ln \frac{r_N}{r_M} - \frac{1}{2} \int_M^N \frac{dx}{r}\right) 2\pi r_M \, dr_M. \tag{5}$$

According to Fig. 1

$$\int_M^N \frac{dx}{r} = \int_M^{A_1} \frac{dx}{r} + \int_{A_1}^{A_2} \frac{dx}{r} + \int_{A_2}^N \frac{dx}{r}.$$

The arc $A_1 A_2$ may, without much error, be replaced by a chord, and then

$$\int_M^N \frac{dx}{r} = -\left[\cot\left(\frac{\pi}{4}+\alpha\right)\ln\frac{r_{A_1}}{r_M} + \cot\left(\frac{\pi}{4}+\frac{\alpha}{2}\right)\ln\frac{r_{A_2}}{r_{A_1}} + \ln\frac{r_N}{r_{A_2}}\right]$$

and Equation (5) assumes the form

$$G = \sigma_S \int_0^{r_0} \left[2 + 2\alpha + \ln\frac{r_N^2}{r_M r_{A_2}} + \cot\left(\frac{\pi}{4}+\alpha\right)\ln\frac{r_{A_1}}{r_M} + \right. \tag{6}$$

$$\left. + \cot\left(\frac{\pi}{4}+\frac{\alpha}{2}\right)\ln\frac{r_{A_2}}{r_{A_1}}\right]\pi r_M\, dr_M$$

or

$$G = \sigma_S \pi r_0^2 (1+\alpha) + \sigma_S \pi \left[\int_0^{r_0}\left(\ln\frac{r_N^2}{r_M r_{A_2}}\right) r_M\, dr_M + \right.$$

$$\left. + \cot\left(\frac{\pi}{4}+\alpha\right)\int_0^{r_0}\left(\ln\frac{r_{A_1}}{r_M}\right) r_M\, dr_M + \cot\left(\frac{\pi}{4}+\frac{\alpha}{2}\right)\int_0^{r_0}\left(\ln\frac{r_{A_2}}{r_{A_1}}\right) r_M\, dr_M\right]. \tag{7}$$

On the basis of Fig. 1 we may write: $r_N = r_0 + R_M\sqrt{2}$ where $K_M = OA_1 = OA_2$, and since $R_M = \frac{r_0 - r_M}{\sqrt{2}\sin\alpha}$, then

$$N \qquad \frac{r_0(\sin\alpha + 1) - r_M}{\sin\alpha}. \tag{8}$$

In the same way we find

$$r_{A_1} = \frac{r_0 \cot\left(\frac{\pi}{4}-\alpha\right) - r_M}{2/(\cot\alpha + 1)}; \tag{9}$$

$$r_{A_2} = \frac{r_0(2\sin\alpha + 1) - r_M}{2\sin\alpha}. \tag{10}$$

By partial integration, we have

$$\int_0^{r_0}\left(\ln\frac{r_N^2}{r_M r_{A_2}}\right) r_M\, dr_M = \left[\frac{r_M^2}{2}\ln\frac{r_N^2}{r_M r_{A_2}}\right]_0^{r_0} - \int_0^{r_0}\frac{r_M^2}{2}\, d\left(\ln\frac{r_N^2}{r_M r_{A_2}}\right) =$$

$$= -\int_0^{r_0}\frac{r_M^2}{2}\, d\left(\ln\frac{r_N^2}{r_M r_{A_2}}\right), \tag{11}$$

since

$$\left[\frac{r_M^2}{2}\ln\frac{r_N^2}{r_M r_{A_2}}\right]_0^{r_0} = 0.$$

Similarly we have

$$\int_0^{r_0}\left(\ln\frac{r_{A_1}}{r_M}\right) r_M\,dr_M = -\int_0^{r_0}\frac{r_M^2}{2}\,d\left(\ln\frac{r_{A_1}}{r_M}\right); \tag{12}$$

$$\int_0^{r_0}\left(\ln\frac{r_{A_2}}{r_{A_1}}\right) r_M\,dr_M = -\int_0^{r_0}\frac{r_M^2}{2}\,d\left(\ln\frac{r_{A_2}}{r_{A_1}}\right). \tag{13}$$

Putting the values of (8), (9), and (10) into Equation (7), taking into account Equations (11), (12), and (13), and remembering that according to the Mises condition $\sigma_S = 2\tau_{\max}$ where σ_S in the present case can be assumed equal to the flow limit in extension, and $\tau_{\max}$, the maximum tangential stress, is equal to the flow limit in shear, or the yield value θ, we have

$$\begin{aligned} P = {} & \pi\theta(2+2\alpha)r_0^2 + \pi\theta\left\{2\int_0^{r_0}\frac{r_M^2\,dr_M}{r_0(\sin\alpha+1)-r_M} + \right. \\ & + \int_0^{r_0} r_M\,dr_M - \int_0^{r_0}\frac{r_M^2\,dr_M}{r_0(2\sin\alpha+1)-r_M} + \cot\left(\frac{\pi}{4}+\alpha\right)\times \\ & \times\left[\int_0^{r_0}\frac{r_M^2\,dr_M}{r_0\cot\left(\frac{\pi}{4}-\alpha\right)-r_M} + \int_0^{r_0} r_M\,dr_M + \right. \\ & \left.\left. + \cot\left(\frac{\pi}{4}+\frac{\alpha}{2}\right)\left[\int_0^{r_0}\frac{r_M^2\,dr_M}{r_0(2\sin\alpha+1)-r_M} - \int_0^{r_0}\frac{r_M^2\,dr_M}{r_0\cot\left(\frac{\pi}{4}-\alpha\right)-r_M}\right]\right]\right\}. \end{aligned} \tag{14}$$

We calculate the definite integrals and carry out the permissible simplifications remembering that $r_0 = h\tan\alpha$; then we have:

$$\begin{aligned} P = {} & \pi\theta h^2\tan^2\alpha\left\{2\alpha - 2(\sin\alpha+1)^2\ln\frac{\sin\alpha}{\sin\alpha+1} + \right. \\ & + \left[1-\cot\left(\frac{\pi}{4}+\frac{\alpha}{2}\right)\right](2\sin\alpha-1)^2\ln\frac{2\sin\alpha}{2\sin\alpha+1} + \\ & + \left[\cot\left(\frac{\pi}{4}+\frac{\alpha}{2}\right)-\cot\left(\frac{\pi}{4}+\alpha\right)\right]\cot^2\left(\frac{\pi}{4}-\alpha\right)\ln\frac{2}{\cot\alpha+1} + \\ & \left. + \cot\left(\frac{\pi}{4}+\frac{\alpha}{2}\right)\left[\cot\left(\frac{\pi}{4}-\alpha\right)-(2\sin\alpha+1)\right]\right\}. \end{aligned} \tag{15}$$

Thus we see that the relationship between θ, G, and h derived by P. A. Rebinder is retained. However, the value of the constant K is determined by an expression different from Formula (2), namely

$$\frac{1}{K} = \pi \tan^2 \alpha \Big\{2\alpha - 2(\sin\alpha + 1)^2 \ln \frac{\sin\alpha}{\sin\alpha + 1} + \\ + \Big[1 - \cot\Big(\frac{\pi}{4} + \frac{\alpha}{2}\Big)\Big](2\sin\alpha + 1)^2 \ln \frac{2\sin\alpha}{2\sin\alpha + 1} + \\ + \Big[\cot\Big(\frac{\pi}{4} + \frac{\alpha}{2}\Big) - \cot\Big(\frac{\pi}{4} + \alpha\Big)\Big]\cot^2\Big(\frac{\pi}{4} - \alpha\Big) \ln \frac{2}{\cot\alpha + 1} + \\ + \cot\Big(\frac{\pi}{4} + \frac{\alpha}{2}\Big)\Big[\cot\Big(\frac{\pi}{4} - \alpha\Big) - (2\sin\alpha + 1)\Big]. \tag{16}$$

This formula was used to calculate values of K for cones with different vertical angles (excluding the value $\alpha = \pi/2$), some of which are given in the table.

Values of the Constant K Calculated From Equation (16)

2α	30°	45°	60°	89°20'
K	0.959	0.416	0.214	0.073

For the angle $2\alpha = 90°$ Equation (14) assumes the form

$$P = \pi\theta(2 + 2\alpha) r_0^2 + \pi\theta \Big[2\int_0^{r_0} \frac{r_M^2\, dr_M}{r_0(\sin\alpha + 1) - r_M} + \\ + \int_0^{r_0} r_M\, dr_M - \int_0^{r_0} \frac{r_M^2\, dr_M}{r_0(2\sin\alpha + 1) - r_M} + \cot\Big(\frac{\pi}{4} + \frac{\alpha}{2}\Big)\int_0^{r_0} \frac{r_M^2\, dr_M}{r_0(2\sin\alpha + 1) - r_M}\Big]. \tag{17}$$

Therefore for a cone with this vertical angle

$$P = \pi h^2 \tan^2\alpha \cdot \theta \Big\{1 + 2\alpha - 2(\sin\alpha + 1)^2 \ln \frac{\sin\alpha}{\sin\alpha + 1} + \\ + \Big[1 - \cot\Big(\frac{\pi}{4} + \frac{\alpha}{2}\Big)\Big](2\sin\alpha + 1)^2 \ln \frac{2\sin\alpha}{2\sin\alpha + 1} - \cot\Big(\frac{\pi}{4} + \frac{\alpha}{2}\Big)\Big(\frac{3}{2} + 2\sin\alpha\Big)\Big\} \tag{18}$$

and the constant K is given by the equation

$$\frac{1}{K} = \pi \tan^2\alpha \Big\{1 + 2\alpha - 2(\sin\alpha + 1)^2 \ln \frac{\sin\alpha}{\sin\alpha + 1} + \\ + \Big[1 - \cot\Big(\frac{\pi}{4} + \frac{\alpha}{2}\Big)\Big](2\sin\alpha + 1)^2 \ln \frac{2\sin\alpha}{2\sin\alpha + 1} - \\ - \cot\Big(\frac{\pi}{4} + \frac{\alpha}{2}\Big)\Big(\frac{3}{2} + 2\sin\alpha\Big). \tag{19}$$

Figure 2 shows K plotted against the cone angle 2α.

The yield values calculated from experimental data by means of Formula (1) with the use of the constant K given by Formula (16) are in good agreement with values of θ determined experimentally by other methods for a number of disperse systems, in the range of 5 to 100 g/cm^2 [7].

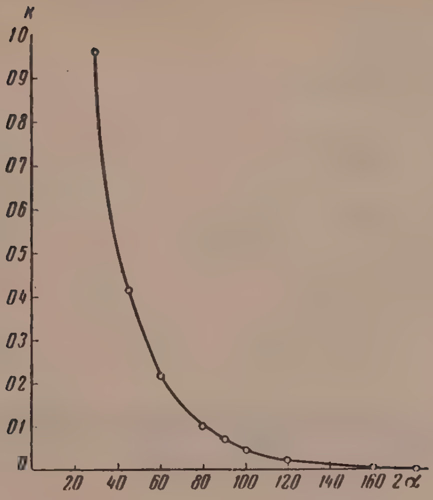

Fig. 2. Constant K as a function of the cone angle.

SUMMARY

1. A theory of the cone plastometer is developed on the basis of the properties of viscoplastic media; this leads to P. A. Rebinder's known formula, but with a different coefficient K.

2. A formula for calculating the coefficient K is derived, and the values of K for cones with different angles are found.

The S. Ordzhonikidze Institute of Aviation, Moscow

Received August 2, 1956

LITERATURE CITED

[1] P. A. Rebinder and N. N. Semenenko, Proc. Acad. Sci. USSR, 64, No. 6 (1949).

[2] P. A. Rebinder and E. E. Segalova, Colloid J., 10, No. 3 (1948).

[3] D. S. Velikovsky, Petroleum Economy, No. 2 (1950).

[4] A. A. Ilyushin, Plasticity, State Tech. Press (1948).

[5] G. Hencky, in Symposium " Theory of Plasticity ", translation edited by Yu. N. Rabotnov, Foreign Lit. Press (1948).

[6] V. V. Sokolovsky, Theory of Plasticity, State Tech. Press (1950).

[7] N. N. Agranat and M. P. Volarovich, Colloid J., 19, 3 (1957).*

---

* Original Russian translation. See. C. B. translation.

15

~~AN~~ ELECTRON-MICROSCOP~~E~~ic STUDY OF STRUCTURE FORMATION IN LOESSes

I. ~~INFLUENCE~~ effect OF THE DISPERSI~~ON~~ing MEDIUM

E. Aripov, Z. Ya. Berestneva, and V. A. Kargin

Electron microscopy has been used by many workers as an analytical method for qualitative investigations of the mineralogical composition of soils. Sedletsky and Ananyev [1] used the electron microscope to study the mineralogical composition of loess of various origins. The specimens were investigated in the form of aqueous suspensions. Vikulova [2] made a more detailed study of particle size in aqueous soil suspensions in relation to the sedimentation time.

For studies of soils by means of the electron microscope, the specimens are usually prepared from aqueous or amyl alcohol suspensions of clays not subjected to preliminary treatments, or from aqueous suspensions of clays previously treated with hydrochloric acid, hydrogen peroxide, or acetic acid, or from separate fractions of aqueous suspensions (separated by the sedimentation method). In all these methods the water-soluble salts present in the material are first removed by decantation of the clear liquids from the suspensions. Repeated decantation of the top liquid layer followed by dilution results in peptization of the clay particles; some authors [2] recommend the addition of ammonia (until a faint odor is apparent) as stabilizer.

These methods may be used in studying the structure of soil or loess particles, but for studying structure formation processes, in which all the components of the loess probably participate, it is necessary to investigate not only the particle structure of the mineral components of the loess, but also their behavior in various media.

It is known that both soils and loesses swell in water, and therefore it is of interest to study, by means of the electron microscope, the influence of the medium on the structure of loess particles. Loess specimens were prepared for this purpose, both by powdering loess in the dry state, and also in the form of aqueous and alcoholic suspensions. Loess of the Tashkent region was used for the work. The investigations were performed with the aid of the EM-3 electron microscope with direct electrono-optical magnification (8000-12000) followed by photographic enlargement.

The specimens were prepared as follows. Copper gauzes with hole diameter not exceeding 0.1 mm were used as supports. These were coated with collodion films 100-150 A thick. The films were made from a solution of collodion in amyl acetate. The films were dried in air under a glass cover to protect them against dust and other contamination. A drop of the suspension to be investigated was then applied to the film and then carefully removed by a piece of filter paper. It was necessary to remove the drops in our investigation because, during slow drying of the drops, structure formation or coalescence of the individual particles due to slow evaporation of the water could occur. This would interfere with interpretation of the results. Removal of the drop results in almost instantaneous evaporation of the remaining moisture. The prepared specimens were stored in Petri dishes placed under a glass cover to protect them against contamination.

The dry loess specimens were made by pulverization of the loess in a dessicator at the bottom of which gauzes with collodion films, serving as supports, were placed. The aqueous and alcoholic suspensions were made by stirring 5-10 g of loess with 200-300 ml of distilled water or ethyl alcohol.

In our electron microscope investigations of loess suspensions, the particles seen in the microphotographs are referred to as "loess particles", irrespective of whether they are clearly defined particles of individual minerals contained in the loess, or amorphous formations consisting of different minerals and salts which are components of the loess.

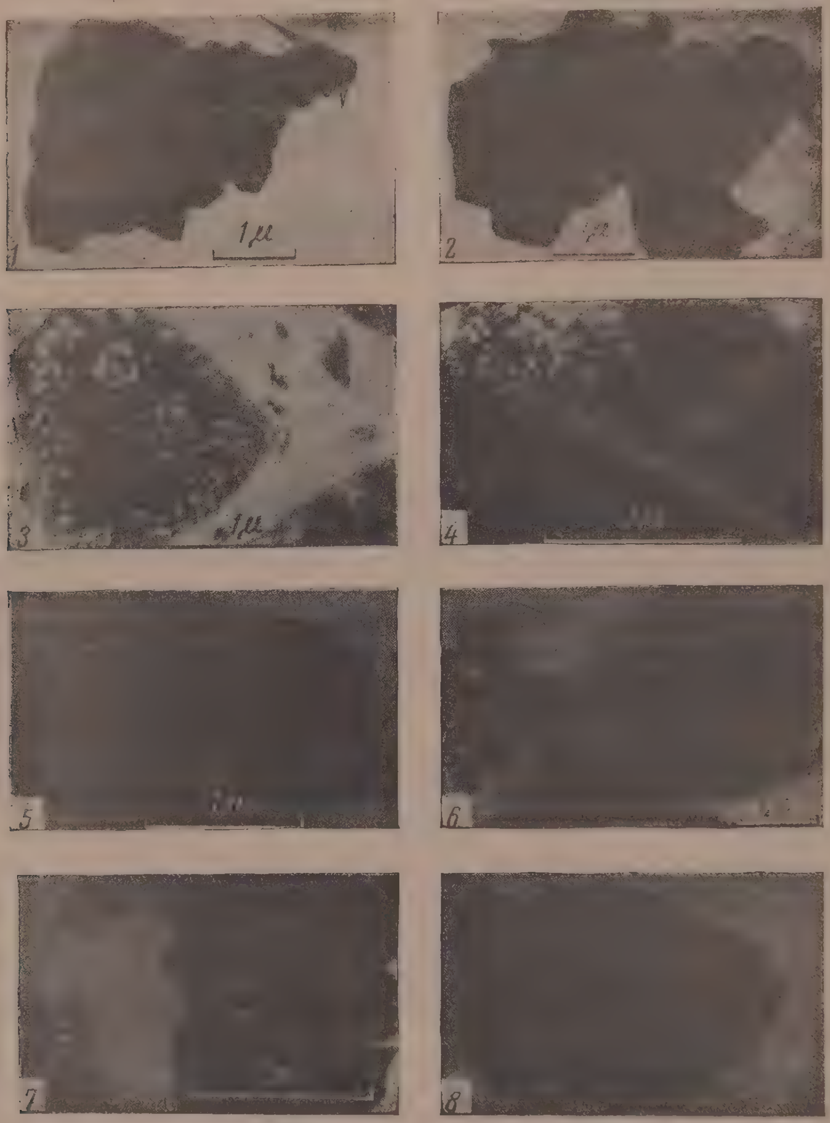

Figs. 1-8. Microphotographs of loess in various media (explanation in text).

Fig. 1 is a microphotograph of specimens prepared by pulverization. The particles consist of scales with dense formations and clear outlines. Loess particles from an alcoholic suspension (Fig. 2) are similar under the electron microscope to specimens prepared by pulverization.

Figs. 3 and 4 are microphotographs of aqueous loess suspensions. The particles retain their external form almost completely but contain pores (Fig. 3). The presence of such pores in loess in aqueous suspensions may be caused by swelling of the loess particles and the consequent formation of a fine porous structure; on the other hand, these porous formations may arise as the result of solution of the easily soluble salts which are always present in loess. In the latter case the formation of a fine porous structure in the loess particles will be irreversible, as the dissolved salts are removed with the water. If the pores are formed as the result of swelling, the effect should be reversible, i. e., pores should be formed during swelling of the loess in water and disappear on drying.

To determine the causes of the formation of a porous structure in loess particles in aqueous suspensions, the structure of the loess particles was studied in aqueous suspensions under the electron microscope, and the water in the suspension was then replaced by ethyl alcohol. Dehydration of the loess by ethyl alcohol was assumed to be permissible as identical electron micrographs are given by loess particles obtained by pulverization and in alcoholic suspensions. The water – alcohol change of medium was performed 5-6 times with the same loess specimen.

It is seen in Fig. 5 that, after the first dehydration, scales with dense formations and sharp edges appear again. This microphotograph is quite similar to those shown in Figs. 1 and 2. When this alcoholic suspension was converted into an aqueous suspension, porosity appeared again, as can be seen in Fig. 6.

Repeated hydration and dehydration of the loess showed that the formation and disappearance of the pores was completely reversible. After the fifth hydration of the suspension a porous structure appeared again (Fig. 7). After the sixth dehydration, dense formations with sharp outlines were again visible (Fig. 8). The reversibility of this process in the transitions between aqueous and alcoholic suspensions indicates that pore formation is caused by swelling of the loess, and not by solution of the salts which are usually present in loess; otherwise the formation and disappearance of the pores would be irreversible.

Water-soluble salts, which may cause the formation of fairly strong surface structures, penetrate to the surface and accumulate on it through the pores formed during swelling in water, by capillary action. This question will be examined separately in the next article.

SUMMARY

1. The structure of loess particles from the Tashkent region has been studied in different media by means of the electron microscope.

2. It is shown that a finely porous structure, which disappears on drying, is formed in an aqueous medium.

3. The process of pore formation and disappearance is reversible, which may be attributed to swelling of the clay mineral particles in loess in water.

The loess specimens were kindly supplied by Prof. Yu. A. Skvortsov, to whom we are grateful.

The L. Ya. Karpov Physicochemical Institute
Moscow

Received September 7, 1956

LITERATURE CITED

[1] I. D. Sedletsky, Proc. Acad. Sci. USSR, New Series, 81, No. 5, 109 (1951); 86, No. 4 (1952); 89,339 (1953); New Series, 70, No. 2, 27 (1953); 96,375 (1954); Sci. Mem. Rostov State Univ., Geol.-Geograph. Faculty, 23, No. 5, 115 (1954); V. P. Ananyev, ibid., 23, No. 5 (1954); I. D. Sedletsky and V. P. Ananyev, Proc. Acad. Sci. USSR, 90, 651 (1953); paper in Symposium "Prevention of Water Filtration in Loess Soils", Acad. Sci. Ukrainian SSR, Kiev (1954).

[2] M. F. Vikulova, Soviet Geol., No. 39,121 (1949); Trans. All-Union Geol. Inst., No. 2 (1950); Electron Microscopy of Clays, State Chem. Press, Moscow (1952).

AN ELECTRON MICROSCOPE STUDY OF STRUCTURE FORMATION IN LOESS

2. INFLUENCE OF LOESS COMPONENTS ON STRUCTURE FORMATION

E. Aripov, Z. Ya. Berestneva, and V. A. Kargin

Loess is a finely granular, porous, loose sedimentary mineral material of a gray-yellow or straw color. Loesses not only serve as parent minerals in soil formation, but are valuable materials used in building, engineering geology, etc. Characteristic properties of loess which distinguish it from other sedimentary rocks are the porosity and looseness of its structure; moreover, the surfaces of loess strata may carry dense formations analogous to the crusts formed on soil surfaces. Geological data relate the loose and porous structure of loess to the deposition conditions, while the question of the influence of mineralogical and mechanical composition on the structure of loess is usually not considered in geological investigations [1].

Most studies of the formation of soil structure in relation to agriculture, dealing with the origins of a lumpy granular (agricultural) structure, associate this with the mineralogical composition of soils [2]. However, such investigations do not deal with causes of formation of a loose and porous structure in loess. In studies of the origins and properties of crusts on soil surfaces [3], these effects are also related to the mineralogical and mechanical composition of soil and the interaction of soil aggregates when the soil is humidified.

The purpose of our investigation was to study the mechanism of structure formation in loess in relation to its mineralogical composition, as the formation of a loose, porous structure and of dense layers on loess is probably primarily associated with its mineralogical composition. Structure formation in disperse systems can be studied by various methods, the most common of which are methods for studying the viscosity and mechanical properties of colloidal solutions and suspensions. Experimental data in this field indicate that structure formation in disperse systems already occurs in the suspensions themselves [4].

The most widely accepted theory of structure formation in disperse systems is the theory developed by Rebinder [5], which has been extensively confirmed by experimental investigations. According to this theory, the formation of secondary structure in disperse systems is attributed to cohesion between the disperse phase particles by means of chemical or van der Waals forces. With this type of cohesion between particles in suspensions, the structures formed are retained after removal of the dispersion medium. Because of this it is possible to study the mechanism of structure formation in aqueous loess suspensions by means of the electron microscope. It is extremely important in the use of this method that the structures formed in the suspensions should persist after removal of water, as the photographs are taken under a high vacuum.

Since the major part of loess is highly disperse in mechanical composition, aqueous suspensions of loess were used for studying processes of structure formation. Electron microscopy was used in our investigations, whereby it is possible to observe changes of shape, dimensions, and relative positions of the loess particles directly, and therefore to study processes of structure formation.

In addition to clay minerals (montmorillonites, kaolinites, etc.), loess contains fairly large amounts of calcium and magnesium carbonates, relatively small amounts of calcium sulfate, and humates. To elucidate the mechanism of structure formation in loess it was necessary to study separately all the loess components as well as their mutual influence on structure formation.

The mechanism of structure formation in loess was studied with the aid of the EM-3 electron microscope with direct electron-optical magnification (7,000-12,000) followed by photographic enlargment. Loess specimens from the Tashkent region were used for the experiments. Ammonium humates obtained from alkaline extracts of chernozem soil were used. Alkali extracts of humic acids contain excess alkali which may influence structure formation in loess. Humic acids were therefore precipitated from the alkaline extracts by addition of concentrated hydrochloric acid. The precipitate was transferred to a filter and washed with distilled water to a negative reaction for chloride ions. The humic acids were then dissolved in ammonia, excess of which can be easily evaporated. The concentration of the ammonium humate solutions was determined gravimetrically, the drying being carried out at 105°. All the samples for investigation were made from freshly prepared suspensions or mixtures of these, and subsequently at various time intervals.

As a check of the reproducibility of the results, each sample to be studied was prepared a number of times; 150 to 250 photographs were taken of each sample. All the samples, with the exception of natural loess, were prepared in the same way: the suspensions and mixtures made from them were shaken before samples were taken for applying the drops to the supports. In this way particles of all sizes present in the suspension were obtained in the specimens. In the case of natural loess the samples were taken from the upper layer of a settled suspension so that very large particles, which might mask the field of vision, could be avoided. However, in this case also control experiments were carried out, in which suspensions of natural loess were diluted and shaken before sampling. It was found that the structure of the larger particles was of the same character as previously (in settled suspensions). Thus the results are based on completely reproducible data.

Natural loess, as is known, consists of many components: clay minerals, various salts (mainly of calcium and magnesium), and remains of plants and microorganisms in the form of humus. These components probably influence structure formation processes in loesses. It was therefore desirable first to study the influence of such surface-active substances as humic acids on the structure of crystals of calcium and magnesium carbonates and calcium sulfate which are present in loess.

It is known that surface-active substances influence the form and dimensions of crystals, and therefore structure formation processes in structurized systems. Ammonium humates, calcium and magnesium carbonates, and calcium sulfate were therefore studied separately under the electron microscope, and then mixtures of these in various proportions were studied.

According to electron microscope data, ammonium humates consist of fine particles, a few hundredths of a micron in size, joined into large flocculent aggregates. Electron micrographs of aqueous calcium carbonate suspensions show that calcium carbonate consists of aggregates of very fine particles of various sizes (but no larger than 0.05-0.07 μ). Magnesium carbonate also consists of aggregates of semitransparent particles 0.2 –0.4 μ in size.

A study of the interaction of ammonium humates with calcium and magnesium carbonates showed that ammonium humates have practically no effect on the structure of calcium and magnesium carbonate particles irrespective of the proportions in which these salts and ammonium humates are taken and of the time elapsing after preparation of the mixtures.

A totally different situation is found in the interaction between ammonium humates and calcium sulfate. According to electron microscope data, calcium sulfate particles in aqueous suspensions are needle-like in shape, reaching 0.8 μ in length and several hundredths of a micron in width. The particles are generally joined into aggregates. Ammonium humates have a considerable effect on the form and dimensions of the calcium sulfate particles. Additions of 0.4 and 1.3% of ammonium humates at once result in recrystallization of the calcium sulfate, the particles of which become progressively larger. As the ammonium humate concentration increases from 6.9 to 17.6%, the calcium sulfate particles are first peptized, and subsequently recrystallization occurs in the mixture, accompanied by considerable growth of the crystals. When the ammonium humate concentration reaches 31.8%, peptization of the calcium sulfate particles first takes place, and subsequently, owing to the blocking effect of the ammonium humates, the recrystallization of the calcium sulfate is retarded.

Recrystallization of the calcium sulfate which occurs in ammonium humate – calcium sulfate mixtures is due to presence of ammonium humates in the mixture, as a pure aqueous suspension of calcium sulfate, allowed to stand 120 days under ordinary laboratory conditions, yields the same electron micrographs as freshly prepared aqueous suspensions of calcium sulfate.

In order to study the effects of calcium and magnesium carbonates, calcium sulfate, and humic acids on structure formation in loess it was first necessary to study loess from which these components had been removed. Removal of calcium and magnesium carbonates from loess was effected by treatment of the loess with 1% acetic acid solution, while the calcium present in the loess was removed by treatment with 0.5% barium chloride solution. It may be assumed that prolonged washing of the loess with water also removed the water-soluble humic acids.

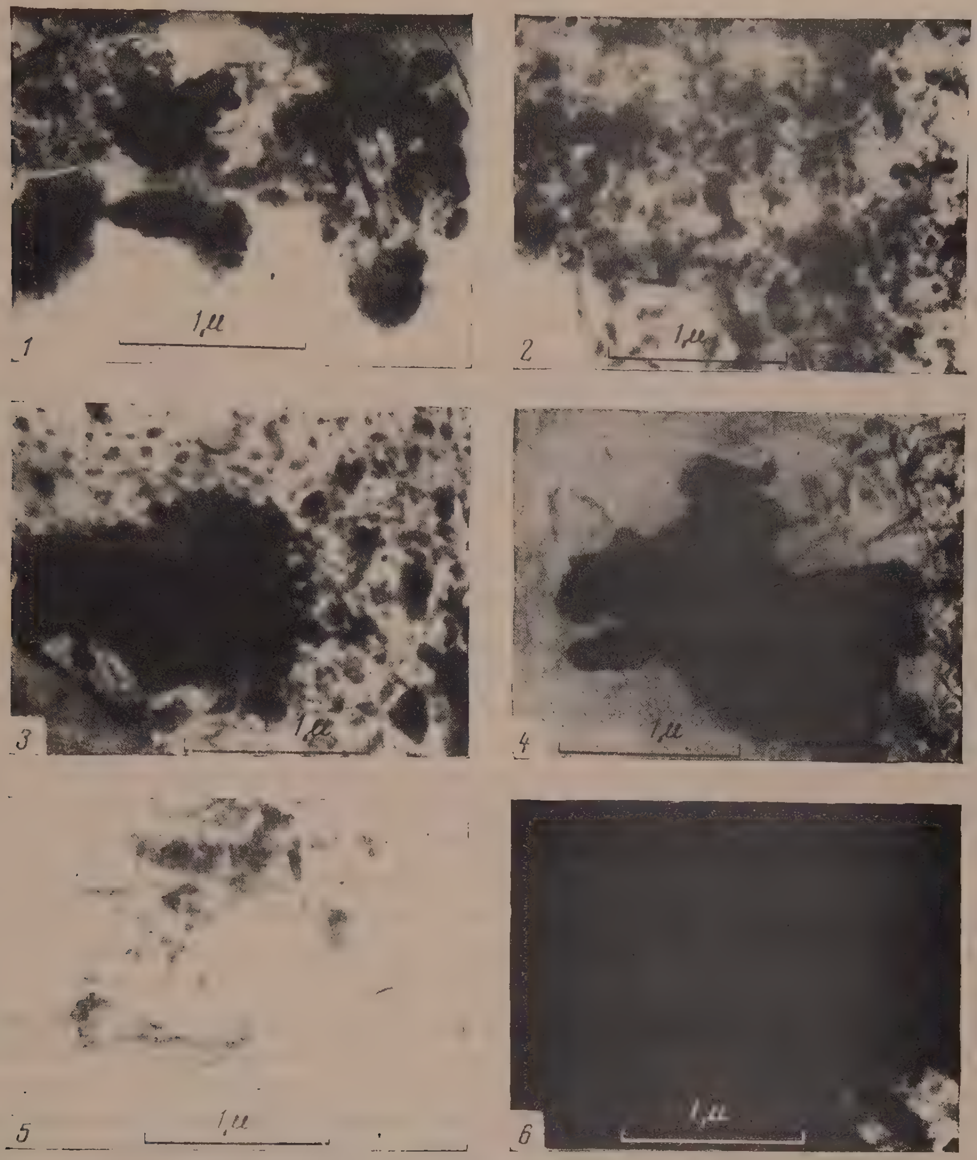

Figs. 1-6. Microphotographs showing variations in the structure of loess under the action of additions.

In our electron microscope investigations of suspensions of loess or of their mixtures with other components, the particles seen in the microphotographs are referred to as "loess particles," irrespective of whether they are clearly defined particles of individual minerals contained in the loess, or amorphous formations consisting of different minerals and salts which are components of the loess. According to electron microscope data, particles of natural loess (Fig. 1) are aggregates 1 to 2 μ in size, consisting of smaller particles.

Acetic acid treatment causes dispersion of the loess, with formation of fine particles of irregular shapes, a few hundreths of a micron in size, and needlelike particles 0.5 – 0.7 μ in length. These needlelike particles have sharp outlines (Fig. 2) in contrast to the particles with a loose structure and indistinct outlines. Loess particles remain practically unchanged after treatment with barium chloride solution (Fig. 3).

The nature of the interaction between loess and calcium and magnesium carbonates is quite different from that between loess and calcium sulfate. Calcium and magnesium carbonate are evidently substances which bind the mineral particles in loess, as dispersion of the loess occurs after removal of the carbonates. Removal of calcium sulfate has practically no effect on the size of the loess particles.

To confirm this hypothesis of the cementing (binding) effect of calcium and magnesium carbonates on loess and to determine the nature of the interaction between calcium sulfate and loess, and also between humates and loess, studies were made of the influence, first of the individual components, and then of their mixtures in various proportions, on structure formation processes in loess. As far as possible, the mixtures consisting of loess, humates, calcium and magnesium carbonates, and calcium sulfate, were made up in the proportions corresponding to natural loess. Loess treated with acetic acid was used. The influence of the individual components and their mixtures was studied with freshly made preparations, and subsequently at various time intervals, in order to observe the course of structure formation in loess. For studies of the effect of calcium carbonate on structure formation in loess, a number of mixtures was prepared consisting of aqueous suspensions of loess with increasing amounts of calcium carbonate. The interaction of loess with calcium carbonate first results in slight aggregation of the loess particles. Subsequently (after 4 days) the aggregates become considerably larger, reaching 2μ and over (Fig. 4). Structure formation in loess is intensified by the combined action of humates and calcium carbonate, large rapidly growing amorphous particles being formed. Addition of calcium carbonate to aqueous suspensions of clay minerals also causes aggregation in these systems.

The interaction of magnesium carbonate with loess is similar to that of calcium carbonate, with the difference that the aggregation processes are considerably slower in the former case.

A study of the combined action of humates and magnesium carbonate on structure formation in loess showed that magnesium carbonate does not exert the cementing action in presence of humates which is found in the case of pure magnesium carbonate. The humates in the mixture, however, also do not influence structure formation in loess, while addition of humates only to loess suspensions causes some aggregation of the loess particles. This suggests that in a mixture consisting of magnesium carbonate, ammonium humates, and loess, magnesium carbonate reacts chemically with the humates to form insoluble magnesium humates, so that the individual components do not exert their influence on structure formation in the loess.

Calcium sulfate in the pure state also has no effect on structure formation in loess, irrespective of time and concentration. Figure 5 shows a microphotograph of a mixture of aqueous suspensions of calcium sulfate and loess washed with acetic acid. Particles can be seen characteristic of loess treated with acetic acid, as seen earlier in Fig. 2.

In the loess – calcium sulfate – humate mixture, according to electron microscope data, aggregation occurs, accompanied by an increase in the density of the aggregates and considerable increases in their size (Fig. 6). This is probably caused by the binding properties of calcium sulfate which are effective in presence of humates, as pure calcium sulfate has no influence on loess, while recrystallization of calcium sulfate occurs in its aqueous suspensions in presence of humates, with increase of crystal size. In this case the rapidly growing calcium sulfate crystals may "seize" the smaller loess particles. Simultaneous addition of the main loess components (carbonates, humates, calcium sulfate) to washed loess induces aggregation processes with formation of rapidly growing aggregates.

Electron micrographs of loess particles washed free from calcium and magnesium carbonates indicate that in this case the loess particles are small (a few hundredths of a micron) and are incapable of forming dense aggregates, while gradual addition to aqueous suspensions of washed loess, first of calcium and magnesium carbonates, calcium sulfate, and humates separately, and then in mixtures of 2 and 3 components, and finally of all these components in a mixture, showed that loess particles are aggregated in presence of these components. Therefore, structure formation in loesses primarily depends on their mineralogical composition. Consequently, the size of the loess particles, the loose and porous nature of its structure, and the formation of dense crusts on surfaces of loess strata, are all associated with the presence of calcium and magnesium carbonate, humic substances, and calcium sulfate in the loess.

DISCUSSION OF RESULTS

The main property which distinguishes loess from other sedimentary minerals is the loose and porous nature of its structure, which persists through practically the whole stratum. The chief mechanical component of loess is fine dust, of which up to 70% is present. It is also known that loesses have a high carbonate content. Therefore it seems likely that carbonates, by binding together the fine loess particles, play the main part in the formation of the loose and porous structure of loess.

In fact, a comparison of electron micrographs of natural loess and of loess washed with acetic acid to remove carbonates showed that the particles in natural loess are aggregates up to 1-2 μ in size, consisting of smaller particles, while treated loess is seen to contain very small randomly scattered particles a few hundredths of a micron in size.

Addition of calcium and magnesium carbonates to aqueous suspensions of loess previously washed free from carbonates induces aggregation of the loess particles, large aggregates being again formed; the loose structure of loess is due to the manner in which these are packed.

The study of the effect of calcium sulfate on loess showed that when it is removed from natural loess the loess particles remain practically the same as before the removal. Addition of pure calcium sulfate to aqueous suspensions of the treated loess has no effect on the loess structure, irrespective of concentration or time. Therefore calcium sulfate in the pure form plays no part in the formation of loess structure. However, in presence of humates recrystallization occurs in aqueous calcium sulfate suspensions, accompanied by rapid growth of the calcium sulfate crystals. Evidently, in presence of humates, calcium sulfate can influence structure formation in loess. In fact, if calcium sulfate is added together with humates to aqueous suspensions of treated loess, structure formation occurs in the loess and very large aggregates are formed.

Simultaneous addition of the principal components of loess (carbonates, humates, etc.) results in aggregation, with growth and condensation of the aggregates. It is known that the surfaces of loess layers with a porous and loose structure may become covered with dense formations similar to the soil crusts formed on cultivated land in Central Asia.

As was shown earlier [6], when loess is humidified the particles swell and small pores form in them, through which water-soluble salts may rise by capillary action and accumulate on the surface. In fact, an aqueous extract of natural loess obtained by ultrafiltration contains dissolved calcium sulfate and magnesium and calcium bicarbonates. Increase of the contents of these substances on the surfaces of loess strata, and especially of the calcium sulfate content, may result in the formation of the dense crusts.

It is known that carbonates and calcium sulfate are present throughout the thickness of the loess stratum, the carbonate contents sometimes reaching 50%, and the calcium content 2%. Therefore an increase of the carbonate content in the surface layer (where it is already high) should not play any important part in the formation of dense crusts on the loess surface, while an increase of the calcium sulfate concentration may have an important effect on structure formation in the loess. In the presence of the humates which are always found in loess, recrystallization of calcium sulfate takes place, with very rapid crystal growth. This favors the formation of large aggregates which create a dense and fairly strong structure on the loess surface.

Since sierozem soils formed on loess deposits have almost the same composition and properties as loess, the mechanism of formation of loose and porous structures and surface crusts on loess strata may also apply to processes of lump and crust formation in sierozem soils of Central Asia.

SUMMARY

1. Structure formation in loesses has been studied by means of the electron microscope.

2. It is shown that ammonium humates added to aqueous suspensions of calcium and magnesium carbonates have practically no effect on their structure, but addition of these humates to aqueous calcium sulfate suspensions results in recrystallization and rapid growth of the calcium sulfate crystals.

3. Calcium and magnesium carbonates influence structure formation in loess, causing formation of aggregates, the nature of the packing of which is the cause of the loose structure of loess.

4. Calcium sulfate in the pure form has practically no effect on structure formation in loess. In presence of humates, recrystallization of calcium sulfate occurs, with rapid growth of its crystals which, by binding the loess particles together, can form either large dense aggregates or structural frameworks which give rise to dense formations on the loess surface.

The alkaline extract of humic acids used in this investigation was kindly provided by Prof. S. N. Aleshin, to thom we express our gratitude. We also thank Prof. I. N. Antipov-Karataev for supplying samples of clay minerals.

The L. Ya. Karpov Physocochemical Institute
Moscow

Received September 7, 1956

LITERATURE CITED

[1] V. A. Obruchev, Trans. II International Conf. Assoc. for Studies of the Quaternary Period of Europe, No. 2, 115 (1933); Trans. V. V. Dokuchaev Soil Inst., 27, 23 (1948); L. S. Berg, Nature, No. 6, 445 (1947); No. 2, 107 (1929); Trans. II. International Conf. Assoc. for Studies of the Quaternary Period of Europe, No. 1, 68 (1932); S. S. Neustruev, Nature, No. 1-3, 47 (1925); I. P. Gerasimov, Bull. Acad. Sci. USSR, Geol.-Geophys. Ser., No. 1, 97 (1939); N. Ya. Denisov, Conctructional Properties of Loesses and Loesslike Loams, State Building and Architecture Press, Moscow (1953).

[2] R. V. Vilyams, Fundamentals of Soil Cultivation, 4th div. gen. Agric. Press, Moscow (1946); K. K. Gedroits, Selected Works, 1, 241 (1955); A. N. Sokolovsky, Pedology, No. 1, 3, (1933); Soil Physics, 5, 9 (1936); A. F. Tyulin, Pedology, No. 3, 9 (1940); Colloidochemical Studies of Soils for Agricultural Purposes, Agric. Press, Moscow (1946); I. N. Gorbunov, The Absorptive Capacity of Soil and Its Nature, Agric. Press, Moscow (1948); I. N. Antipov-Karataev, V. V. Kellerman, and V. V. Khan, Soil Aggregates and Methods of Their Investigation, Acad. Sci. USSR (1948); P. V. Vershinin and V. P. Konstantinova, Physicochemical Principles of Artificial Soil Structure, Agric. Press, Moscow-Leningrad (1935); G. Ya. Rozen, Nature, No. 5, 88 (1956); Z. S. Filippovich, Pedology, No. 2, 16 (1956); E. O. Sushko, Chemical Melioration of Soils, Agric. Press, Moscow-Leningrad (1936).

[3] A. N. Izyumov, Pedology, No. 10, 00 (1938);* I. A. Kaspirov, Pedology, No. 7, 60 (1940); Soil Crust and Its Prevention, Agric. Press, Moscow-Leningrad (1951); N. I Gorbunov and N. E. Bekarevich, Cotton Growing, No. 7, 52 (1951); Soil Crust in Cotton Irrigation, Acad. Sci. USSR Press, Moscow (1955); N. K. Balyabo, Increase of Soil Fertility in the Irrigated Cotton Zone of the USSR, Agric. Press, Moscow (1954); M. I. Lomonovich, Loess in Kazakhstan and Its Significance in the National Economy, Acad. Sci. Kazakh SSR Press, Alma-Ata (1955).

[4] I. N. Putilova, Practical Manual of Colloid Chemistry, Chem. Press, Moscow (1947); P. A. Rebinder, Synopsis of a General Course in Colloid Chemistry, Moscow State Univ. Press, Moscow (1950).

[5] Rebinder P., Disc. Far. Soc., No. 18, 151, 1954; E. E. Segalova, P. A. Rebinder, and O. P. Lukyanova, Bull. Moscow State Univ., 2, 17 (1954); N. V. Mikhailov and P. A. Rebinder, Colloid J., 17, 107 (1955).

[6] E. Aripov, Z. Ya. Berestneva, and V. A. Kargin, Colloid J., 19, 14 (1957).

---

* As in original — Publisher's note.

THE EFFECT OF AIR IONIZATION ON THE DISPERSE PHASE OF AEROCOLLOIDS

I. I. Belyaeva, A. E. Mikirov, and N. S. Smirnov

It was shown in the previous comunication [1] that artificial increase of air ionization by ultraviolet and X-rays and β-particles results in a 3-4 fold increase of the concentration of ultramicroscopic particles and a more than 10-fold increase of the number of condensation nuclei. Wilson [2] observed mists in pure moist air without water vapor supersaturation upon irradiation by "strong ultraviolet." M. Curie [3] introduced radon into small chambers (30-55 cc) and observed the formation of mists in air of relative humidity from 100 to 7%; she noted that the mists were visible for 10-20 days after introduction of radon into the chambers and disappeared only when the radon concentration in the chamber fell considerably as the result of disintegration. Finally, Strieder et al. [4]irradiated pure moist air by X-rays and obtained mists at a relative humidity of ~ 100%. Our object in the present work was to study the scattering power and stability of such mists.

EXPERIMENTAL

The optical system used in the experiments in shown in Fig. 1. Rays from the light source S, passing through the condenser K, the diaphgram D, and the objective O_1 are rendered parallel. The light then passes through the objective O_2 and reaches the screen E situated at the focus of the objective O_2 giving a real image of the diaphgram D of natural size. The screen is 3 × 3 mm. A photomultiplier type FEU-1 is situated behind the screen. The aerosol cell a-c, 1.6 liter in capacity with plane-parallel sides, was placed between the objectives O_1 and O_2. Thus, if no optical inhomogeneities are present between the objectives O_1 and O_2 (with the cell empty) no light reaches the photocathode, and the microammeter in the photomultiplier circuit registers the dark value of the current (I_0).

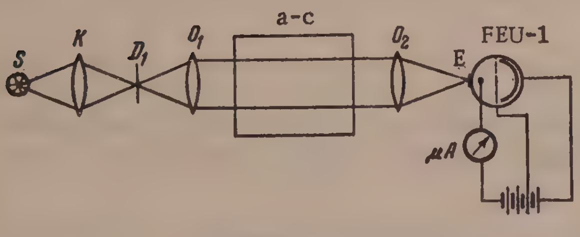

Fig. 1. Optical diagram of the experiments.

When an aerosol forms in the cell, the light scattered by the particles will pass around the black screen and reach the photocathode, and as a result current (I) will flow through the microammeter. The magnitude of this current is a measure of the scattering power of the mist, and depends on the concentration and size of the particles.

The optical diagram shows that the indicatrix of light scattering by the particles is rationally utilized. As is known [5], most of the light (80%) scattered by a particle is directed forward and is contained in an angle of 45-50°. This made it possible to measure fairly accurately variations of the scattering power of turbid media with time.

Ionization of the air in the cell (chamber) was effected by α-particles from Po^{210} of different activities by introduction of the sources into the chamber.

Results of Determinations. In all cases in which air of relative humidity not greater than 100% was ionized by a α-particles, a visible mist was formed, the rate of formation of which depended on the activity of the source. The mists were very stable in these humidity conditions, and were destroyed very slowly after removal of the radioactive source.

The increase of the light scattering power of the mist with the time of irradiation by sources differing in activity by one order of magnitude is given in Table 1.

TABLE 1

Light Scattering by Mist Formed as the Result of Irradiation of Moist Air by α-Particles

Activity of source 200 mcurie		Activity of source 20 mcurie	
Irradiation time, min.	Scattering power I/I_0	Irradiation time, min.	Scattering power I/I_0
00	1.00	00	1.00
20	1.02	30	1.00
45	1.09	70	1.01
50	1.12	85	1.03
55	1.22	115	1.06
60	1.37	130	1.08
65	1.42	160	1.12
		175	—

TABLE 2

Variation of Light Scattering by a Mist With Age

Age of mist in minutes	Scattering power I/I_0	Age of mist in minutes	Scattering power I/I_0
00	1.38	205	1.22
15	1.38	220	1.12
55	1.37	—	—
175	1.31	—	—

The same apparatus was used to determine the stability of the mists by the changes of their light scattering power with time.

After the radioactive source had been removed from the chamber, the scattering power of the mist decreased, and usually after several hours I/I_0 became practically equal to unity. The results of such a determination are given in Table 2.

The results of our experiments confirm the visual observations of Wilson [2], M. Curie [3], and Strieder et al. [4].

Moreover, our experimental data show that artificial increase of the ionization of moist air of relative humidity not over 100% not only increases the concentration of the submicroscopic condensation nuclei) and ultramicroscopic fractions of the disperse phase of aerocolloids [1], but produces a visible stable mist. Measurements of the light scattering power of such mists showed that it increases with irradiation time and source activity. For example, on irradiation by a source of 200 mcurie, a mist was formed in 5-10 minutes, and after 65 minutes its light scattering was 42% greater than that of the same air before irradiation. The action of a 20 mcurie source produced a mist visible after 20 minutes, and 175 minutes after irradiation the light scattering was 12% higher than before the irradiation. It was shown experimentally that such mists are stable; i. e., in our conditions they persisted for several hours.

SUMMARY

1. Increased ionization of the air (the dispersion medium) increases the concentration of submicroscopic particles (condensation nuclei) and ultramicroscopic fractions in the disperse phase of aerocolloids and results in formation of a visible mist.

2. The rate of formation of such aerocolloids depends on the activity of the ionizing radiation source, and therefore on the rate of formation and the concentration of ions in the dispersion medium.

3. Such mists are stable in the conditions studied, and increase light scattering by 12-40%, according to the activity of the source and the time of irradiation.

Geophysical Institute, Acad. Sci. USSR
Moscow

Received May 5, 1956

LITERATURE CITED

[1] K. M. Merzhanov, N. I. Peterimova, and N. S. Smirnov, Colloid J., 18, No. 5, 574 (1956).

[2] C. T. R. Wilson, Phil. Trans. Roy. Soc., London, Ser. A. 192, 403, 1899.

[3] M. Curie, C. r.* 145, 1145, 1907.

[4] F. Strieder et al, Ann. Phys. 46, H–7, 989, 1915.

[5] See, e. g., K. S. Shifrin, Light Scattering in Turbid Media, GITTL (1951).

---

* C. r. = Comptes rend. – Publisher's note.

INTERMOLECULAR STRUCTURE OF HIGH POLYMERS

COMMUNICATION 22. MODIFICATION OF THE MOLECULAR STRUCTURE OF HIGH POLYMERS BY THE INCLUSION METHOD

A. N. Bykov and A. B. Pakshver

Inclusion can serve as one of the methods for modifying the molecular structure of high polymers. By inclusion of molecules of an inert substance in the molecular structure of a polymer previously loosened by a substance which causes swelling, it is possible to preserve the loose structure. In this way it is possible to increase the reactivity of high polymers (cellulose, polyamides, acetylcellulose, etc.) in solution, dyeing, and sorption of acids and bases.

Only a few investigations, relating to hydrate cellulose fibers, and cellulose, have so far dealt with inclusion in high polymers. Nikitin [1], in a study of the esterification of cotton linters, noted that after preliminary swelling in water and treatment with pyridine (inclusion) cellulose is much more rapidly esterified. Hydrate cellulose treated with pyridine remained highly reactive even after drying.

Rogovin [3] attributes the increased reactivity of cellulose containing included substances to impossibility of removing the included substances for steric reasons. Because of the presence of the included substance within the fibers the distance between the macromolecules increases and formation of hydrogen bonds between adjacent macromolecules is hindered. Krässig [4] included various organic liquids: benzene, acetone, pyridine, etc., in cellulose swollen in water. The reactivity of the cellulose increased, and it reacted readily with hexamethylene diisocyanate, combining with up to 0.25 mole of hexamethylene diisocyanate per 1 mole of glucose residue. The result of inclusion treatment of cellulose depends both on the molecular size of the included substance, and on the degree of preliminary swelling of the cellulose or hydrate cellulose fibers.

No publications have yet appeared on inclusion in synthetic polymers, although Scharf [5], who studied the action of mineral and organic acids on polyamide fibers, was in fact dealing with inclusions in polyamides. The increased sorption of dye anions in the regions damaged by acid can only be explained by inclusions in the polyamide.

The present paper is the first communication on a series of investigations on modification of the molecular structure of high polymers by the inclusion method in order to increase their reactivity.

EXPERIMENTAL

The inclusion treatment was carried out as follows. A sample of the fiber, cellulose, or flake ~2g in weight was treated with a substance causing swelling of the polymer and weakening the forces between the macromolecules. For polyamides, phenol solutions (15, 20, and 25 g / liter) and 15% H_2SO_4 solutions; for cellulose, 5 and 10% NaOH solutions; and for acetylcellulose, 10, 30 and 40% aqueous acetone solutions and 20% HCOOH solution were used for this purpose. The samples were pressed out after the treatment and the swelling liquid was replaced by the inclusion substance: benzene, acetone, alcohol, ether, or water (in the case of capron and acetylcellulose). The replacement was performed consecutively, for example:

Phenol (or NaOH) → water → alcohol → benzene (or ether)
Phenol (or NaOH) → water → acetone → benzene (or alcohol)
Acetone (or HCOOH) → water → alcohol → benzene (or ether)

The inclusion treatment time was 30 minutes for polyamides and 60 minutes for acetylcellulose and cellulose. The treatment temperature was 20°. The treated polymer was dried at 50° for 1 hour.

Various methods were used to evaluate the influence of inclusion on the polymer properties: sorption rates of dyes, acetic acid, and phenol; also, for polyamides, the time required for solution, the rate of dye sorption for acetylcellulose, and the rate of dye sorption and viscose filtration blockage coefficient for cellulose.

An acid brown dye was used for polyamide dyeing (pH 3; dyeing time 10 minutes). Acetic acid was used at 0.01 N concentration. The phenol used as the sorbed substance after inclusion had a concentration of 8 g/liter; the sorption time was 10 minutes. The amount of substance sorbed was determined from the concentrations in solution before and after treatment. The solubility of capron resin was determined in concentrated solution of calcium chloride in methyl alcohol at 60°.

The dye used for acetylcellulose was Acetoquinone Blue. The sulfite cellulose was previously shredded and treated with NaOH solution to remove hemicellulose.

Cellulose reactivity before and after the inclusion treatment was determined by the method of the All-Union Scientific Research Institute for Artificial Fibers [6], i. e., by the retardation of the filtration rate of viscose solution, and also by the rate of dye sorption (Congo Red, dyeing time 10 minutes, dye concentration 0.5 g/liter). The capron resin was reprecipitated from solution in 88% phenol. Ethyl alcohol was used to precipitate the resin from this solution.

The tensile strength and extensibility of the fibers were determined with the aid of a recording dynamometer.

Tables 1 and 2 give the results of studies of the effects of inclusion of various substances on the properties of polyamides (flake and fibers), cellulose, and acetylcellulose. The properties of the original polymers are taken as 100% in all cases.

These results show that polymer reactivity can be increased by inclusion in all cases. The sorption of dyes and acids by capron resin and fibers is increased by a factor of 1.4-2.2, and the sorption of phenol, nearly 4-fold. The solution time of carpon resin is decreased by 30%. Cellulose and acetylcellulose take up 1.2-1.8 times more dye after inclusion treatment.

The viscose-making properties of cellulose are also improved, and filtration blockage rate is considerably decreased. All this is explained by the fact that preliminary treatment of the polymer by the swelling agent causes rupture of intermolecular bonds and weakening of molecular interaction. This change of structure becomes fixed by incorporation of the included substance, the presence of which prevents re-intensification of the weakened forces between the macromolecules. The higher the concentration of the substance causing swelling of the high polymer, the greater is the inclusion effect and the reactivity of the treated polymer.

It is true that an increase of acetone concentration above 10% in the treatment of acetylcellulose somewhat lowers its reactivity (dye sorption). However, this is probably caused by removal of the more active low molecular portion of the acetylcellulose, soluble in 30-40% acetone solutions.

Some increase in the reactivity of the inclusion-treated polymer also occurs with increasing molecular weight of the inclusion substance. Sorption of dyes and acids increases somewhat, polyamide solution time decreases, and the viscose filtration blockage rate is lowered. It seems that an included substance of higher molecular weight, on incorporation between the polymer macromolecules, creates greater obstacles to the restoration of the molecular bonds broken during swelling.

Reprecipitation of capron resin leads to a sharp increase of reactivity, as the reprecipitated resin has a looser structure with fewer molecular bonds, and the active polyamide groups become more accessible to dyes and acids. The solution time of such resin is also considerably less. The physicomechanical properties of drawn capron yarn are changed by inclusion treatment: the fiber strength is decreased by 10-25%, and the extension at break increases by 25-30%.

TABLE 1

Effects of the Inclusion of Various Substances on the Properties of Capron Resin and Fibers

Substance studied	Swelling solution	Method of evaluation	% Change after inclusion (for 60 min. at 20°) of			
			benzene	acetone	ethyl alcohol	water
Capron resin	20 g/liter phenol	Dye sorption	163	138	138	—
		Solution time	68	65	71	—
Ditto, after reprecipitation*	20 g/liter phenol	Dye sorption	803	711	710	—
		Solution time	43	49	49	—
Undrawn capron yarn	25 g/liter phenol	Dye sorption	187	—	—	—
		Sorption of acetic acid	172	148	—	—
	15 g/liter phenol	Dye sorption	172	145	—	—
		Sorption of acetic acid	135	133	—	—
Ditto, drawn	Sorption of acetic acid	Sorption of phenol	390	329	—	245
		Tensile strength	81	71	—	79
		Extension at break	125	131	—	128

---

* After reprecipitation, capron flake without inclusion takes up 636% of dye and the solution time decreases to 57%.

TABLE 2

Effects of the Inclusion of Various Substances on the Properties of Cellulose and Acetylcellulose

Substance	Swelling solution	Method of evaluation	% Change after inclusion (for 60 min. at 20°) of			
			benzene	acetone	ethyl alcohol	ether
Sulfite cellulose*	5% NaOH	Filtration blockage rate	—	78	—	—
		Dye sorption	—	122	—	—
	10% NaOH	Filtration blockage rate	78	91	100	113
		Dye sorption	188	186	130	170 (вода)
Acetylcellulose	10% acetone	Dye sorption	154	—	—	—
	30% acetone	Ditto	128	—	—	130
	40% acetone	» »	99	—	—	—
	20% formic acid	» »	137	—	—	116

---

* All the data refer to sulfite cellulose from which hemicellulose had been removed by treatment with 17.5% NaOH solution. This treatment increases the filtration blockage rate to 158% and dye sorption to 115%.

SUMMARY

1. Inclusion treatment increases the reactivity of high polymers, considerably raising the sorption rates of dyes and acids by polyamides, and of dyes by acetylcellulose and cellulose.

2. The viscose-making properties of cellulose are improved and the solution times of polyamides are decreased.

3. The greater the preliminary weakening of the high polymer structure, the greater is the effect produced by the inclusion and the higher is the polymer reactivity.

LITERATURE CITED

[1] N. I. Nikitin, Paper Ind., No. 3, 38 (1941).

[2] H. Staudinger, W. Döhle, J. Heick, Prakt. Chem. 161, 191, 219, 1942; Staudinger H., Döhle W., Makr. Chem. 9, 2, 188, 1953.

[3] Z. A. Rogovin, High Molecular Compounds, No. 9, 1 (1949); Z. A. Rogovin and N. N. Shorygina, Chemistry of Cellulose and Associated Substances, State Chem. Press, p. 87 (1953).

[4] H. Krässig, Makr. Chem. 10, I, 1953; H. Krässig, E. Schroft, Bull. Inst. text. France, No. 49, 47, 1954, Makr. Chem. 13, 2/3, 179, 1954.

[5] R. Scharf, Textil and Faserstoff, 5, No. 10, 573, 1955.

[6] All-Union State Standard 5982-51, Group K-51, Refined Viscose Cellulose, p. 10.

EQUILIBRIUM OF A VISCOPLASTIC DISPERSE SYSTEM ON A ROTATING DISK

A. M. Gutkin

Tyabin, Shklyar, Mosikhin, and Vinogradov [1] have described a centrifugal method for studying the rheological properties of greases, based on investigations of the equilibrium and flow of a thin layer of grease on a rotating disk. This method can be used for studying any viscoplastic disperse system. However, the theory of the method as put forward by the authors cannot be accepted as correct. The defects of the theory are largely due to the fact that it is based on the "general equation for the flow of a viscoplastic medium," proposed by M. V. Tyabin. Comments on this equation and on its practical applications have already been published [2].

The problem of equilibrium in a layer of a viscoplastic disperse system on a rotating disk is considered below. Since the case of the flow of the medium is not discussed, plastic viscosity does not enter the solution of the problem. This then reduces to the problem of the elasticoplastic equilibrium of the disk, differing in boundary conditions from the problem of elasticoplastic equilibrium of rotating disks which was examined by Sokolovsky [3]. The difference in boundary conditions significantly influences the method and solution of the problem.

Suppose that a layer of viscoplastic medium of thickness h lies on a disk rotating with angular velocity ω. It is assumed that adhesion takes place between the disk and the grease layer, i. e., that the displacement u of the medium on the disk surface is zero: $u_z = 0$ and $u_r = 0$ when $z = 0$. With these boundary conditions the problem can be solved in terms of deformations.

In the elastic deformation region the components of the stress tensors in a cylindrical system of coordinates are expressed as follows:

$$\sigma_r = -p + 2G\frac{\partial u_r}{\partial r},\quad \sigma_\varphi = -p + 2G\frac{u_r}{r},\quad \sigma_z = -p + 2G\frac{\partial u_z}{\partial z};$$

$$\tau_{rz} = G\left(\frac{\partial u_r}{\partial z} + \frac{\partial u_z}{\partial r}\right);\quad \tau_{r\varphi} = 0;\quad \tau_{z\varphi} = 0, \tag{1}$$

where G is the shearing modulus, $p = -{}^1/_3\ (\sigma_r + \sigma_\varphi + \sigma_z)$.

The equations

$$u_\varphi = 0;\quad \frac{\partial u_r}{\partial \varphi} = 0;\quad \frac{\partial u_z}{\partial \varphi} = 0$$

are a consequence of circular symmetry.

In the given conditions the equilibrium equations have the form:

$$\frac{\partial \sigma_r}{\partial r} + \frac{\partial \tau_{rz}}{\partial z} + \frac{\sigma_r - \sigma_\varphi}{r} + \rho\omega^2 r = 0; \tag{2}$$

$$\frac{\partial \tau_{rz}}{\partial r} + \frac{\partial \sigma_z}{\partial z} + \frac{\tau_{rz}}{r} = 0. \tag{3}$$

In addition to Equations (2) and (3), the equation for continuity of displacements must be satisfied:

$$\frac{\partial u_r}{\partial r} + \frac{u_r}{r} + \frac{\partial u_z}{\partial z} = 0. \tag{4}$$

In order that Equation (4) should be satisfied identically, we introduce a certain function ψ, such that

$$u_r = -\frac{1}{r}\frac{\partial \psi}{\partial z}; \quad u_z = \frac{1}{r}\frac{\partial \psi}{\partial r}. \tag{5}$$

Replacing the stress tensor components in Equations (2) and (3) by their expressions in the form of (1) where displacements are first expressed in terms of ψ, we have:

$$-\frac{\partial p}{\partial r} = \frac{G}{r}\frac{\partial}{\partial z}\Delta\psi - \rho\omega^2 r; \tag{6}$$

$$\frac{\partial p}{\partial z} = \frac{G}{r}\frac{\partial}{\partial z}\Delta\psi, \tag{7}$$

where Δ denotes the operator

$$\Delta = \frac{\partial^2}{\partial r^2} - \frac{1}{r}\frac{\partial}{\partial r} + \frac{\partial^2}{\partial z^2}. \tag{8}$$

Eliminating p from Equations (6) and (7), we have a differential equation for ψ :

$$\Delta\Delta\psi = 0. \tag{9}$$

Differential Equation (9) must be solved for the boundary conditions:

$$\frac{1}{r}\frac{\partial \psi}{\partial r} = 0, \quad \frac{1}{r}\frac{\sigma\psi}{\partial z} = 0, \qquad \text{when } z = 0; \tag{10}$$

$$\tau_{rz} = G\left(\frac{\partial u_r}{\partial z} + \frac{\partial u_z}{\partial r}\right) = 0, \quad \sigma_z = 0, \qquad \text{when } z = h. \tag{11}$$

The medium is assumed to be unlimited in the direction r . The function ψ is found to be:

$$\psi = r^2(az^3 + bz^2).$$

The constants a and b are to be determined from the boundary conditions (11), which have not yet been satisfied.

Since $\frac{\partial u_z}{\partial r} = 0$ everywhere, it follows from the first boundary condition in (11) that

$$\frac{\partial u_r}{\partial z} = -r\,(6az + 2b) = 0, \quad \text{when } z = h,$$

and hence

$$6ah + 2b = 0 \tag{12}$$

The second boundary condition in (11) may be transformed into

$$\frac{\partial p}{\partial r} = 0, \text{ when } z = h \tag{13}$$

From Equation (6) it follows that

$$-\frac{\partial p}{\partial r} = r\,(6aG - \rho\omega^2).$$

To satisfy Condition (13), the following equation must be true:

$$6aG = \rho\omega^2. \tag{14}$$

From Equations (12) and (14) the constants a and b can be found. Thereby the function ψ and the values of u_r, u_z, τ_{rz} are also found.

The pressure p is found to be

$$p = \rho\omega^2\,(z - h)^2. \tag{15}$$

The boundary of the elastic deformation zone is found from the condition

$$\frac{1}{6}\,[(\sigma_r - \sigma_z)^2 + (\sigma_z - \sigma_\varphi)^2 + (\sigma_r - \sigma_\varphi)^2] + \tau_{rz}^2 = \theta^2, \tag{16}$$

i. e., by equating the tangential stress intensities to the yield stress.

Equation (16) leads to equation for the boundary surface separating the elastic and plastic deformation regions:

$$\rho^2\omega^4\,[3z^2\,(z - 2h)^2 + r^2\,(z - h)^2] = \theta^2. \tag{17}$$

If the thickness of the layer is small, the first term in the square brackets may be neglected, and Equation (17) is simplied to

$$\rho\omega^2 r\,(h - z) = \theta. \tag{18}$$

Thus, the region of plastic deformation approaches most closely to the axis of the disk at the periphery

$$z = 0,\ r_0 = \frac{\theta}{\rho\omega^2 h}\,. \tag{19}$$

If r_0 is known, θ can be found:

$$\theta = \rho\omega^2\,r_0 h. \tag{20}$$

If the radius of the layer is less than or equal to r_0, the medium will not flow.

The solution found for this case is not exact, as the medium is assumed to be unlimited in the direction of the axis r. The boundary conditions for the lateral surface of the layer of medium therefore did not enter into the formulation of the problem. However, the error introduced if the boundary conditions at the lateral surface are not satisfied cannot be large, because the height of the layer is small.

If the radius of the layer is greater than r_0 the medium will flow and the position of the elastic zone boundary will depend not only on θ, but also on the viscosity and flow rates. Formula (20) can be used to find θ experimentally, by studying the behavior of the medium on a rotating disk. The formula gives the most accurate results if the layer of medium with radius R is applied and the angular velocity is then gradually increased until the medium begins to flow.

Let us determine the yield value of a lubricant grease by means of Formula (20) on the basis of the experimental results described in [1]. The results treated in this way are given in the table.

Table of Yield Values

Revolutions of disk per min.	Radius of elastic zone in cm	Height of grease layer in elastic zone, in mm	θ calculated from Formula (20), in dynes/cm^2
400	5.6	3	3000
500	4.3	3	3600
600	3.75	3	4500
700	3.4	2.8	5000
800	2.8	2.8	5600
900	2.5	2.5	5600
1200	1.75	2.3	6400
1600	1.15	1.8	5900

The values of θ found from the results of the first three experiments must be considered low, as the radii of the elastic zone in these experiments were less than the radii calculated from Formula (20). The reason for this was that, in addition to its plastic properties, the viscous properties of the grease also influenced its behavior, as in these experiments the viscoplastic grease covered the whole disk and was in a state of flow on it before the measurements were made.

The last five experimental determinations give values for the yield stress of the grease which are in fairly good agreement with each other. These values are close to the yield value (6000 dynes / cm^2) which, as is noted by the authors [1], was obtained by K. I. Klimov for this grease by another method.

SUMMARY

1. Deformation and stress distributions in a layer of a plastic medium in equilibrium on a rotating disk have been determined.

2. A relationship has been derived between the limiting radii of the medium in the equilibrium state and the yield value.

3. The formula has been used to calculate yield values from the experimental results of N. V. Tyabin, L. A. Shklyar, E. P. Mosikhin, and G. V. Vinogradov.

The Molotov Institute of Power Engineering
Moscow

Received March 26, 1957

LITERATURE CITED

[1] N. V. Tyabin, L. A. Shklyar, E. P. Mosikhin, and G. V. Vinogradov, Trans. S. M. Kirov Inst. Chem. Tech., Kazan, No. 16, Tatar State Press, Kazan (1951).

[2] M. P. Volarovich and A. M. Gutkin, Colloid J., 15, No. 2 (1953).*

[3] V. V. Sokolovsky, Theory of Plasticity, State Tech. Theoret. Press, Moscow—Leningrad (1950).

---

* Original Russian pagination. See C. B. translation.

INVESTIGATION OF THE STRUCTURE AND PROPERTIES OF CARBON CHAIN POLYMERS IN DILUTE SOLUTIONS

2. SOLUTIONS OF VINYL CHLORIDE – ACRYLONITRILE COPOLYMER

S. G. Zelikman and N. V. Mikhailov

Copolymerization is one of the most widely used methods for the production of polymers with a great variety of properties. Copolymers are becoming increasingly important in the production of synthetic fibers. At the present time fibers based on caprolactam and AH salt copolymers (trelon, eftrelon), acrylonitrile and vinyl acetate, acrylonitrile with small amounts of other monomers, etc., are widely used.

Synthetic fibers made from vinyl chloride – acrylonitrile copolymer have certain specific properties which distinguish them advantageously from most other types of carbon chain fibers. These properties include high stability to heat and light, easier dyeing, stability in many organic solvents, absence of shrinkage, and high strength in the wet and dry states. Because of the good fiber properties and wide availability of the raw materials, this is one of the most promising copolymers [1].

The present paper describes a study of the properties of vinyl chloride – acrylonitrile copolymers. The properties of the pure polymers were described previously [2].

EXPERIMENTAL

Three copolymers were used for the study, with the following ratios of acrylonitrile to vinyl chloride: 40:60, 29:71, and 13:87% by weight. The physicochemical properties of these copolymers and methods for their fractionation have not been described in the literature.

The 40:60 and 29:71 copolymers were fractionated from acetone solutions. The solvent used for the copolymer containing 13% acrylonitrile was a 5:1 mixture of acetone with dimethylformamide.

The fractionation procedure for the 40:60 copolymer was as follows: a mixture of methanol and acetone (10:13) was added dropwise with stirring to a 2% solution of the copolymer in acetone until a flocculent precipitate was formed. After settling and decantantion the precipitate was washed with methanol and dried. These operations were repeated to precipitate the following fractions. The last fraction was precipitated by an excess of pure methanol. The copolymers containing 29 and 13% acrylonitrile were precipitated by a 3:1 mixture of acetone and water. The last fraction was precipitated by an excess of water. Three fractions, differing in specific viscosity, were isolated from each of the copolymers. These fractions were used for studying the viscosity and osmotic pressure of the copolymers. The nitrogen contents of the fractions were determined by the Kjeldahl method. It was found that the fractions of a given copolymer, while differing in molecular weight, had equal nitrile group contents. The differences between the fractions corresponded to ~ 0.5% nitrile groups, which is within the error limits of the nitrogen determination.

The variations of viscosity with concentration in the 0.25-1.0% range, and also variations of viscosity with temperature (from 20 to 60°) were studied for all the copolymers. The osmotic pressure was determined at 20, 35, and 50°. To determine molecular weights, π/c graphs were used and the reduced osmotic pressures were extrapolated to zero concentration. The methods of viscosity and osmotic pressure determinations were described previously [2].

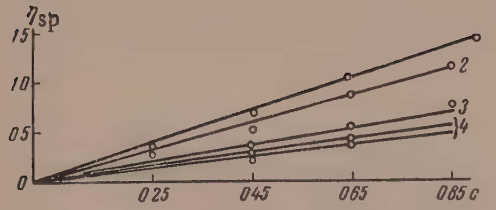

Fig. 1. Variation of specific viscosity with concentration of copolymer solutions: 1) fraction I of 40:60 copolymer; 2) fraction I of 29:71 copolymer; 3) fraction I of 13:87 copolymer; 4) fraction III of copolymers of all compositions.

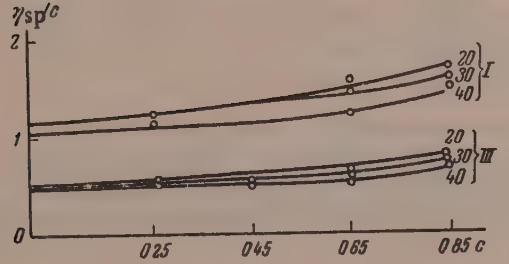

Fig. 2. Variation of reduced viscosity at 20, 30, and 40° with concentration of 40:60 copolymers: I) fraction I, mol. wt. 54,000; III) fraction III, mol. wt. 30,000.

TABLE 1.

Molecular Weights of Copolymer Fractions at 20,35, and 50°

Copolymer	Fraction	Molecular weight of copolymer at temperature, °C		
		20	35	50
Copolymer 40 : 60	I III	54 000 30 000	53 000 30 000	48 000 30 000
Copolymer 29 : 71	I III	53 000 33 000	52 000 32 000	51 000 32 000
Copolymer 13 : 87	I	55 000	55 000	52 000

The variations of specific and reduced viscosity with concentration for copolymers of different composition are shown in Figs. 1,2, and 3.

The variation of viscosity with temperature for fraction I of the 40:60 copolymer is shown in Fig. 4. In the temperature range studied, the variation of specific viscosity with temperature was linear for all the copolymers. The slope of the $\eta_{sp} - t$ curves depends on the molecular weight of the fractions and the solution concentration: the slope increases with increasing molecular weight and concentration.

As is seen from Figs. 2 and 3, the relationship between reduced viscosity and concentration is practically linear for all the copolymers in the concentration region 0.25 – 0.85%. Figure 5 shows the variation of reduced osmotic pressure with concentration for the two extreme fractions (I and III) of all the copolymers at 20, 35, and 50°. The molecular weights of the copolymers are given in Table 1.

Table 1 shows that the molecular weights of any given copolymer fraction practically coincide at different temperatures. The molecular weight variations with the temperature are very small, and are within the limits of experimental error.

Thus, like the pure polyvinyl chloride and polyacrylonitrile polymers, their copolymers W of various compositions form true solutions at infinite dilution, and no molecular aggregation occurs. The absence of aggregation is also indicated by the linear course of the $\eta_{sp} - c$ curves. A comparison of the copolymer properties shows that the viscosities of the copolymers of all compositions practically coincide at low molecular weights (fraction III). Some differences are found for the fractions of higher molecular weight (Fig. 6).

The curve shows that copolymer viscosity increases with increasing nitrile group content. Small deviations from additivity are found even for dilute solutions (0.65%). To evaluate the flexibility of the copolymers studied, the values of μ were calculated (Table 2).

A comparison of the values of μ for polymer fractions of approximately equal molecular weight shows that the 40:60 polymer has the greatest flexibility. The flexibility of copolymers with lower nitrile group contents approaches the flexibility of polyvinyl chloride. Variations of μ with composition (for fractions of similar molecular weight) are shown in Fig. 7.

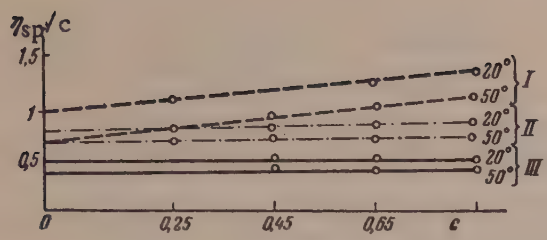

Fig. 3. Variation of reduced viscosity at 20 and 50° with concentration: I) fraction I of 29:71 copolymer; II) fraction I of 13:87 copolymer; III) fraction III of 29:71 and 13.87 copolymers.

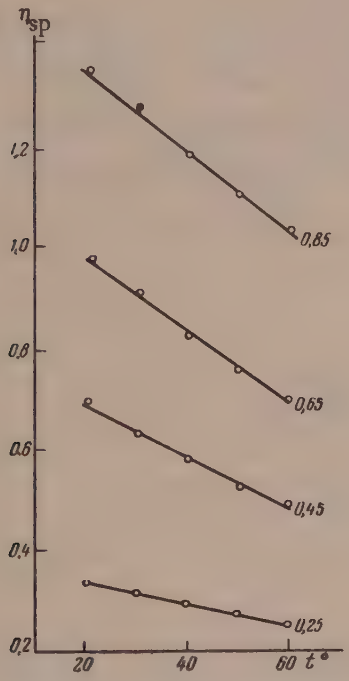

Fig. 4. Variation of specific viscosity of 40:60 copolymer with temperature at different concentrations.

TABLE 2

Values of μ for Copolymers of Different Compositions

Copolymer	Molecular weight of fraction	μ
Copolymer 40 : 60	54 000 30 000	0.38 0,46
Copolymer 29 : 71	53 000 33 000	0.41 0.47
Copolymer 13 : 87	55 000	0.44

This leads to the conclusion that copolymer flexibility decreases with decreasing molecular weight. Copolymers of all compositions with molecular weight ~ 30,000 fraction III), and polyacrylonitrile, consist of rigid molecular chains. These results agree with the findings of Flory [3] and Lang and Münster [4] that the second virial coefficient of osmotic pressure depends on the molecular weight of the polymer.

The temperature – osmotic pressure relationship was used to calculate the changes in the thermodynamic functions (free energy ΔF, enthalpy ΔH, and entropy ΔS); the results are given in Table 3.

The appreciable differences between the properties of the copolymers and the pure polymers can probably be explained if the dipole interactions of the CN and Cl groups are taken into account. Both polyvinyl chloride and polyacrylonitrile are polar polymers. The dipole moment of Cl^- (for example, in 1,3-dichloropropane) is $2.5 \cdot 10^{-18}$, and the dipole moment of nitrile group is $3.5 \cdot 10^{-18}$ In the case of copolymers a decrease of polymer polarity caused by intramolecular action between Cl and CN groups can probably be assumed. In fact, introduction of CN groups into the polyvinyl chloride molecule disturbs the regular arrangement of the chain segments, which favors easier coiling of the molecules into globules. If a Cl group is then found close to a nitrile group carbon, dipole attraction will prevail over repulsion.

In presence of such intramolecular saturation, the polarity of the molecules should decrease somewhat, and this should lead to increased polymer flexibility, decrease of intermolecular interaction, increased solubility, etc. Similar views on dipole interaction within molecular polymer chains were advanced earlier by Mikhailov [5].

This view is confirmed by studies of the properties of mixtures of pure polymers, in which fairly stable (CN – Cl) bonds are formed between the molecules, leading to considerable changes in the behavior of such mixtures in solution and in the solid state.

TABLE 3

Changes of the Thermodynamic Functions for Copolymers of Various Compositions (dimethylformamide solvent)

Copolymer	Fraction	Concentration in g/100 g solution	$\Delta F_1 \cdot 10^2$ cal./mole			$\Delta H_1 \cdot 10^2$ cal./mole		$\Delta S_{1\,exp} \cdot 10^5$ cal./mole		$\Delta S_{id} \cdot 10^5$ cal./mole
			293° K	308° K	323° K	300,5° K	315,5°K	300,5° K	315,0° K	
Copolymer 40 : 60	I	0.25	0.213	0.231	0.274	0.14	0.65	1.2	2.8	0.65
		0.45	0.394	0.428	0.496	0.27	0.95	2.3	4.5	1.20
		0.65	0.565	0.625	0.736	0.60	1.65	4.0	7.4	1.75
		0.85	0.907	0.981	1.113	0.54	1.73	2.3	11.2	2.30
	III	0.25	0.385	0.411	0.428	0.12	0.06	1.7	1.1	1.20
		0.45	0.702	0.753	0.796	0.30	0.13	3.4	2.8	2.16
		0.65	1.044	1.096	1.164	0.03	0.30	3.6	4.5	3.17
		0.85	1.370	1.438	1.506	—0.05	—0.03	4.5	4.5	4.55
Copolymer 29 : 71	I	0.25	0.231	0.240	0.257	0	0.10	0.6	1.1	0.69
		0.45	0.411	0.445	0.487	0.25	0.45	2.2	2.9	1.29
		0.65	0.605	0.659	0.727	0.45	0.56	3.6	3.9	1.70
		0.85	0.976	1.079	1.198	1,04	1.37	6.9	8.0	2.35
	III	0.25	0.342	0.368	0.394	0.17	0.17	1.7	2.3	1.10
		0.45	0.608	0.651	0.719	0.05	0.75	4.6	4.5	1.98
		0.65	0.873	0.913	1.027	—0.23	1.38	6.3	6.3	2.90
Copolymer 13 : 87	I	0.25	0.184	0.223	0.257	0.49	0.47	2.3	2.3	0.64
		0.45	0.351	0.411	0.462	0.82	0.64	4.0	3.4	1.20
		0.65	0.514	0.599	0.676	1.15	0.98	5.7	5.1	1.69
		0.85	—	0.907	1.027	—	1.56	—	8.0	2.25

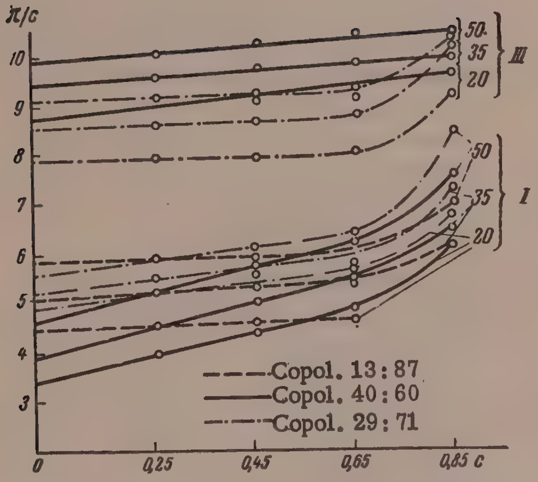

Fig. 5. Variation of reduced osmotic pressure with concentration; I) fraction I of all copolymers; III) fraction III of all copolymers.

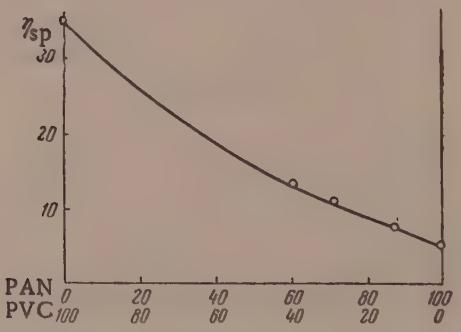

Fig. 6. Specific viscosity of 0.65 % solutions as a function of the composition (PAN = polyacrylonitrile, PVC = polyvinyl chloride).

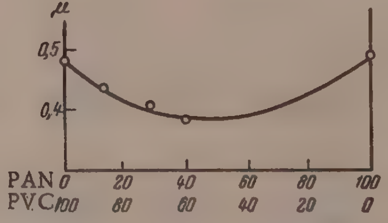

Fig. 7. Values of the constant μ as a function of the composition for polymers of similar molecular weight.

SUMMARY

1. The variation of the viscosity of vinyl chloride – acrylonitrile copolymers of various compositions with temperature has been studied in the range 20-60°; the specific and intrinsic viscosities of the copolymers in dimethylformamide have been determined.

2. The molecular weights of copolymer fractions have been determined at 20, 35, and 50° (by the osmotic method) and the changes in their thermodynamic functions have been calculated.

3. The view is put forward that the differences in the copolymer properties (increased solubility and molecular flexibility, decreased solution viscosity, change in the heat stability) are explained not only by the irregular structure of the copolymers, but also by intramolecular interaction between polar groups; in this instance, between chlorine and carbon of the nitrile groups.

All-Union Scientific Research Institute
for Artificial Fibers, Mytishchi

Received August 2, 1955

LITERATURE CITED

[1] Z. A. Rogovin, Chemistry and Technology of Artificial Fibers, State Light Industry Press (1952).

[2] N. V. Mikhailov and S. G. Zelikman, Colloid J., 18, No. 6, 717 (1956).

[3] P. Flory, J. Chem. Phys. 13, 453, (1945).

[4] X. Lang, A. Münster, Naturwissenschaft. 3, 68 (1946).

[5] G. P. Mikhailov, Progr. Chem., 24, No. 7, 875 (1955).

DISTRIBUTION OF A WEAK ELECTROLYTE IN THE DOUBLE LAYER

I. G. Ivanter

The existing theory of strong electrolytes [1] is based on the assumption that a self-consistent field may be used. * The distribution of positive and negative ions is therefore purely Boltzmann in character. It is natural to assume that the existence of a relationship between the dissociation constant and the field strength must influence this distribution in some way [2]. The derivation of this distribution must be based not on the existence of a self-consistent field, but on the general Gibbs method.

Debye and Hückel applied the idea of a self-consistent field [2] to calculating the deviations from ideality of the thermodynamic functions of dilute solutions of strong electrolytes. Fowler [3] derived the condition for the applicability of the self-consistent field to dilute neutral solutions of strong electrolytes. Kramers [4] calculated the statistical integral and found the deviations of the thermodynamic functions from ideality without using the self-consistent field concept. Although the self-consistent field method can be applied to neutral solutions only at very low concentrations, it has been used by various authors for calculations of interactions in the ionic double layer, where the ionic concentrations can by no means be regarded as low. In establishing the applicability of this method to ionic double layers, Frenkel [5] pointed out that the slow decrease of the field with distance (in proportion to 1/r) should result in small fluctuations, and thus make the use of the self-consistent field legitimate. However, at first sight Fowler's work appears to contradict this. Moreover, the view is widely held that the self-consistent field may be used up to concentrations at which the interaction between two particles is less than the thermal energy, i. e., until $e^2/r_{ij} \ll kT$.

It will be shown that Fowler's calculations are applicable only to neutral solutions, ** and that when repulsive forces are predominant the self-consistent field may in any case be used up to concentrations at which intermolecular forces begin to operate.

Application of the Fowler Method to Double Layers of Strong Electrolytes

Fowler considers the statistical integral (partition function)

$$B(T) = \int \dots \int e^{-U/kT} \, d\Gamma \; ^{***}$$

---

* The self-consistent field method is an approximate method in which the interaction energy between particles is replaced by the sum of the interaction energies of one particle with the others. The latter set up a force field with the property that the probability distribution of each particle in this field is $\sim e^{-e\varphi/kT}$ and with this density distribution the particles themselves create this field, which is termed self-consistent.

** Here and subsequently this refers to the electric charge and not acidity.

*** U is the potential energy of particle interactions as a function of their coordinates, the product of the differentials of which is expressed conventionally as dT^{1}.

and, if U contains long-range forces, he formally introduces the function W, defined by

$$Ce^{-W/kT} = \int \dots \int e^{-U/kT}\, d\Gamma'^{i}, \tag{1}$$

where the integral is not taken over the coordinates of the i-th particle.

In a double layer of strong electrolytes, in the absence of specific adsorption forces, U represents the interaction energy of the charged particles among themselves and with the external field

$$U = e^2 \sum_{ij} \frac{Z_j\, Z_i}{r_{ij}} + \sum_i eZ_i\varphi_0,$$

where φ_0 is the external field.

Differentiating Equation (1) with respect to x_i,

$$\frac{\partial W}{\partial x_i} \cdot Ce^{-\frac{W}{kT}} = \int \dots \int e^{-U/kT} \frac{\partial U}{\partial x_i}\, d\Gamma'_i$$

or

$$\frac{\partial W}{\partial x_i} \cdot Ce^{-W/kT} = \frac{\partial W}{\partial x_i} \int \dots \int e^{-U/kT}\, d\Gamma'_i = \int \dots \int e^{-U/kT} \frac{\partial U}{\partial x_i}\, d\Gamma'_i. \tag{2}$$

Fowler [3] points out that W in Equation (2) can be interpreted as the average energy of the i-th particle.

After differentiating again, performing the same operations with respect to y_i and z_i, and adding the three equations, we have:

$$\left[\Delta W - \frac{1}{kT} \sum_{\alpha=1}^{3} \left(\frac{\partial W}{\partial x_{i_\alpha}}\right)^2\right] \cdot \int \dots \int e^{-U/kT}\, d\Gamma^{i'} =$$
$$= \int \dots \int e^{-U/kT} \left[\Delta_i U - \frac{1}{kT} \sum_{\alpha-1}^{3} \left(\frac{\partial U}{\partial x_{i_\alpha}}\right)^2\right] d\Gamma^{i'}. \tag{3}$$

Fowler notes that the electrostatic energy U_i always satisfies Laplace's equation

$$\Delta_i U_i = -\frac{4\pi\rho e_i}{D},$$

and therefore

$$\Delta W + \frac{4\pi\bar{\rho} e_i}{D} = \frac{1}{kT} \sum_{\alpha=1}^{3} \left[\left(\frac{\partial W}{\partial x_{i_\alpha}}\right)^2 - \overline{\left(\frac{\partial U}{\partial x_{i_\alpha}}\right)^2} \right], \tag{3a}$$

from which we can find the root mean square deviation of the force acting on the i-th particle.

In evaluating the applicability of the Debye–Hückel theory, Fowler assumed that the deviations will be small if $\frac{\partial W}{\partial x_i}$ is mainly determined by a constant field which does not depend on the particle distribution. However, this evaluation cannot be applied to a charged electrolyte. As will be shown, the field formed by the particles distributed in it is stable in a number of cases. This is because the root mean square deviation of the derivative of the energy from its mean value will be much less than the mean value itself, if it is possible to divide the region of the double layer into a large number of layers, in each of which the difference between the space-average of the density at any time and its time-average is much less than the latter. A more exact evaluation may be obtained directly from Equations (3) and (3a).

For simplicity, we consider the one-dimensional case:

$$\left[\left(\frac{\partial W}{\partial x_i}\right)^2 - \overline{\left(\frac{\partial U}{\partial x_i}\right)^2} \right] = \overline{\left[\frac{\partial W}{\partial x_i} - \frac{\partial U}{\partial x_i} \right]^2} = e^4 \overline{\left[\int_0^x \{\bar{f}(\xi) - f(\xi)\}\, d\xi \right]^2}. \tag{4}$$

But, since the greatest density deviations occur when the deviations are independent and the numbers of particles are not related in a way such that an increase of their number in one region results in a decrease in another, we have

$$\int_0^x [\bar{f}(\xi) - f(\xi)]\, d\xi = \int_0^{\Delta x} [\bar{f}(\xi) - f(\xi)]\, d\xi = [\bar{f}(\xi^*) - f(\xi^{*\prime})]\, \Delta x \tag{4a}$$

ξ^* and $\xi^{*\prime}$ lie between 0 and Δx. It is assumed that the greatest deviations exist in the neighborhood of 0; here Δx is a layer for which it is still permissible to introduce an average density.

However, for the particle density we have, according to Equation (4), $\overline{(f - f)^2} = \frac{\bar{f}}{d\Gamma}$ and hence

$$\overline{[\bar{f}(\xi^*) - f(\xi^{*\prime})]^2 (\Delta x)^2} = \frac{\bar{f}(\Delta x)^2}{d\Gamma}. \tag{4b}$$

Here $\bar{f}$ is normalized to the density in the volume d Γ. Substitution of Equation (4b) into Equation (4) gives

$$\left[\left(\frac{\partial W}{\partial x}\right)^2 - \left(\frac{\partial U}{\partial x}\right)^2\right] = \frac{e^4\,\bar{f}\,(\Delta x)^2}{d\Gamma}\,.$$

By comparing the terms in Equation (3a), we can formulate the condition:

$$\bar{f}e^2 4\pi \,/\, D \gg \bar{f}e^4\,(\Delta x)^2 \,/\, d\Gamma kT$$

or

$$1 \gg De^2\,(\Delta x)^2 \,/\, 4\pi\, d\Gamma\, kT. \tag{5}$$

However, to satisfy Equation (4a) it is necessary that f (ξ *) differ little from (ξ *'), otherwise it is necessary to consider large values of Δx, i. e., Δx may be decreased so long as the deviations of the density from the mean are small. In other words, the approximation in question becomes increasingly valid if we can increase the number of parts into which we can divide the whole space interval over which the potential changes; these parts must however, be such that in each one the deviation of the particle density is small,

i. e., $\sqrt{(\bar{f} - f)^2} \ll \bar{f}$

We shall use the Boltzmann distribution for the evaluation; f (ξ *') and f (ξ*) should not differ greatly. Primes denote average values at a given interval. We require that

$$f\,(\xi^*) - f\,(\xi^{*\prime}) = B\,(e^{-e\varphi^*/kT} - e^{-e\varphi^{*\prime}/kT}) \ll Be^{-\varphi^* e/kT}$$

or

$$1 - e^{-(\varphi^{*\prime}-\varphi^*)/kT} \ll 1,\ \text{i. e.,}\ \ \varphi^* - \varphi^{*\prime} \ll \frac{kT}{e}\,. \tag{6}$$

On the other hand, it is also necessary that

$$\overline{f\,(\xi)^2} \gg \overline{[f\,(\xi) - \overline{f\,(\xi)}]^2} \doteq \frac{\bar{f}\,(\xi)}{d\Gamma} \doteq \frac{\bar{f}\,(\xi)}{\Delta x\,\Delta y\,\Delta z} = \frac{\bar{f}\,(\xi)\,\varphi_x'}{\Delta y\,\Delta z\,\Delta\varphi} = \frac{\bar{f}\,(\xi)\cdot\varphi_x'}{\Delta y\,\Delta z\,pkT/e}\,. \tag{7}$$

But, from the first integral of the Laplace – Boltzmann equation we have:

$$\varphi'_x \sim (\sqrt{AcK}\, kT)^{1/2} \cdot e^{-\varphi e/2kT}; \tag{8}$$

the number of particles is

$$dn = \sqrt{cKA}\, e^{-\varphi e/kT}\, dx\, dy\, dz \tag{8a}$$

where $\sqrt{cKA}$ is the density in the volume. Substituting the values of the densities $f(\xi) = Be^{-\varphi e/kT}$ and $f(\xi') = Be^{-\varphi' e/kT}$ into Equation (7), taking into account (8) and (8a), we have

$$e / \sqrt{kT}\, p\Delta y\Delta z \ll (cKA)^{\frac{1}{4}} \cdot e^{-\varphi e/2kT}, \tag{9}$$

where $1/p$ is the number of subdivisions. Condition (9) is satisfied even for very small values of p.

$$p_{\text{lim}} = \frac{e \exp(\varphi e / 2kT)}{\sqrt{kT}\, \Delta y\, \Delta z_{,} (cKA)^{1/4}};$$

$$\Delta x_{\text{lim}} = \frac{pkT}{e\varphi'_x} = \frac{1}{\Delta y\, \Delta z.}\, \frac{1}{f(\xi)} = \frac{1}{\Delta y\, \Delta z}\, \frac{1}{\sqrt{cKA}}\, e^{-\varphi e/kT}; \tag{10}$$

where A is Avogadro's number; K is the dissociation constant. Thus by the set of Equations (6) and (10) we have shown that application of an average self-consistent field to strong electrolytes is quite legitimate for double layers of sufficient extent. This has been demonstrated here for a plane double layer, but it must be pointed out that the proof may be extended to cases involving several variables with the condition that sufficiently large electrodes are considered. It must be pointed out that fluctuations decrease with increasing ion concentration in the double layer. The above considerations, however, do not apply if it is not possible to select a macroscopic volume $d\Gamma$, or exact $\Delta y\Delta z$, which is the case for neutral solutions, for which Fowler's reasoning is valid.

Distribution of a Weak Electrolyte in the Double Layer

As for strong electrolytes, we consider the statistical integral

$$B(T) = \int \ldots \int e^{-U/kT}\, d\Gamma. \tag{11}$$

Since the dissociation energy plays an important role in consideration of weak electrolytes, we introduce intramolecular energy and forces into our reasoning. The average values of these forces may depend on the surrounding medium.

We shall consider ions only, and a distinction is made between their situation within and outside the molecular volume. The energy of the system will be given by the sum of the energies of all the ions. We first consider a binary 1:1 electrolyte. The energy U of the whole system is

$$U = \sum_{ij} \left\{ \left[Z_i \frac{e^2 Z_j}{D r_{ij}} + e Z_i \varphi_0 \right] (1 - \bar{\delta}_{r_{ij}}) + W_{\text{mol}} \bar{\delta}_{r_{ij}}, \right.$$

where $\bar{\delta}_{r_{ik}} = 1$, if $Z_k = Z_i$, r_{ik} within the molecular volume,

$x\bar{\delta} r_{ik} = 0$, if $Z_k = Z_i$,

$\delta_{r_{ik}} = 0$, is outside the molecular volume.

A function of this type was used by Kramers [4] for calculation of deviations of thermodynamic functions from ideality; this was required in order to make the integral convergent.

We first determine the probability (P_{lm}) of the l-th positive ion forming a molecule with the m-th negative ion. This is the same as finding the probability of the l-th positive ion being in the volume of the m-th negative ion, and we must integrate along the coordinate of the m-th negative ion

$$P_{lm} = \frac{1}{B(T)} \int dV_m \int d\Gamma''^{ml} \left(\exp \left[\frac{1}{kT} \sum_{ij}^{ml} \ldots \right] \right) \int e^{-1/kT} W_{\text{mol}\, lm} \, dV_l .$$

The integration with respect to $d\Gamma''$ is performed for all the volumes except the molecular volume of the m-th ion, and with respect to dV_l, for the molecular volume of the m-th ion. The sum of the probabilities that all the particles will be in the molecular state or, after appropriate rearrangement, the average number of molecules at the point $\vec{r}$ is given by

$$N_{\text{mol}(\vec{r})} = \frac{N_0 d\vec{r}}{B(T)} \int d\Gamma''^{ml} \, (iden) \int\limits_{\substack{\text{molecular volume} \\ \text{around } \vec{r}}} e^{-1/kT} W_{\text{mol}\, lm} \, dV_l , \tag{12}$$

where the integration is performed as stated above; N_0 is the total number of molecules.

The probability of the i-th ion being in the unbound state is:

$$P_i = \frac{1}{B(t)} \int dV_i \int \exp \left\{ -\frac{1}{kT} \left[\sum_{qs} \left(\frac{Z_q Z_s}{D r_{qs}} + e r_q \varphi_0 \right) (1 - \bar{\delta}_{r_{qs}}) + W_{\text{mol}} \bar{\delta}_{r_{qs}} \right] d\Gamma'^i . \right. \tag{13}$$

Correspondingly, the average number of ions around a certain point $\vec{r}$ will be obtained if in Equation (13) integration over the whole volume of the i-th ion is replaced by integration around a fixed point only, followed by multiplication by the total number of ions.

As was done by Fowler, we formally introduce the function ω_{mol}, defined by the following equation:

$$Ce^{-\omega_{mol}/kT} =$$

$$= \int \ldots d\Gamma''^{ij} e^{-\sum_{kn}^{''ij} (W_{kn\,electr} + W_k + W_{kn\,mol})} \int_{\text{around } \vec{r}_j} e^{-W_{ij\,mol}/kT} dV_i .$$

It is easily shown by differentiation that ω_{mol}. is the average energy. It must be noted that the average value with respect to the inner integral is the most important $W_{kn_{mol}}$ represents the sum of the energies of interaction between the k-th and n-th particles and between each of these and each of the others, with the condition that they are all in direct proximity. In some important cases it is possible to neglect, in this sum, the terms which represent interaction with molecules.

We apply the term average intramolecular energy $\tilde{\omega}_{ij\,mol}$

$$\tilde{\omega}_{ij\,mol} = \int_{\text{around } \vec{r}_j} W_{ij\,mol} \exp\left[-W_{ij\,mol}/kT\, dV_i\right].$$

Here $\tilde{\omega}_{ij\,mol}$ will depend on the coordinates of all the other particles. We shall assume, since this interaction is of a purely statistical nature, that it may be reduced to interaction with a certain average field. This field will be mainly determined by the ion distribution; the influence of molecular distribution will be slight, and therefore the estimates of the fluctuations given previously should be of the same order of magnitude as before. Introduction of this average field is therefore permissible. It must be pointed out, however, that the field will not be self-consistent in the sense of satisfying the Laplace – Boltzmann equation, as molecules will also influence this field.

Consequently, if fluctuations are not taken into account, $\tilde{\omega}_{mol}$ may be regarded as function of the strength of an average field (the strength because the molecular dimensions are small in comparison with the thickness of the double layer). In other words, interaction of the dipole type is taken into consideration, and hence

$$\tilde{\omega}_{mol} = \tilde{\omega}_{ij\,mol}[\vec{F}(\vec{r}_j)].$$

We determine the ion distribution by means of perturbation theory, assuming as a first approximation that the energy of interaction of ions with molecules is much less than the energy of interaction with ions. Then after suitable rearrangement, we may remove $-\frac{1}{kT}\sum_{ks} W_{mol\,ks}\,\tilde{\delta}_{ks}$ in Eq. (13), but this gives an expression coinciding with the probability for strong electrolytes, and therefore we have $n_{\pm} = n_0 K_{\infty} e^{\pm e\varphi/kT}$. On the other hand, $n^+ n^- = Kn_{mol}$ by definition of the dissociation constant. The possibility that the latter may depend on the field strength (according to Onsager [2]) must be taken into account, but

$$n^+n^- = K_{\text{to}\,\infty}\, n_{\text{mol to}\infty}\,, \tag{14}$$

$$\frac{K(\infty)}{K(x)} = \frac{n_{\text{mol}}(x)}{n_{\text{mol}}(\infty)}\,. \tag{15}$$

On the other hand, we have from Equation (3)

$$\frac{n_{\text{mol}}(x)}{n_{\text{mol}}(\infty)} = e^{[-\omega_{\text{mol}}(x)+\omega_{\text{mol}}(\infty)]\,/\,kT}, \tag{16}$$

and hence

$$\ln\{K(x)\,/\,K(\infty)\} = \frac{\omega_{\text{mol}}(x) - \omega_{\text{mol}}(\infty)}{kT} \tag{17}$$

or

$$\Delta \ln K(x) = \Delta\omega_{\text{mol}}(x)\,/\,kT\,. \tag{18}$$

This last expression is a generalization of a well known thermodynamical expression of the case when K depends on the field. In order to obtain the second approximation and an equation for the electrostatic field, we assume that

$$\tilde{\omega}_{\text{mol}ij} = kTK(x_j)\,\overline{\delta}_{r_{ij}}. \tag{19}$$

This is equivalent to replacing the electrostatic forces by their average field in their action on a molecule.

To find the distribution of the ions, we again use Fowler's theory:

$$Ce^{-W/kT} = \int d\Gamma' e^{-U/kT}, \tag{20}$$

where W is the average interaction with all the molecules and ions (as may be shown by differentiation of the integral), as in [3]. Differentiation with respect to x_i gives for the derivative of the total energy

$$\frac{\partial W}{\partial x_i} - \frac{\partial \overline{W}_{\text{ion}}}{\partial x_i} = \frac{\partial}{\partial x_i} \sum_{kn} \overline{\omega}_{kn} (Exn). \tag{21}$$

We note that averaging $\frac{\partial}{\partial x_i} \sum_{kn} \tilde{\omega}_{kn}$ has given the last term of Equation (21); it may be written in the form $\frac{\partial}{\partial x_i} = \epsilon_{\text{mol}}$;

$$\epsilon_{\text{mol}} = \int \tilde{\omega}(x)\, n_{\text{mol}}(x)\, dV, \tag{22}$$

where ϵ_{mol} is the total energy of all the molecules or, introducing the average electrostatic field,

$$\epsilon_{\text{mol}} = \int \tilde{\omega}(\varphi'_{(x)})\, n_{\text{mol}}(\varphi'_{(x)})\, dV, \tag{23}$$

and hence

$$\frac{\sigma}{\partial x_i} \epsilon_{\text{mol}} = \int \frac{\partial \tilde{\omega} n}{\partial \psi'(x)} \frac{\partial \psi'(x)}{\partial x_i} dV. \tag{24}$$

Equation (24) may, as a first approximation, be written as

$$\int f(x) \frac{\partial \psi'(x)}{\partial x_i} dV \rightarrow \int f_1(x)\, dx \cdot q,$$

where q is the charge of one particle.

Thus, integration with respect to x gives the average value of the expression

$$\frac{\partial(\tilde{\omega} n)}{\partial \psi'(x, x_i)} \cdot q.$$

By its physical meaning this must be the derivative of the total energy of interaction of the i-th ion with the molecules.

Let us now calculate directly the energy of interaction of the i-th ion with the molecules. Suppose that the i-th ion is introduced at some point of the space. Suppose that before this a field ψ' was given in all space; then the total energy of the molecules was

$$\varepsilon_{\text{mol}} = \int \tilde{\omega}(\psi')\, n_{\text{mol}}(\psi')\, dV. \tag{25}$$

After introduction of the i-th ion at the point (x_i, y_i, z_i), the field was changed, and the energy of the system becomes:

$$\varepsilon^{*}_{\text{mol}} = \int \tilde{\omega}(\psi' + \psi_i')\, n_{\text{mol}}(\psi' + \psi_i')\, dV.$$

The difference between these two energies is the required energy of interaction

$$\varepsilon^{*}_{\text{mol}} - \varepsilon_{\text{mol}} = \int [\tilde{\omega}(\psi' + \psi_i')\, n_{\text{mol}}(\psi' + \psi_i') - \tilde{\omega}(\psi')\, n_{\text{mol}}(\psi')]\, dV. \tag{26}$$

If ψ_i' is small relative to the whole field, the expression under the integral may be replaced by $\frac{\partial(\tilde{\omega}n)\,\psi_i'}{\partial\psi'}$

Here the expression $\frac{\partial(\tilde{\omega}n)}{\partial\psi'}$ does not depend on the i-coordinate, i. e., Equations (24) and (26) are in agreement.

Consequently, the total energy given in Equation (20) is

$$W = W_{\text{ion}} + \int \frac{\partial(\tilde{\omega}n)}{\partial\psi'}\, \psi_i'\, dV. \tag{27}$$

Introducing the average field concept, we obtain Laplace's equation

$$\Delta_i \psi = -\frac{4\pi}{D}\rho,$$

where ρ is taken to be the density of the ions only. The dipole correction is taken into account only in Equation (28). For the densities of the ions we have:

$$n \pm \sim e^{\pm\frac{\psi z e}{kT}}\, e^{\pm\frac{1}{kT}\int \frac{\partial(\tilde{\omega}n)}{\partial\psi'}\,\psi'_{ki}\, dV}. \tag{28}$$

Returning to Equations (14) and (15), we have the condition that Equation (28) must not contradict Equation (15). There will be no contradiction if the factor is small or if it vanishes (the corrections for (−) and (+) ions balance out). However, it will vanish only if the distribution itself does not depend on the sign of the charge.

In considering the range of applicability of the above theory it is first necessary to note that introduction of an average field strength is permissible only if the influence of the field set up by the nearest ion is considerably less than the influence of the total field at the point under consideration. This can only be the case if the charge distribution is fairly continuous. The sign of the charge of the ion is immaterial if charges of one sign predominate over charges of the other sign (this is due to the fact that the field of a plane is finite, and that of a point is infinite at the point).

The following is the condition for the applicability of the theory: the interaction of one ion with all the molecules must be much less than the interaction of all the ions with one molecule, as only then are the approximations (16), (18), and (28) valid.

The first interaction is of the order

$$\frac{\int W(x)\, n(x)\, dx}{\int n_{\text{ion}}(x)\, dx} \sim \frac{\overline{W} n_{\text{mol}}}{n_{\text{ion}}}, \tag{29}$$

where $\overline{W}$ is the total energy of interaction of the molecules with the ions. It is therefore sufficient that $\frac{n_{\text{mol}}}{n_{\text{ion}}} \ll 1$.* (The concentrations refer to the double layer region. Therefore our equations can always be applied at sufficiently high potentials. However, we are concerned not with abstract values of n, but with those corresponding to the limiting concentrations: $n_{\infty} \ll 1/V_m$, where V_m is the volume of a gram-molecule. For these conditions we may use the results of the theory of double layers of strong electrolytes, and substitute the appropriate expression into Equation (15). Integration over the whole depth of the layer gives the total negative adsorption (desorption). However, this value is not of as much interest as it might appear, as it is small in comparison with the positive adsorption of ions, and its influence on surface tension will be slight. Nevertheless, such negative adsorption may be significant in reactions at electrodes, as neither molecules themselves nor definite parts of them may be found at one of the electrodes (for example, if we are dealing with organic acids, neither the undissociated acid nor its negative ions will be found at one of the electrodes). Possibly this may be related to some forms of catalysis.

We write in explicit form the relationship between concentration and potential

$$n = n_{\infty}/F \tag{30}$$

where F is the Onsager function [2]

$$F = 1 + \bar{b} + \sum_{k=r}^{\infty} \frac{(2\bar{b})^k}{k!\,(k+1)!}\text{, where } \bar{b} = \frac{\psi' e^3}{2Dk^2 T^2}; \tag{30a}$$

---

* It would be formally possible to use a method analogous to (16-28) to consider the reverse case $n_{\text{mol}}/n_{\text{ion}} \gg 1$ thus obtaining the change of the ion distribution, but in view of the necessity pointed out above, for the space charge to be fairly continuous, this cannot be done. This is because replacement of the dipole (ionic—molecular) interaction by an interaction with an average field is inadmissible, because of the prevailing role of fluctuations. In particular, the form of the formula for the capacity is quite obscure in this case.

it is known from the theory of the double layer [1] that

$$\psi' = (\sqrt{n_\infty K_\infty A})^{1/2} e^{\left| \frac{e\varphi}{kT} \right|} \qquad \cancel{(30b)}$$

(if the influence of ions of the opposite sign is ignored; this is necessary, as our theory is not applicable to the region in which this cannot be done).

A second result of the theory is that, at sufficiently high potentials, the theory derived for strong electrolytes is applicable to double layers of weak electrolytes. It must be emphasized that we have throughout considered the case of a double layer in absence of appreciable amounts of strong electrolytes. In conclusion, we must draw attention to the close connection between the change in the energy of molecules along the thickness of the double layer, if the dissociation constant depends on the field (and therefore on the coordinate), and the Onsager principle of microscopic equilibrium.

In fact, it can be shown that equilibrium can be established by a noncyclic process, with a dissociation constant which varies along the thickness of the double layer, only under the condition that the activity coefficient also varies with the coordinate. In the present instance this is equivalent to the molecule-field interaction varying with the coordinate, and it also indicates that this interaction is not small relative to kT.

SUMMARY

1. Electric field strength fluctuations in the double layer at electrodes of sufficiently large size are small, and introduction of the average field is permissible. Conditions are derived for which deviations of the field strength from the average value are small.

2. In the double layer region, where the number of molecules is much less than the number of ions (in practice, for dilute solutions, throughout the double layer if the potential differences are not too small), it is permissible to apply all the consequences of the double layer theory of strong electrolytes, including those relating to capacity, if the values of the concentration and the dissociation constant in the depth of the solution are taken.

3. It is shown that the distribution of neutral molecules varies in inverse proportion to the dissociation constant. The relationship between the distribution and the field has been derived in explicit form for cases to which Onsager's theory of dissociation of weak electrolytes is applicable.

4. Decrease of the number of neutral molecules at the electrode surface may be of importance in the occurrence of chemical and electrochemical reactions at the electrode surfaces.

I express my gratitude to Prof. V. G. Levich for proposing the problem and for criticism of the first version of the paper, and to Academicians M. A. Leontovich, V. I. Kogan, and I. Z. Fisher for their interest, discussions, and valuable advice.

The Minsk Tractor Works Mechanical Laboratory,
Central Factory Laboratory

Received December 15, 1955

LITERATURE CITED

[1] A. N. Frumkin et al., Kinetics of Electrode Reactions, Moscow (1952).

[2] H. Harned and B. Owen, Physical Chemistry of Electrolytic Solutions, Foreign Lit. Press, Moscow (1952).

[3] R. H. Fowler, Proc. Cambridge Philos. Soc. 22, 861, 1925; Statistical mechanics, 1929 (cited through B. Falkenhagen, Electrolytes, United Sci.-Tech. Press, Theoret. Chem., 1935).

[4] H. A. Kramers, Proc. Royal Acad. Sci. Amsterdam 30, 145, 1927 (in Russian in V. K. Semenchenko, Physical Theory of Solutions, ONTI, Moscow-Leningrad (1941).

[5] I. Ya. Frenkel, Statistical Physics, Moscow – Leningrad (1948).

COMPATIBILITY OF NITROCELLULOSE WITH BUTADIENE–ACRYLONITRILE COPOLYMERS

3. DEPENDENCE OF THE GLASS TRANSITION TEMPERATURE AND FLOW OF NITROCELLULOSE FILMS ON THEIR CONTENTS OF VARIOUS BUTADIENE–ACRYLONITRILE COPOLYMERS

L. E. Kalinina, V. I. Alekseenko, and S. S. Voyutsky

Studies of the changes of deformation of polymer mixtures in relation to the component ratios and temperature extend our knowledge of the compatibility of polymers and of the plasticization of rigid polymers by high-molecular softeners. Moreover, determination of the effects of butadiene – acrylonitrile copolymers on the transition temperatures of nitrocellulose is important from the practical standpoint, as it provides information on the behavior of such systems in use under various temperature conditions.

The studies were performed on films made from solutions of nitrocellulose and butadiene – acrylonitrile copolymers with the following acrylonitrile group contents:

Copolymers	1	2	3	4
Acrylonitrile group contents, %	18.4	28.6	37.7	44.4

The preparation of the films is described in one of our previous communications [1].

The deformability of the films over a wide temperature range was determined by means of V. A. Kargin's modified dynamometric balance, in which the specimens were subjected to periodic extension at a gradually increasing temperature. The temperature was raised uniformly during the tests, by approximately 2° per minute. The deformation of the specimens was measured at 5-10° intervals; the load was 15 kg/cm^2. The specimens were always of standard size. The width of each specimen was 5 mm, and the length of the working section was 20 mm. The deformation was always read off 3 seconds after application of the load.

Figure 1 shows the thermomechanical curves obtained, which represent variations of extension deformation with temperature under constant load for nitrocellulose films containing various amounts of different butadiene–acrylonitrile copolymers.

It follows from Fig. 1, which refers to experiments with copolymer 1, that the relative extension of nitrocellulose itself is very small, and increases very little with temperature. Additions of from 20 to 60% of the weakly polar copolymer 1 produce relatively slight increases of deformation. With higher contents of copolymer 1 in the films the deformation – temperature curve is shifted in the direction of lower temperatures. The sharp inflections in the curves for films with high contents of copolymer 1 indicate that in this case there is a direct transition from the glassy to the viscofluid state with increase of temperature, at temperatures below zero. The absence of regions corresponding to a state of high elasticity on the curves can be taken as indicating mutual insolubility of the two components, and therefore inability of copolymer 1 to elasticize nitrocellulose. The system is evidently heterogeneous at all the component ratios studied, and probably consists of microvolumes of one phase dispersed in the other, the mechanical properties of the film being, of course, determined mainly by the properties of the external phase. From this viewpoint, the different deformations of films with low and high contents of butadiene – acrylonitrile copolymer must be attributed to the fact that in the first case the external phase is nitrocellulose (or, more accurately, a dilute solution of butadiene – acrylonitrile copolymer in nitrocellulose) and in the second, butadiene – acrylonitrile copolymer (or, more

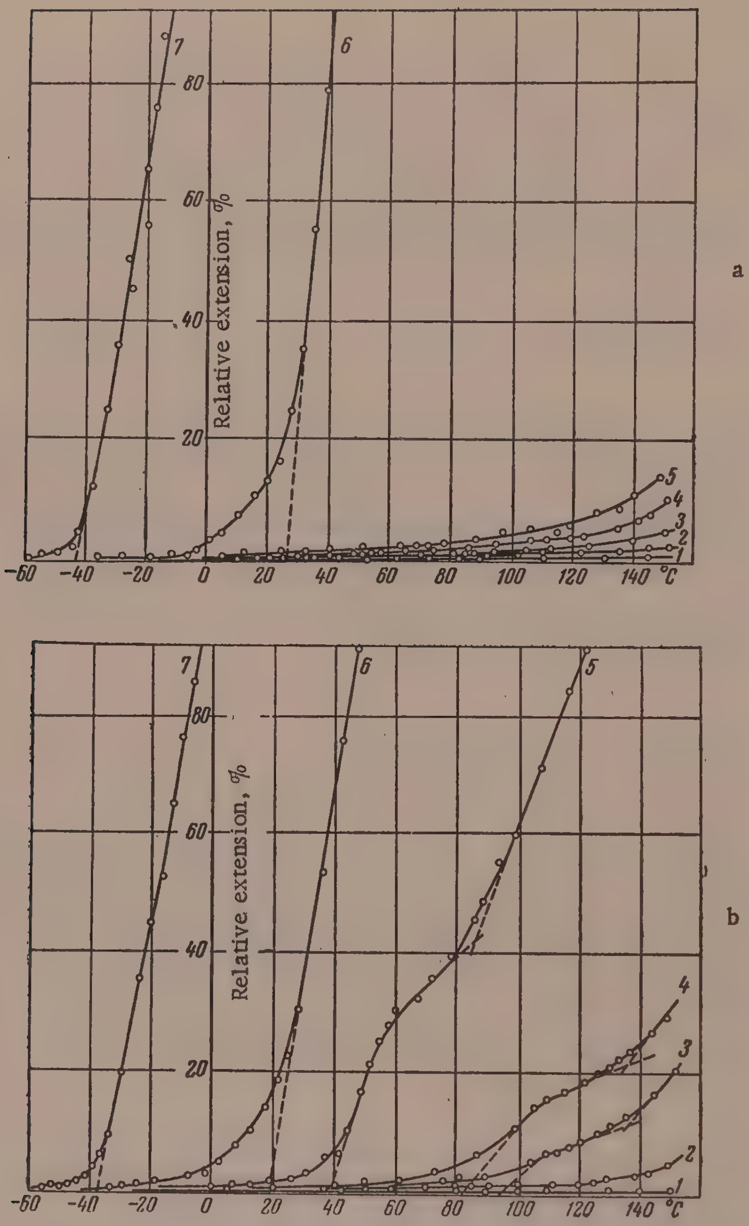

Figs. 1,a and 1,b. Effect of temperature on the deformation of nitrocellulose films with different contents of butadiene—acrylontrile copolymers: a) copolymer 1, b) copolymer 2; 1) nitrocellulose film; 2) ditto, with 20% copolymer; 3) ditto, with 40%; 4) ditto, with 50%; 5) ditto, with 60%; 6) ditto, with 80%; 7) film of copolymer 1 only.

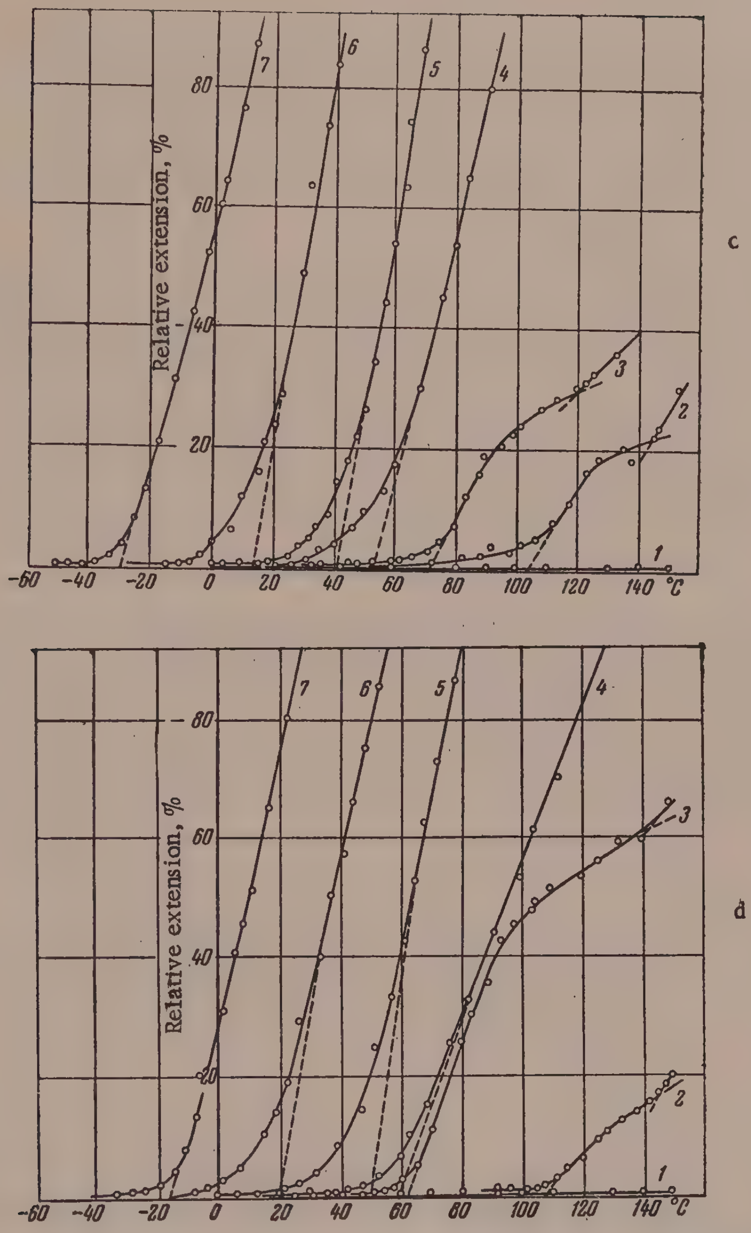

Figs. 1,c and 1,d. Effect of temperature on the deformation of nitrocellulose films with different contents of butadiene–acrylonitrile copolymers: c) copolymer 3; d) copolymer 4); 1) nitrocellulose film; 2) ditto, with 20% copolymer; 3) ditto, with 40%; 4) ditto, with 50%; 5) ditto, with 60%; 6) ditto, with 80%; 7) film of copolymer 1 only.

accurately, a dilute solution of nitrocellulose in butadiene – acrylonitrile copolymer). Phase inversion occurs, to judge by the positions of the curves in Fig. 1, when the system contains 60-80% butadiene– acrylonitrile copolymer.

The situation is somewhat different for films containing the more polar copolymer 2. As Fig. 1, b shows, the thermomechanical curves for films with fairly high contents (40-60%) of this copolymer have inflections characteristic of high-elastic materials. This indicates that the butadiene – acrylonitrile copolymer 2 can elasticize nitrocellulose, and is therefore compatible with it. At very high contents of copolymer 2 the inflexions on the curves degenerate – with increase of temperature the material passes directly from the glassy into the viscofluid state. It is likely that intermolecular forces are weakened to a greater extent than intramolecular by the introduction of large amounts of the copolymer. It is significant that in the case of nitrocellulose films containing various amounts of copolymer 2 the thermomechanical curves are arranged much more uniformly on the diagram. This indicates that phase inversion does not occur in the system with increase of copolymer 2 content, as is the case in mixtures of nitrocellulose and copolymer 1. It also confirms that the two components are compatible.

The thermomechanical curves for films containing copolymers 3 and 4 are also situated uniformly on the diagram, and are, in general, similar to the curves discussed above. However, a comparison of the curves in Figs. 1, c and 1, b shows that copolymer 3 has a greater effect than copolymer 2 on the displacement of the transition temperatures of the mixtures from one state into the other, into the lower temperature region. Moreover, the curve for the mixture of 80% nitrocellulose and 20% copolymer 3 is already clearly S-shaped. This indicates that copolymer 3 lowers the energy level of the potential barrier of rigid molecules; i. e., that it has a stronger elasticizing effect than copolymer 2 on nitrocellulose. However, degeneration of the curve (disappearance of the region corresponding to a state of high elasticity) occurs in this case at a lower content of the copolymer. The curves for films containing copolymer 4 indicate considerably greater extensions in the temperature range of high elasticity, as Fig. 1, d clearly shows.

The deformation – temperature relationships shown in Fig. 1 can be readily used to determine glass transition temperatures T_g, flow temperatures T_f, and differences between these values $T_g - T_f$ for mixtures containing different butadiene – acrylonitrile copolymers and nitrocellulose in various proportions. The graphical method often used for this purpose [2, 3] was applied. The glass transition temperature was taken to be the temperature corresponding to the intersection of the abscissa axis with extension of the linear portion of the curve in the region of transition from the glassy into the high-elastic or viscofluid states. The flow temperature was taken to be the temperature corresponding to the intersection of the extensions of the linear portions of the curves in the high-elastic region and at the beginning of the viscofluid region.

The results are given in the table following. It must be pointed out that T_g and T_f could not be determined for mixtures containing up to 60% butadiene – acrylonitrile copolymer 1, since the inflections on the curves for such mixtures lie above the temperatures investigated. Moreover it should be noted that the values found for T_g and T_f are extremely conventional, as they depend on the methods used for their determination [4, 5].

As the table shows, the maximum difference between T_f and T_g, which represents the temperature range of the high-elastic state, increases with increasing acrylonitrile group content in the copolymers. This indicates that the elasticizing action increases with increasing polarity of the butadiene – acrylonitrile copolymer. Since the rigidity of a high-molecular plasticizer usually increases with polarity, the only explanation of this effect is that the compatibility of nitrocellulose with the copolymer increases with rising acrylonitrile group content.

It also follows from the table that, for butadiene – acrylonitrile copolymers compatible with nitrocellulose, increase of polarity leads to a decrease of the amount required for elasticization. For example, in the case of copolymer 2 an elasticizing effect is found only with 50-60% of the copolymer. In the case of copolymer 4, an elasticizing effect occurs with 20-40% of the copolymer. With higher contents of this strongly polar copolymer the system passes directly from the glassy into the viscofluid state with increase of temperature. This also can only be explained by the better compatibility of strongly polar copolymers with nitrocellulose.

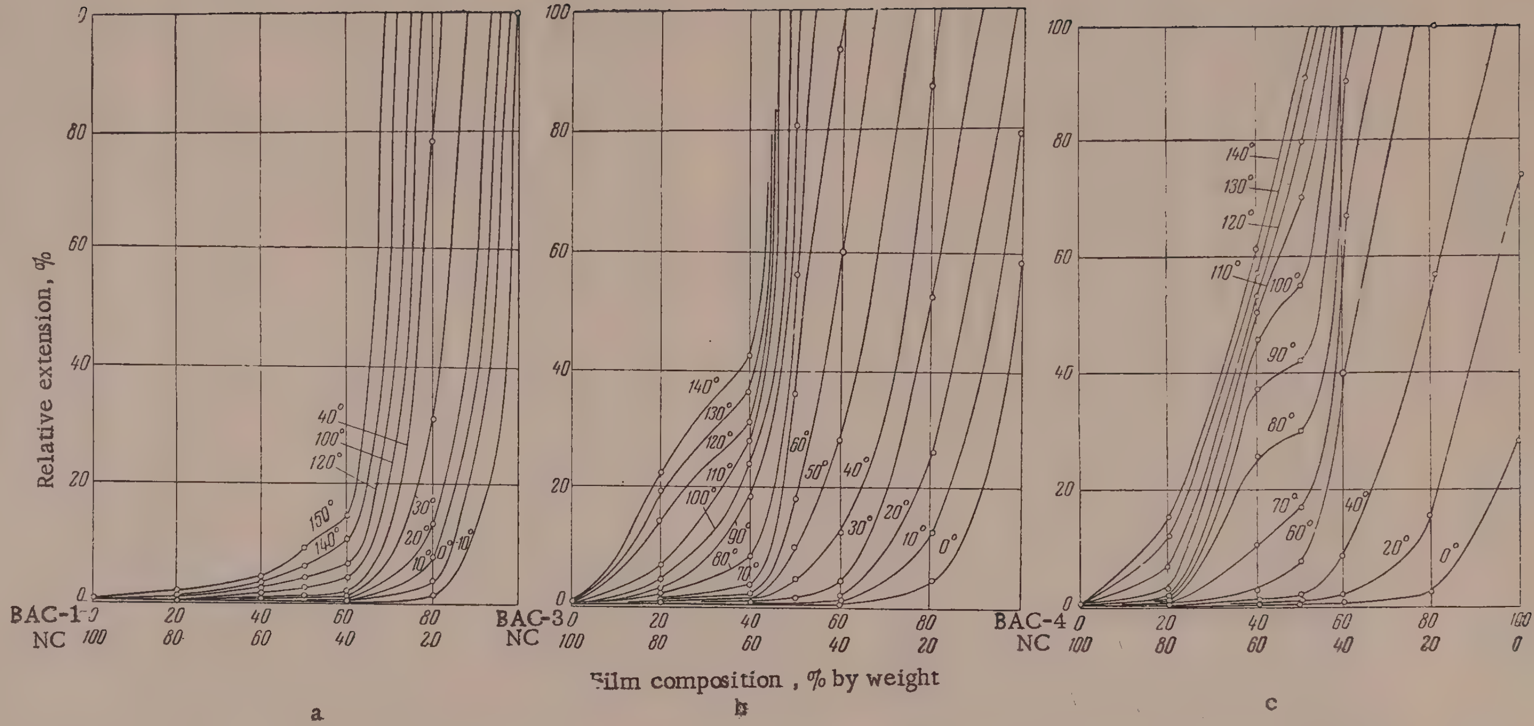

Fig. 2. Dependence of deformation on the contents of butadiene – acrylonitrile copolymers (BAC) in nitrocellulose (NC) films: a) copolymer 1; b) copolymer 3; c) copolymer 4.

TABLE

Glass Transition Temperatures T_g, Flow Temperatures T_f, and Differences $T_f - T_g$ for Nitrocellulose Films with Different contents of Butadiene – Acrylonitrile Copolymers

Copolymer contents, wt. %	Copolymer 1			Copolymer 2			Copolymer 3			Copolymer 4		
	T_g	T_f	$T_f - T_g$	T_g	T_f	$T_f - T_g$	T_g	T_f	$T_f - T_g$	T_g	T_f	$T_f - T_g$
20	—	—	—	—	—	—	104	145	41	104	144	40
40	—	—	—	93	139	46	61	123	62	62	142	80
50	—	—	—	82	138	56	52	52	0	58	58	0
60	—	—	—	37	87	50	45	45	0	50	50	0
80	+27	+27	0	+18	+18	0	+21	+21	0	+20	+20	0
100	−30	−30	0	−30	−30	0	−17	−17	0	− 7	− 7	0

The data in Fig. 1, which represent the effect of temperature on the extension of nitrocellulose films with different contents of various butadiene – acrylonitrile copolymers, may be represented in the form of curves showing the variation of deformation with film composition at different temperatures. Such curves are shown in Fig. 2.

It is seen that in the case of nitrocellulose films containing copolymer 1 (Fig. 2, a) the deformation increases first slowly and then rapidly with increasing copolymer content. An inflection corresponding to a high-elastic state of the mixture is found only in curves corresponding to 140-150°. Films containing copolymer 2 shows similar behavior. In the case of the nitrocellulose film containing copolymer 3 (Fig. 2, b) an inflection is already found on the curve for 120°.

Finally, in the case of nitrocellulose containing the highly polar polymer 4 (Fig. 2, c)inflections are visible on curves corresponding to temperatures above 60°. However, at temperatures of 110° and over these inflections disappear probably because at these temperatures all specimens containing copolymer 4 are capable of flow. It must be noted that similar behavior was found in studies of the plasticizing action of a true low-molecular plasticizer, dibutyl phthalate, on polyvinyl chloride [2].

A comparison of Figs. 1 and 2 reveals a definite resemblance between the curves. Deformation increases both with rise of temperature and with increasing content of the butadiene – acrylonitrile copolymer in the film. Some of these curves have inflections, which may be interpreted as being due to the fact that the mixtures have high-elastic properties in the corresponding ranges of temperature or butadiene – acrylonitrile copolymer concentration. Degeneration of the inflections in the curves in Fig. 2, c for high temperatures corresponds to degeneration of the inflections in Curves 2, 3 and 4 (Fig. 1) which represent mixtures with high contents of the butadiene – acrylonitrile copolymer.

This similarity between the deformation – temperature and deformation – composition curves is quite understandable. Both types of curves represent variations of deformation with rupture of intra - and intermolecular bonds at polar groups, but in one case this rupture is caused by temperature and in the other by presence of a high-molecular plasticizer.

The data in Fig. 1 can also be represented in the form of curves showing variations of deformation with the content of polar acrylonitrile groups in the polymer used for plasticizing the films. Examination of such curves shows that deformation of the films first increases and then decreases with increasing content of acrylonitrile groups in the copolymer added to the nitrocellulose. Maximum deformation is found in mixtures containing copolymer 3. It seems likely that this copolymer also has the maximum effect on nitrocellulose. This entirely agrees with the result derived by analysis of extension diagrams for nitrocellulose films containing various butadiene – acrylonitrile copolymers [1]. A comparison of these curves also shows that deformation of the films increases sharply with increasing contents of butadiene – acrylonitrile copolymers in the films.

In the case of films of pure butadiene – acrylonitrile copolymers, the curves for deformation as a function of the acrylonitrile group content in the copolymer are of a different character – deformation decreases sharply with increasing polarity of the copolymer.

SUMMARY

1. The nature of the relationship between deformation and temperature for nitrocellulose films with various contents of butadiene – acrylonitrile copolymers indicates that a weakly polar copolymer containing 18.4% acrylonitrile groups is not compatible with nitrocellulose and cannot plasticize it. Copolymers with higher acrylonitrile group contents are compatible with nitrocellulose and can plasticize or elasticize it.

2. The difference $T_f - T_g$, which represents the temperature range of the high-elastic state of nitrocellulose films containing butadiene – acrylonitrile copolymers, increases with increasing acrylonitrile group content in the copolymers. This indicates an increase of the elasticizing action of butadiene – acrylonitrile copolymer on nitrocellulose with increasing polarity.

3. Curves for the variation of deformation with content of butadiene – acrylonitrile copolymer in the nitrocellulose are similar in form to the deformation – temperature curves. It is suggested that this similarity is the consequence of the similar effects of temperature and copolymer addition on the rupture of intramolecular bonds at polar groups.

4. The maximum influence on the deformation of nitrocellulose films is produced by the addition of a butadiene – acrylonitrile copolymer containing 37.7% acrylonitrile groups to nitrocellulose.

Central Scientific Research Institute for Leather Substitutes
Moscow

Received March 17, 1956

LITERATURE CITED

[1] L. E. Kalinina, V. I. Alekseenko, and S. S. Voyutsky, Colloid J., 18, 180 (1956).

[2] R. A. Reznikova, A. D. Zaionchkovsky, and S. S. Voyutsky, J. Tech. Phys., 25, 1045 (1955).

[3] A. P. Aleksandrov and Yu. S. Lazurkin, Proc. Acad. Sci. USSR, 43, 396 (1944).

[4] G. M. Bartenev, Proc. Acad. Sci. USSR, 69, 373 (1949).

[5] G. M. Bartenev and I. A. Lukyanova, J. Phys. Chem., 29, 1486 (1955).

THIXOTROPIC STRUCTURE FORMATION AND ELASTICOPLASTICOVISCOUS PROPERTIES OF ASKANGEL SUSPENSIONS

E. I. Kobakhidze and M. E. Shishniashvili

As is known, thixotropic structure formation and the structural and mechanical properties of bentonite suspensions are among the most important of their varied characteristics. Studies of these properties are, on the one hand, of independent scientific importance in relation to the mechanism and principal laws of structure formation, and, on the other, the structural and mechanical characteristics are used for evaluation of the properties of structurized systems used in various branches of the national economy. In particular, thixotropic bentonite suspensions are extensively used in oil-well drilling, the success of which largely depends on the thixotropic and the structural and mechanical properties of these suspensions [1].

It has been shown in the numerous investigations by Rebinder and his school [1—3] that the process of thixotropic structure formation is completely reversible, and after complete or partial breakdown the thixotropic structure is again fully restored. In such systems, cohesion between the elements of the structural network is effected by van der Waals coagulation forces, weakened by very thin layers of the dispersion medium. The relatively easy breakdown and easy restoration of coagulative cohesion ensures complete reversibility of the system. It has also been shown [4] that completely reversible spatial structures, such as the structures in bentonite clay suspensions, are conventionally solid-like plastic bodies, with conventional flow limits.

The present investigation consisted of a study of the mechanism of thixotropic structure formation and the structural and mechanical properties of askangel suspensions in relation to the equilibrium pH on treatment with 1 N NaOH solution.

Askangel is a highly disperse, strongly swelling bentonite, and it forms thixotropic suspensions with low solid-phase contents. Askangel has very promising applications in various branches of the national economy, especially for drilling processes [5]. Suspensions of natural, and particularly of chemically treated askangel, are high quality suspensions with clearly defined thixotropic properties; they produce a thin but strong crust, not easily permeable to water, on the borehole walls, thus decreasing possibilities of caving. Because of their good thixotropic properties, askangel suspensions satisfactorily retain the cuttings in a suspended state if the circulation in the borehole stops, and eliminate the danger of drill clogging.

It must be pointed out that additions of even small amounts of natural askangel greatly improve the inferior suspensions of clays of other origins, confer thixotropic properties on them, raise their stability, and diminish water loss [5].

The above advantages of askangel suspensions are due to their special physocochemical and especially structural and mechanical properties. Because of this, apart from its independent scientific importance, the present investigation is also of practical value for determining the best methods for the production of drilling muds and for quantitative evaluation of their working properties.

Investigations in our laboratory have shown that high quality clay suspensions, satisfying the demands of complex deep oil-well drilling, must be made from highly disperse fractions of bentonite clays. We therefore isolated highly disperse fractions of natural askangel, in powder form, for the investigation. The highly disperse askangel powders were prepared from dilute (~ 3%) aqueous suspensions which were settled for three days to deposit the coarse fractions, with subsequent evaporation of the settled suspensions on the water bath.

The structural and mechanical properties of 4% suspensions prepared from the powders so obtained were equivalent to the properties of 7% suspensions of the original askangel.

The thixotropic properties of the systems were studied by the increase with time of the yield value P_m, which is conventionally taken to represent the strength of the structure. On the basis of these results, the systems were kept at rest in a dessicator until thixotropic buildup was complete; their elasticoplasticoviscous properties were then studied by Rebinder's method [3], based on investigation of the deformation kinetics at constant shearing stress.

Askangel suspensions were studied with the aid of a Veiler – Rebinder type instrument [6], and askangel pastes with the aid of the Tolstoi instrument [7].

Investigation of the kinetics of thixotropic structure formation in askangel suspensions in relation to the solid-phase concentration showed that the time for thixotropic structure formation increases with increasing solid-phase concentration. Thixotropic buildup of dilute (3, 4, and 5%) askangel suspensions is largely completed in 120-300 hours; the strengthening of askangel pastes (7, 8, and 10%) continues for 20-30 days. However, the coefficient of thixotropy [8]

$$K_T = \frac{P_m - P_0}{P_0}$$

(where P_0 is the original strength of the system, and P_m is the strength after time τ) decreases sharply, probably in consequence of retarded orientation of the particles.

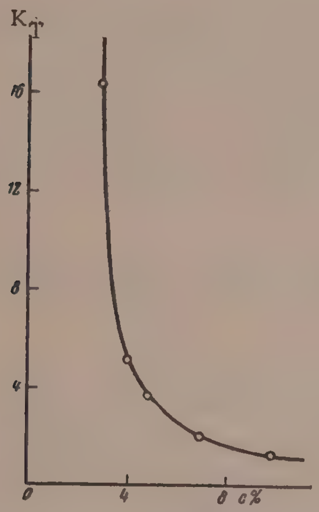

Fig. 1. Variation of the coefficient of thixotropy K_T of an askangel suspension with solid-phase concentration (τ_b = 120 hours).

Figure 1 shows a graph of the variation of the coefficient of thixotropy with solid-phase concentration during the time of thixotropic buildup, 120 hours. According to the literature [8, 9] the coefficient of thixotropy of clay suspensions first increases to a maximum and then decreases with increasing solid-phase concentration. Evidently because of the highly disperse nature of the askangel particles, the maximum of the coefficient of thixotropy is displaced into the low concentration regions (< 3%), while the decrease of K_T is restricted to a narrow concentration range.

In studies of the kinetics of structural buildup, the structure was broken down mechanically and its restoration was verified. It was found that the thixotropic structures in askangel suspensions and pastes are eventually converted into thixolabile structures.

Figures 2 and 3 show curves for the kinetics of thixotropic buildup of a 4% suspension and a 7% paste of askangel. It is seen that only a part of the bonds existing between the elements of the structural network is destroyed by mechanical action. In consequence, the rate of restoration of the broken-down structure is higher than the rate of the original thixotropic structure formation. Therefore the strength of the restored structure is considerably increased. With increasing age of the structure, its breakdown becomes less effective, and after several breakdowns the system appears to lose its thixotropic nature.

The formation of thixolabile structures culminates in syneresis of the system. The syneresis is increasingly pronounced with decreasing concentration of the solid phase.

The incomplete reversibility of askangel suspensions and pastes is probably to be explained by their gradual and lengthy buildup and formation of compact aggregates during breakdown, which ultimately leads to loss of thixotropic properties.

For comparison, a study was also made of the kinetics of thixotropic buildup in 10% suspensions of natural Oglanli bentonite. The results are shown graphically in Fig. 4. The thixotropic buildup time and the strength of the structure in 4% askangel suspension (see Fig. 2) are considerably greater ($\tau_b \sim$ 190 hours; P_m = 250 dynes/cm^2) than in 10% suspension of Oglanli bentonite ($\tau_b \sim$ 40 hours; P_m = 170 dynes /cm^2).

The viscosity of Oglanli bentonite suspensions does not vary with time. The viscosity of askangel suspensions, on the other hand, increases sharply with time (Fig. 5).* The explanation is that completely reversible thixotropic structures are formed in the first, while in the second the structures are not completely reversible.

For complete quantitative characterization of the structural and mechanical properties of askangel suspensions, $\epsilon = f(\tau)$ curves for the deformation kinetics at various shearing stresses were plotted, with subsequent measurements of the decay of deformation after removal of the load. The elastic, plastic and viscosity parameters were calculated from the results. For illustration, Fig. 6 shows curves for the deformation kinetics of 8 % askangel paste. Elasticity, plasticity, and viscosity data for different solid-phase concentrations are given in Table 1.

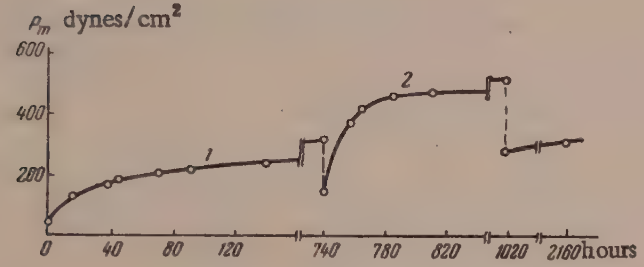

Fig. 2. Kinetics of thixotropic buildup in a 4% askangel suspension (the broken line indicates structural breakdown).

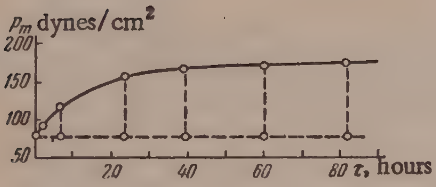

Fig. 4. Kinetics of thixotropic buildup in a 10% suspension of Oglanli bentonite.

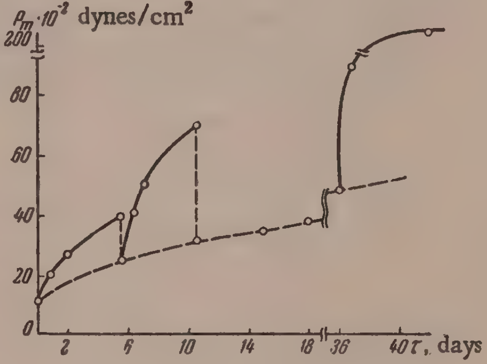

Fig. 3. Kinetics of thixotropic buildup in 7% askangel paste.

These investigations showed that suspensions and pastes of natural askangel have a flow limit P_f which coincides with the elastic limit, below which flow cannot be detected experimentally during any period of time which the experimental technique allows.

The curves in Fig. 6 show that stresses $P < P_f$ produce completely reversible instantaneous-elastic and elastic deformations, which disappear after removal of the load. This region is accordingly characterized by the instantaneous E_1 and elastic E_2 moduli. The elastic viscosity η_2, which determines the rate at which elastic deformation develops, was also calculated.

---

* A Hoeppler viscosimeter was used for measuring the viscosities of the suspensions. The suspensions were vigorously agitated with a stirrer before each determination.

TABLE 1

Elastic, Plastic, and Viscous Properties of Askangel Suspensions with Various Solid-Phase Concentrations

	4% askangel, $P_f = 76$ dynes/cm²				8% askangel, $P_f = 9.7 \cdot 10^3$ dynes/cm²					10% askangel, $P_f = 12.5 \cdot 10^3$ dynes/cm²				
P dynes/cm²	$E_1 \cdot 10^{-4}$ dynes/cm²	$E_2 \cdot 10^{-4}$ dynes/cm²	$\eta_1 \cdot 10^{-8}$ poises	$\eta_2 \cdot 10^{-8}$ poises	$P \cdot 10^{-3}$ dynes/cm²	$E_1 \cdot 10^{-5}$ dynes/cm²	$E_2 \cdot 10^{-5}$ dynes/cm²	$\eta_1 \cdot 10^{-9}$ poises	$\eta_2 \cdot 10^{-9}$ poises	$P \cdot 10^{-3}$ dynes/cm²	$E_1 \cdot 10^{-5}$ dynes/cm²	$E_2 \cdot 10^{-5}$ dynes/cm²	$\eta_1 \cdot 10^{-9}$ poises	$\eta_2 \cdot 10^{-9}$ poises
25	0.86	3.0	–	0.63	4.0	5.8	5.8	–	1.41	5	8.68	8.68	–	2.6
50	0.86	3.0	–	0.63	8.7	5.8	5.8	–	1.53	10	8.66	8.66	–	2.6
67	0.88	2.7	–	0.57	10.7	5.3	4.9	3.0	1.54	15	8.14	8.64	6.2	2.7
85	0.85	2.9	0.92	0.56	15.7	5.5	5.0	4.9	1.43	20	8.0	8.7	7.1	2.7
106	0.9	3.18	1.2	0.65	17.7	5.5	5.5	4.7	1.53	30	8.66	8.66	7.0	2.5
119	0.84	–	–	–	22.7	6.0	5.6	5.0	1.57	35	8.50	9.15	6.5	2.7
135	0.85	–	–	–	24.7	5.4	4.5	4.7	1.27	40	9.0	9.0	7.4	2.7
122	0.81	–	–	–	25.7	4.6	4.6	4.0	1.38	45	7.16	8.1	0.9	1.72

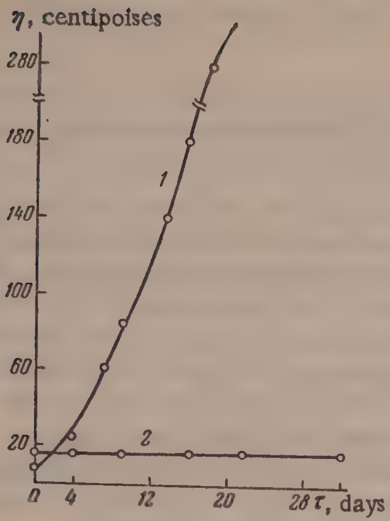

Fig. 5. Viscosity variations with time 1) 4 % askangel suspensions; 2) 10% Oglanli bentonite suspensions.

Under the action of stresses only slightly greater than the flow limit, flow at a very high and constant viscosity occurs, i. e., when $P > P_f$ flow occurs almost without structural breakdown. Flow at constant viscosity continues over a wide range of shearing stresses, with the instantaneous and elastic deformations fully retaining their original values. Very rapid breakdown of the structural framework occurs only when the limiting deformation is reached, with corresponding decreases in the elasticity and viscosity data.

Rheological $d\epsilon/d\tau = f(P)$ curves (Fig. 7) for these systems consist of straight lines which cut off intercepts on the stress axis equal to the values of P_f determined directly from the curves for the deformation kinetics. Thus, askangel suspensions and pastes are characterized by a flow limit P_f, conventionally-instantaneous elastic modulus E_1 and elastic after-effect modulus E_2, plastic viscosity η_1 and after-effect viscosity η_2.

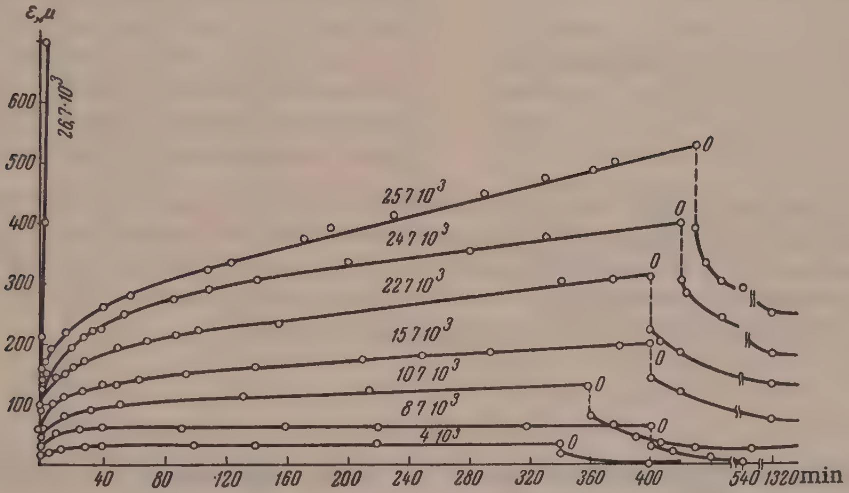

Fig. 6. Deformation kinetics of 8% askangel paste at various shearing stresses P in dynes/cm^2 (shown on the curves).

The data in Table 1 show that all the elasticity and viscosity characteristics remain constant over a wide range of shearing stresses and increase sharply with increasing concentration of the solid phase. Increase of the concentration from 4 to 10% produces nearly a 100-fold increase of E_1, a 30-fold increase of E_2, a 68-fold increase of η_1, a 44-fold increase of η_2, and a 164-fold increase of P_f.

We also studied the effects of added electrolytes on the thixotropic and rheological properties of askangel suspensions. The suspensions were first treated with 1 N NaOH solution until equilibrium pH was established.

When the suspensions are treated with NaOH solution, some of the alkali is converted into carbonate by the action of atmospheric carbon dioxide; this carbonate may undoubtedly influence the structural and mechanical properties. To investigate the effect of this factor, the askangel suspensions were treated with alkali both in presence of atmospheric carbon dioxide, and in closed vessels in absence of carbon dioxide. The results are given in Table 2. Table 2 shows that a longer time is needed to reach equilibrium pH in open vessels, with a considerably higher alkali consumption.

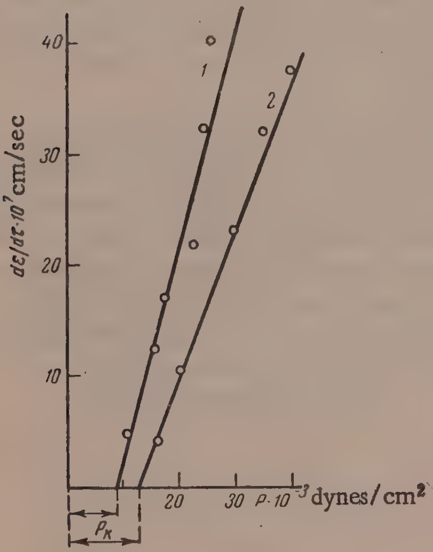

Fig. 7. Rheological curves for askangel pastes: 1) 8%; 2) 10%.

The askangel suspensions differed in viscosity, initial strength of structure, and thixotropic properties, according to the conditions of treatment.

Treatment of the suspensions with NaOH solution in closed vessels resulted in considerable liquefaction (decrease of viscosity and initial shearing stress) caused by the peptizing action of the alkali, resulting in structural breakdown. The liquefaction effect increases with rising pH. At pH 10.5 and 11 thixotropic structure formation does not occur at all. If the suspensions are treated in open vessels, increase of pH increases the viscosity and initial shearing stress,* so that the Hoeppler viscosimeter cannot be used to measure the viscosity.

Studies of the kinetics of thixotropic structure formation at different equilibrium pH values (Fig. 8) showed that thixotropically reversible structures are formed in these suspensions. The thixotropic buildup times and the coefficients of thixotropy are considerably less (τ_b is 20-50 hours; K_T = 1.2-0.6) than for 4% aqueous suspensions of natural askangel. The observed thixotropic buildup in these systems is probably caused by the action of carbonates, formed by the chemical action of atmospheric CO_2 with the alkali.

Investigation of the deformation kinetics of these suspensions shows that the deformation which arises in the system at any small shearing stress, despite its apparent slowing down and tendency to a limit, actually does not reach it but continues to increase gradually at a very low rate, of the order of 10^{-8}-10^{-9} cm/sec, without significant breakdown of the structural network. At these shearing stresses all the elastic and viscous parameters are constant and increase with increasing pH (Fig. 9, Table 3).

TABLE 2

4% Suspension of Natural Askangel, Treated with 1N NaOH Solution to Give Suspensions with Different Equilibrium pH Values

Treatment conditions	pH	Amount of 1 N NaOH consumed, in ml per 100 ml suspension	Time to reach equilibrium, days	Viscosity in centipoises	P_0 dynes/cm^2
In closed vessels	10.0	0.46	12	97.7	100
	10.5	0.65	14	65.7	90
	11.0	1.02	19	45.8	80
In open vessels	9.5	0.65	30	Could not be measured	180
	10.0	1.65	44		550
	11.0	6.49	60		800

---

* The possibility of concentrational changes in the suspensions during the experiments was excluded.

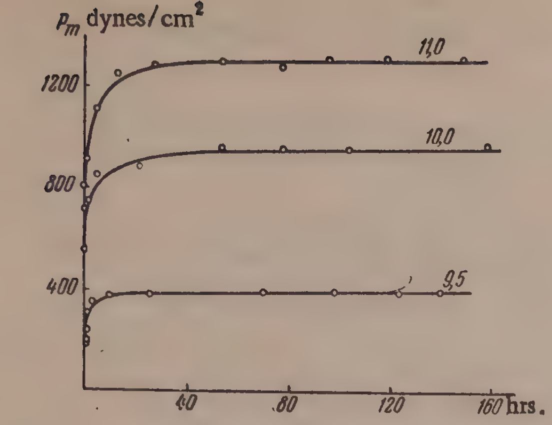

Fig. 8. Kinetics of thixotropic buildup in 4 % askangel suspension at various equilibrium pH values (shown on the curves).

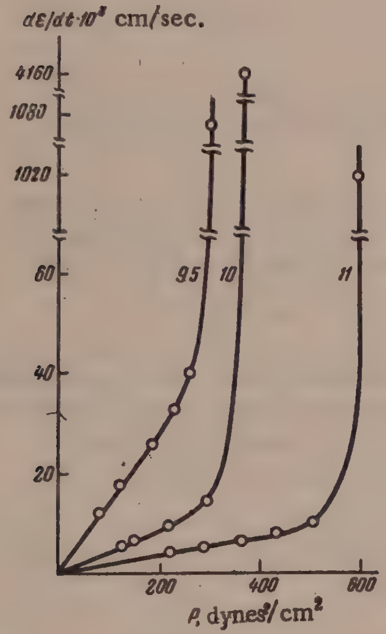

Fig. 10. Rheological curves for 4% askangel suspension at various equilibrium pH values (shown in the curves).

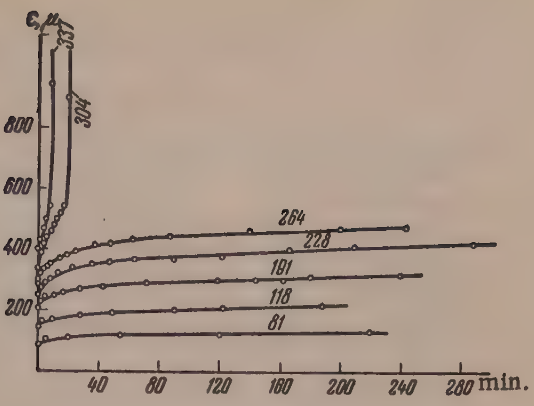

Fig. 9. Deformation kinetics of 4% askangel suspension of pH 9.5, at various shearing stresses P in dynes/cm ² (shown on the curves).

It is seen from Fig. 9 that a slight increase of the shearing stress results in very rapid development of structural breakdown processes, so that the viscosity drops suddenly and flow results in decreasing viscosity. It is evident that at these shearing stresses the flow rate exceeds the rate of bond restoration, and the destroyed structures do not have time to be built up again. Accordingly, the rheological curves for these systems (Fig. 10) consist of two regions: the first is linear, corresponding to flow of the suspension at constant viscosity, with the structure still intact, and the second rises steeply. This portion of the curve represents flow of the suspension with partially destroyed structure.

As is known, the shearing stress corresponding to the boundary between the region of flow at high constant viscosity and the region of flow at variable viscosity is regarded as the conventional flow limit P_{cl} . Systems having a conventional elastic region are classified with the solid-like plastic systems [10, 4].

The conventional flow limit of the suspensions studied is much lower than the yield value P_m (the strength of the structure), and increases considerably with increasing equilibrium pH (Fig. 10, Table 3).

The results of our experiments justify the classification of askangel suspensions with the solid-like plasticoviscous systems.

TABLE 3

Elastic, Plastic, and Viscous Properties of 4% Askangel Suspension at Various Equilibrium pH Values

pH 9.5; P_m = 400 dynes/cm²					pH 10.0; P_m = 960 dynes/cm²					pH 11.0; P_m = 1300 dynes/cm²				
P dynes/cm²	$E_1 \cdot 10^{-4}$ dynes/cm²	$E_2 \cdot 10^{-4}$ dynes/cm²	$\eta_1 \cdot 10^{-9}$ poises	$\eta_2 \cdot 10^{-8}$ poises	P dynes/cm²	$E_1 \cdot 10^{-4}$ dynes/cm²	$E_2 \cdot 10^{-4}$ dynes/cm²	$\eta_1 \cdot 10^{-9}$ poises	$\eta_2 \cdot 10^{-8}$ poises	P dynes/cm²	$E_1 \cdot 10^{-4}$ dynes/cm²	$E_2 \cdot 10^{-4}$ dynes/cm²	$\eta_1 \cdot 10^{-9}$ poises	$\eta_2 \cdot 10^{-8}$ poises
81	1.2	2.77	0.64	0.74	132	1.76	4.52	2.47	1.74	218	4.75	10.46	6.0	5.31
118	1.0	2.83	0.64	0.76	148	1.77	4.44	2.55	1.70	292	5.00	10.01	5.6	4.9
191	1.14	2.86	0.72	0.76	221	1.82	4.80	2.23	1.80	363	5.44	10.89	5.5	5.38
228	1.09	2.74	0.67	0.73	298	1.78	4.45	2.10	1.74	437	5.52	11.00	5.1	5.2
264	1.13	2.64	0.65	0.70	331	1.73	—	0.01	—	510	5.56	10.2	5.1	5.0
304	1.07	—	0.03	—	367	1.75	—	0.008	—	583	5.00	—	0.06	—
337	1.10	—	0.01	—	418	1.73	—	—	—	619	4.64	—	—	—

SUMMARY

1. The thixotropic structures formed in aqueous suspensions and pastes of askangel pass in course of time into thixolabile structures, resulting in syneresis of the system.

2. Treatment of such systems with 1 N NaOH solution in open vessels sharply decreases the time of thixotropic structure formation and the coefficient of thixotropy. The structures formed have complete thixotropic reversibility.

3. Aqueous suspensions and pastes of askangel belong to solid-like plastic systems by their structural and mechanical properties, with flow limits coinciding with the elastic limits (within the sensitivity range of the instrument used). Their elastic, plastic, and viscous characteristics remain constant over a wide range of shearing stresses, and increase sharply with increasing concentration of the solid phase.

4. The less strong and thixotropically completely reversible structures formed when askangel suspensions are treated with NaOH solution are conventionally classified with the solid-like systems. These systems have a conventional flow limit, below which they flow at very high constant viscosities. At these shearing stresses all the elastic and viscous characteristics remain constant, but increase with increasing pH. Above the conventional flow limit the viscosity decreases sharply and flow occurs at variable viscosity as the result of very rapid breakdown of the structural network which develops in the system.

The authors express their deep gratitude to Academician P. A. Rebinder and to N. A. Serb-Serbina for their help in this investigation.

The P. N. Melikishvili Institute of Chemistry,
Acad. Sci. Georgian SSR
Colloid Chemistry Laboratory Tbilisi

Received May 7, 1956

LITERATURE CITED

[1] P. A. Rebinder, Symposium, Viscosity of Liquids and Colloidal Solutions, Vol. 1, Acad. Sci. USSR Press, Moscow-Leningrad, p. 361 (1941); N. N. Serb-Serbina, ibid, p. 381.

[2] N. N. Serb-Serbina and P. A. Rebinder, Colloid J. 9, 381 (1947); N. N. Serb-Serbina and S. A. Nikitina, Colloid J. 8, 63 (1946).

[3] P. A. Rebinder, New Methods of Physicochemical Investigation of Surface Phenomena, vol. 1, Acad. Sci. USSR Press, p. 5 (1950); E. E. Segalova and P. A. Rebinder, Colloid J. 10, 223 (1948; P. A. Rebinder and E. E. Segalova, Proc. Acad. Sci. USSR, 71, 85(1950); E. E. Segalova, P. A. Rebinder, and L. I. Sentyurikhina, Colloid J., 13, 6(1951).

[4] L. A. Abduragimova, P. A. Rebinder, and N. N. Serb-Serbina, Colloid J., 17, 184(1955).

[5] S. Filatov, Symposium, The Bentonite Clays of Georgia and their Use in the National Economy, Acad. Sci. Georgian SSR Press, Tbilisi, p. 27 (1953); E. Pondoeva, ibid, p. 83.

[6] S. Ya. Veiler and P. A. Rebinder, Proc. Acad. Sci. USSR 49, 354 (1945).

[7] D. M. Tolstoi, Colloid J., 10, 133 (1948).

[8] E. M. Tarasova, Candidate's Dissertation, Moscow (1919).

[9] S. A. Kudrina, Candidate's Disseration, Tashkent (1950).

[10] N. V. Mikhailov and P. A. Rebinder, Colloid J., 17, 107(1955).

GELATINIZED EMULSIONS

13. O/W TYPE EMULSIONS OF MAXIMUM CONCENTRATION WITH A THIXOTROPIC DISPERSION MEDIUM

L. Ya. Kremnev

We have demonstrated, by a number of examples, the possibility of greatly increasing the sedimentational and aggregative stability of concentratedemulsions(with disperse phase contents considerably less than 74% of the volume of the system) as the result of thixotropic structure formation in the dispersion medium. Spatial structure formation was induced by addition of small amounts of cetyl alcohol [1] or cholesterol [2] to the dispersion medium — aqueous solution of sodium oleate, stearate, or palmitate. Such solutions have very high rates of thixotropic buildup of the structures broken down in emulsification. This factor is decisive for prevention of coalescence of the droplets incorporated in the spaces of the spatial networks, and for the formation of a highly disperse emulsion.

A thixotropic dispersion medium, both in bulk and in thin layers, has higher structural and mechanical characteristics: elasticity in shear, structural viscosity, and considerable strength. An indication of these properties is given by the results of viscosity determinations by means of the capillary viscosimeter. As an example, Fig. 1 shows the variations of efflux rate $v \approx 1/\tau$ (where τ is the time) of 1 % aqueous sodium oleate solution containing different concentrations of cetyl alcohol. According to Rebinder [3], this behavior of the protective layers on the particle surfaces provides a universal means for an extremely great increase of the aggregative and sedimentational stability of disperse systems. This explains why in our experiments with thixotropically structurized soap solutions [1, 2] the stability of concentrated emulsions was increased by thousands of times.

In the course of our investigations which led to the conclusion that emulsions based on alkali soaps are stabilized by unsaturated adsorption monolayers [4], it was of interest to study emulsions of maximum concentrations with thixotropically structurized dispersion media, and to investigate the state and structure of the protective layers in them. Emulsions of benzene, of maximum concentration, were prepared in aqueous solutions of sodium oleate mixed with cetyl alcohol were prepared for this purpose.

The soap solutions were boiled for 20-30 minutes with weighed quantities of cetyl alcohol in a flask under reflux. The cooled solutions were fairly thixotropic, and were used as dispersion media for the emulsions. The emulsification was carried out by our method by the use of a spiral moving through the system [5]. As usual, the end of emulsification (formation of maximum strength emulsion) was established by the end of absorption of benzene by the emulsion. The emulsions were subjected to complete dispersion analysis by the microscopic method, the emulsion characteristics being based on the results.

Thixotropic solutions are obtained with various proportions of soap and cetyl alcohol, but all such solutions are suitable for emulsification, irrespective of the component concentrations.

The Table gives the characteristics of maximum strength emulsions based on aqueous sodium oleate solutions of three different concentrations, containing 0.025 mole/liter of cetyl alcohol. The Table gives: the maximum volume V_∞ of emulsified benzene in 1 ml of dispersion medium, the maximum surface S_∞ of the protective adsorption-solvation layers per 1 ml of the aqueous solution, the minimum thickness δ_{crit} of the layers, and the area S_0 per oleate molecule in the droplet surfaces.

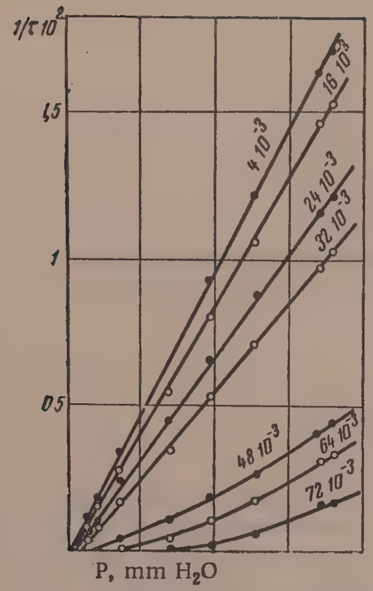

Fig. 1. Effect of cetyl alcohol on structure formation in aqueous sodium oleate solutions (the numbers on the curves represent the concentrations of cetyl alcohol in mole/liter).

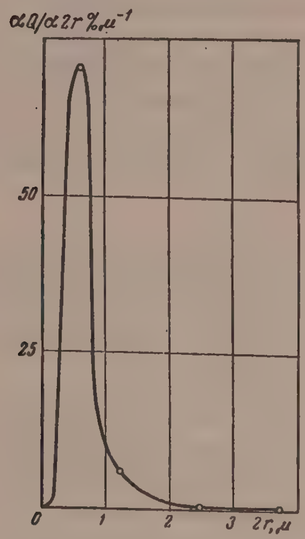

Fig. 2. Differential droplet size distribution curve for a maximum strength emulsion in thixotropic sodium oleate solution.

TABLE

Maximum Strength Emulsions in Thixotropic and Aqueous Solutions of Sodium Oleate

Soap concentration in mole/liter	V_∞ in ml	S_∞ in m^2	S_{crit} in μ	S_0 in A^2
Thixotropic solutions of Sodium Oleate				
0.033	20	146	0.0146	350
0.098	46	150	0.0066	270
0.164	74	250	0.0040	225
Aqueous solutions of Sodium Oleate				
0.032	33	33	0.030	160
0.096	88	69	0.014	115
0.160	140	100	0.010	100

The maximum volume of the disperse phase V_∞ increases with soap concentration in the mixture at a constant content of cetyl alcohol in the dispersion medium, but the values of V_∞ are much lower than in experiments with sodium oleate alone [6] because of greater dispersion of the droplets. Indeed, the degree of dispersion and homogeneity of the emulsions is very high. To illustrate this, Fig. 2 shows a differential curve of droplet size distribution in a maximum strength emulsion in a dispersion medium containing 0.164 mole sodium oleate and 0.025 mole cetyl alcohol per liter.

The maximum on the distribution curve corresponds to a droplet diameter of the order of 0.6 μ, while in maximum strength emulsions based on soap solutions without cetyl alcohol the maximum is always found at a diameter of ~ 1μ, which is in accordance with an analysis of the emulsification process [7]. The shift of the maximum in the direction of smaller drop size is due to the thixotropic properties of the dispersion medium, as the spatial structures, being rapidly restored after breakdown, prevent coalescence of the smaller droplets formed during the emulsification. In the emulsions studied the droplet diameter never exceeded 5 μ.

The shift of the maximum in the direction of smaller droplet size results in an appreciable decrease of V_∞ in comparison with the values of V_∞ obtained earlier with sodium oleate.

Returning to the table, we see that the minimum thickness of the protective layer δ_{crit} decreases with increasing soap concentration, while the maximum layer area S_{∞} increases. As regards the packing density of the soap molecules on the droplet surfaces, the values of S_0 leave no doubt that the adsorption layers are considerably unsaturated monolayers. It is particularly interesting to note in this connection that the structural and mechanical properties of the protective layers are effective in monomolecularly attenuated adsorption layers.

It is useful to compare the data obtained with the results of a study of maximum strength emulsions in sodium oleate without cetyl alcohol [6]. The table therefore contains some earlier data for maximum strength emulsions in aqueous sodium oleate solutions.

A comparison of the data in the table leads to the conclusion that addition of cetyl alcohol to the soap solution does not produce any radical changes in the characteristics of maximum strength emulsions and protective layers. However, spatial structure formation in the dispersion medium results in a sharp decrease in the thickness of the adsorption – solvation layers which can stabilize the droplets. This is probably to be explained by the higher structural and mechanical properties of thixotropic stabilizer solutions both in a large volume and in thin layers. Accordingly, the surface area S_{∞} of the layers formed from 1 ml of solution increases in proportion to the decrease of their thickness. At the same time the adsorption layers become more attenuated, and the emulsifying power of the sodium oleate, quantitatively represented by the values of S_{∞}, increases.

SUMMARY

1. Maximum strength o/w type emulsions have been prepared in thixotropic sodium oleate solutions. In agreement with Rebinder's views, the main factors determining the stability of such emulsions are the structural and mechanical properties of the protective adsorbed solvate layers.

2. Thixotropic structure formation in the dispersion medium of the emulsion results in an appreciable increase of the emulsifying power of the stabilizer and a decrease of the critical thickness of the protective layers.

3. The protective adsorbed layers are monomolecular and unsaturated.

4. Emulsions with a thixotropic dispersion medium have a very high degree of dispersion and are homogeneous in droplet size.

The Lensoviet Technological Institute
Leningrad

Received April 16, 1956

LITERATURE CITED

[1] L. Ya. Kremnev, Colloid J., 10, 18 (1948); Trans. Leningrad Tech. Inst., No. 17, 73 (1950); L. Ya. Kremnev and E. I. Kvit, Trans. Leningrad Tech. Inst., No. 17, 89 (1950).

[2] L. Ya. Kremnev and T. A. Volkova, Trans. Leningrad Tech. Inst., No. 21, 50 (1951).

[3] P. A. Rebinder, Introduction to translation of W. Clayton's "Emulsions", Foreign Lit. Press, Moscow (1950).

[4] L. Ya. Kremnev and S. A. Soskin, Colloid J., 9, 269 (1947); L. Ya. Kremnev and R. N. Kagan, Colloid J., 10, 436 (1948).

[5] L. Ya. Kremnev, Proc. Acad. Sci. USSR, 79, No. 4, 655 (1951); Colloid J., 13, 394 (1951).

[6] L. Ya. Kremnev and S. A. Soskin, J. Gen. Chem., 16, 2004 (1946); Colloid J., 9, 269 (1947).

[7] L. Ya. Kremnev and A. A. Ravdel, Colloid J., 16, 17 (1954).

INVESTIGATION OF STRUCTURIZED SUSPENSIONS

E. F. Kurgaev

In coagulation and softening of water by the precipitation method a flocculent suspension is formed; the floc particles are independent structurized systems which at a definite concentration unite into a loose spatial structure [1]. Experiments performed by the Veiler – Rebinder method [2] have been used to determine the shearing stress and relaxation time of such structures [3, 4]. At the same time, technological investigations of the operation of water clarification equipment have involved the determination of such parameters of the suspension as its volume concentration in the dispersion medium, compressive strength, density, and the cohesive forces which cause aggregation of the particles and assist the removal of mechanical impurities from the water. The technique of such determinations has been developed by the author; it is based on an analysis, given below, of the results of observations of the kinetics of lowering of the boundary of the suspension allowed to settle simultaneously in several glass cylinders. The suspension in all the cylinders has the same initial concentration, but different layer heights H_0.

Observations show that at the start of the settling the boundary of the suspension layer sinks at a constant rate, independent of the layer height H_0. The rate then decreases, gradually becoming zero, and the boundary becomes stabilized at a certain height H_f. While the boundary sinks at a constant rate, the suspended particles in the layer (with the exception of its lower part, consisting of a zone of settled particles) retain their individual outlines and are in a state of appreciable circulation in various directions. This suggests that collective subsidence of the particles occurs; this is confirmed by a comparison of the calculated rates of such subsidence for different initial suspension concentrations.

The start of the change in the rate of sinking of the layer boundary is accompanied by cessation of particle circulation, and formation of a continuous spatial network. The subsequent sinking of the layer boundary is the result of condensation of this network by contraction of the pores between the particles forming it. This is followed by stabilization of the height of the layer. Similar stages in the process were also observed by Zuev [5].

We have carried out special investigations over a wide range of initial layer heights H_0; it was found up to values below a certain value H_{cr}, the ratio of H_0 to the stabilized height H_f remains constant, while after H_{cr} is exceeded this ratio begins to increase. There are no pores between the particles of the suspension when the layer height has become stabilized. This is shown both by visual observations and by the fact, established by special experiments, that the layer is impermeable to water.

There is reason to believe that in the initial height range below H_{cr} the stabilized layer is a structurized system of the same density as the particles of the suspension forming it. At heights greater than H_{cr} the pressure of the layer exceeds the compressive strength of the structure and causes the latter to condense. From this it is possible to determine the volume concentration of the suspension in its original form, i. e., as a disperse phase in a structureless medium, which is the state of the layer of the particles in the suspension at its initial height H_0. This concentration is evidently equal to the ratio of the stabilized height to the initial height of the layer, for values of the latter not exceeding H_{cr}; i. e., $c_0 = H_f/H_0$ when $H_0 < H_{cr}$.

Having determined the weight concentration (c_w) of the solid phase of the suspension in grams per milliliter in the original volume of the layer by the usual method, we can find the solid phase content in unit volume of the suspension structure from the expression $\gamma_1 = c_w/c_0$ Hence we can find the density of the suspension floc from the formula

$$\gamma_2 = 1 + \gamma_1 (1 - 1/\gamma_d)\ \mathrm{g/ml}$$

where γ_d is the density of the dry substance contained in the suspension structure, in g/ml.

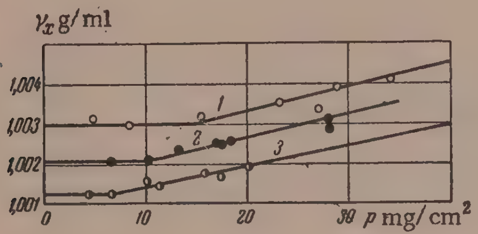

Fig. 1. Variation of suspension density with pressure: 1) 50% $Al(OH)_3$ + 50% $Fe(OH)_3$, $p_{cr} = 14\ \mathrm{mg/cm^2}$; $\alpha = 0.064\ \mathrm{cm^{-1}}$; 2) 75% $Al(OH)_3$ + 25% $Fe(OH)_3$; $p_{cr} = 10\ \mathrm{mg/cm^2}$; $\alpha = 0.059\ \mathrm{cm^{-1}}$; 3) $Al(OH)_3$, $p_{cr} = 7\ \mathrm{mg/cm^2}$, $\alpha = 0.052\ \mathrm{cm^{-1}}$.

The amount of water (density of which is unity) relative to the volume of the dry substance in the suspension is $\varphi_0 = (\gamma_d - \gamma_1)/\gamma_1$ and relative to the weight of the dry substance, $\varphi_w = \varphi_0/\gamma_1$.

The above data on the critical layer height H_{cr} and the suspension parameters may be used to calculate the value of its maximum normal uniaxial compressive stress p_{cr} from the formula

$$p_{cr} = c_0 H_{cr} \gamma_1 (1 - 1/\gamma_d)\ \mathrm{g/cm^2}$$

or

$$p_{cr} = H_{cr} c_0 (\gamma_2 - 1)\ \mathrm{g/cm^2}.$$

Observed data on the ratios of the initial and final layer heights when $H_0 > H_{cr}$ make it possible to follow the variations of the suspension density, of the amount of water present in its structure, and of the compressive deformation stress as a function of pressure.

Figure 1 shows the variations of density γ_x with pressure p for suspensions formed in coagulation of water by aluminum and iron salts.

It was found experimentally that, for these suspensions, the relationship $\gamma_x = f(p)$ can be represented as

$$\gamma_x = \gamma_2 + (p - p_{cr}) \cdot \alpha\ \mathrm{g/ml}.$$

Almost the same value of α (0.06 $\mathrm{cm^{-1}}$) was obtained for different coagulants, which may be a sign that their structural bonds are of the same character.

The amount of water in the suspension structure decreases as p_{cr} is exceeded; the above data may be used to calculate the loss of water from the suspension by increase of the externally applied pressure.

The cohesive forces between the particles may be quantitatively estimated by parallel observations of the condensation kinetics of suspension layers of different initial heights. For this, we determine the rates of condensation of the layers from the instant at which continuous structurized systems are formed in them to the instant at which the density of the system becomes equal to the density of its constituent suspension particles. As has been stated earlier, when $p < p_{cr}$ this state is reached when the height of the layer has become stabilized. The average value of the required rate V can be approximately calculated by dividing the difference between the heights of the layer at the beginning and the end of the condensation period by the duration of the latter.

The average rate can be found more exactly by integration of the relationship between the condensation rate and time, which varies in the course of the process. For this, the $V_{cond} = f(\tau)$ graph is plotted and $\bar{V}$ is then determined from the expression

$$\bar{V} = \frac{1}{T} \int_{\tau_1}^{\tau_2} V_{cond}\, d\tau,$$

where $1/T = \tau_2 - \tau_1$.

It was found experimentally that the suspension condensation rate increases with increasing initial layer height H_0 and pressure p, the relationship $\bar{V} = f(p)$ being of the form shown in Fig. 2. This relationship, expressed in the form $\bar{V} = ap + b$, shows that condensation of the structurized system is caused not only by gravitational forces, but also by other forces, which may be assumed to be forces of cohesion between the particles of the suspension. This relationship is used to find the magnitude of the cohesion forces from the suspension condensation rate V_a, corresponding to zero value of the pressure p. For this, the pressure increment p_a corresponding to the rate V_a is determined. A simple transformation of the above expression for $\bar{V}$ shows that the required value of p_a corresponds to the ordinate $2V_a$.

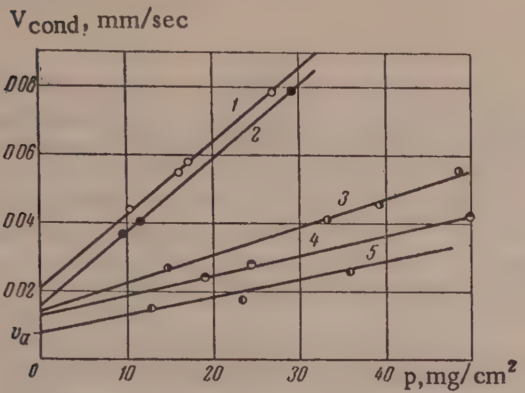

Fig. 2. Variation of the condensation rate of the suspension layer with pressure: 1) 80 % Al $(OH)_3$ +20% Fe $(OH)_3$; p_a = 10.0 mg/cm²; 2) Al $(OH)_3$ p_a = 7.5 mg/cm²; 3) 25% Al $(OH)_3$ + 75% Fe$(OH)_3$; p_a = 18.5 mg/cm²; 4) Fe$(OH)_3$; p_a = 22.2 mg/cm²; 5) 50% Al$(OH)_3$ + 50% Fe$(OH)_3$; p_a = = 17.0 mg/cm².

It must be pointed out that if the observations are made at values of $p > p_{cr}$ for calculation of V_a, the end of the condensation period cannot be taken to be the instant when the height of the layer becomes stabilized, as an additional process is superposed here, due to disturbance of the natural state of the suspension structure as the result of its condensation. However, the results of such experiments can also be used if the period of condensation of the suspensions for a cylinder with the minimum value of p, less than p_{cr}, is taken as equal for all the cylinders. This gives satisfactory agreement with experiments in which $p < p_{cr}$ in all the cylinders.

In addition to the above values, the following were determined: the magnitude of the cohesion forces per unit weight of the dry substance forming the suspension, p_a/γ_1 (which we term the adhesion coefficient K_a), and the critical concentration by weight c_{cr} at which a continuous structural network is formed.

The experimentally determined values of the physical parameters are given in the table.

Quantitative Characteristics of the Suspensions Studied

Composition of suspension	Physical parameters				
	γ_2, g/ml	mg/cm²	$\frac{p_a}{\gamma_1}$	φ_W	c_{cr} %
Al $(OH)_3$	1.0012	7.5	3.75	500	0.07
Fe $(OH)_3$	1.0026	22.2	5.94	270	0.15
Fe $(OH)_3$	1.0064	9.6	1.04	109	0.46 *
Fe $(OH)_2$	1.0061	11.6	1.33	115	0.43
75% Al $(OH)_3$ + 25% Fe$(OH)_3$	1.0020	10.0	3.13	332	0.13
50% Al $(OH)_3$ + 50% Fe $(OH)_3$	1.0029	17.0	3.98	233	0.17
25% Al $(OH)_3$ + 75% Fe $(OH)_3$	1.0048	18.5	2.65	144	0.32
Mg $(OH)_2$	1.0026	3.5	0.78	222	0.07
25% Mg $(OH)_2$ + 75% $CaCO_3$	1.0300	26.0	0.53	20.4	1.47
15% Mg $(OH)_2$ + 85% $CaCO_3$	1.0860	66.0	0.44	7.2	6.95

---

* After condensation for 40 hours and dispersion of the precipitate by water.

The data in the table show that the particles in the suspension include very large amounts of water, considerably exceeding the dry substance in weight; this quantity is determined by the nature of the structure of the suspension. The suspension densities vary over a wide range, and are not directly related to the density of the dry substance. The critical concentrations also vary over a wide range.

In combined coagulation of aluminum and iron salts the density and subsidence rate of the suspension are higher than for a suspension of aluminum hydroxide alone. The values of the adhesion coefficient are greater in combined coagulation than for ferrous hydroxide, which is usually present in the coagulum in incomplete hydrolysis of iron salts. The quantitative values of these parameters explain the improved water clarification effect and the extension of the range of its optimum ionic composition in combined coagulation with iron and aluminum salts, as compared with coagulation by one of these reagents. Moreover, it is possible to determine the optimum component ratio: this was 1:1 in our experiments.

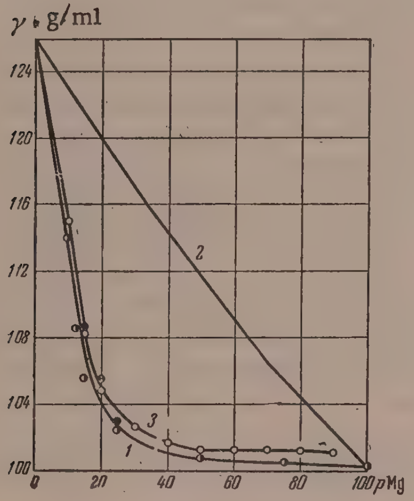

Fig. 3. Densities of suspensions consisting of calcium carbonate and magnesium hydroxide in various proportions: 1) $\gamma_{cm} = f(p_{Mg})$ from experimental data; 2) $\gamma_{cm} = f(p_{Mg})$ calculated for $\gamma_{Ca} = 1.26$ g/ml; 3) – $\gamma_{Ca} = f(p_{Mg})$ from experimental data;

$$p_{Mg} = \frac{Mg(OH)_2}{Mg(OH)_2 + CaCO_3} \cdot 100\%$$

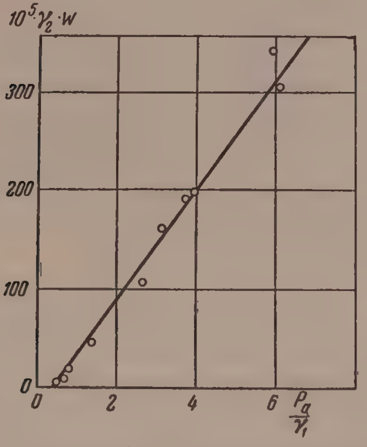

Fig. 4. Variation of the mass of floc particles with the magnitude of the cohesion forces.

Data showing the influence of "aging" and repeated mechanical peptization on the suspension parameters were obtained for ferric hydroxide.

The particle diameters calculated from the values of γ_2 and from the experimentally determined subsidence rates were in agreement with the generally observed dimensions of such particles.

A study of the physical parameters of the suspensions formed in water softening showed that the presence of magnesium hydroxide alters the character of the structure formation in calcium carbonate suspensions. With increasing magnesium content the structure formation passes from the condensation-crystallization to the coagulation type. Calculations showed that this is accompanied by a sharp decrease in the density of the calcium carbonate suspensions (Fig. 3).

Observations by the electron and optical microscopes revealed an approximately 400-fold decrease in the volume of the calcium carbonate crystals and a change in the nature of the structural bonds. Instead of aggregation at the plane faces, the crystals join by their corners (sharp projections) and are coated with magnesium hydroxide. This is in entire agreement with the laws for the effects of surface-active substances on structure formation established by Rebinder and his associates [6].

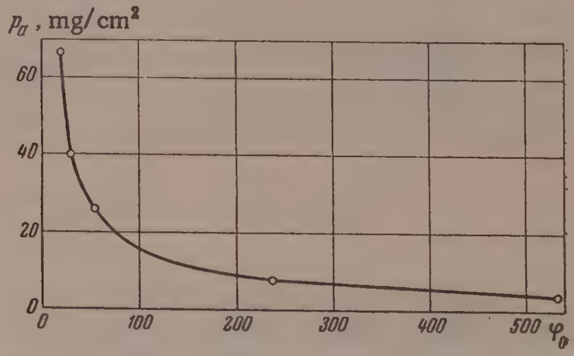

Fig. 5. Relationship between cohesion forces and the amount of water immobilized by the structural network of a suspension consisting of calcium carbonate and magnesium hydroxide.

Our experiments showed that a linear relationship, shown in Fig. 4, exists between the adhesion coefficient and the particle mass $\gamma_2 W$ (here W is the volume of a particle).

Interesting relationships were found between the cohesion forces p_a and the amount of water contained in the structural network. Figure 5 shows such a relationship for a suspension of calcium carbonate and magnesium hydroxide.

SUMMARY

1. A new method has been used to determine the following physical parameters of flocculent suspensions formed in water coagulation and softening processes: density, strength in normal uniaxial compression, amount of water immobilized by the structural network of the suspension, and quantitative values of the cohesion forces causing floc aggregation.

2. A linear relationship exists between the specific cohesion force (coefficient of adhesion) and the mass of a floc particle.

3. When a calcium carbonate suspension is formed in presence of magnesium hydroxide, the character of its structure formation changes and its density alters. With increasing magnesium content the structure gradually passes from the condensation-crystallization to the coagulation type, and the density of the calcium carbonate floc decreases.

4. A relationship, represented by a curve close to a hyperbola, exists between the cohesion forces and the amount of water immobilized in the structural network of a suspension consisting of calcium carbonate and magnesium hydroxide. The vertex of the hyperbola represents transition to a predominant influence of one of the above types of structure formation.

5. In combined coagulation with aluminum and iron salts the suspension has optimum physical properties with equal amounts of aluminum and iron hydroxides.

6. The quantitative data on the physical parameters of flocculent suspensions can be used in the design of equipment for water purification, and the relationships between these parameters, for investigation and control of water coagulation and softening processes.

I express my deep gratitude to Academician P. A. Rebinder for valuable advice and guidance in generalization of the experimental results.

All - Union Scientific Research Institute
for Railroad Transport
Moscow

Received June 23, 1956

LITERATURE CITED

[1] P. A. Rebinder, Bull. Div. Math. Nat. Sci. Acad. Sci. USSR, Chem. Ser., 5, 603 (1936); P. A. Rebinder and E. E. Segalova, Science and Life, No. 5 (1955).

[2] S. Ya. Veiler and P. A. Rebinder, Proc. Acad. Sci. USSR, 49, No. 5 (1946).

[3] E. N. Teterkin and N. S. Lebedeva, Trans. Inst. Water Supply and Hydrogeol. Eng., Inform. Material No. 3, Moscow, p. 23 (1952).

[4] T. I. Baryshnikova, Dissertation, Sverdlovsk Polytech. Inst. Urals (1954).

[5] Yu. S. Zuev, Colloid J., 10, No. 4, 281, No. 6, 431 (1948).

[6] N. N. Serb-Serbina and P. A. Rebinder, Colloid J., 9, 381 (1947); E. E. Segalova and P. A. Rebinder, Colloid J., 10, No. 3, 223 (1948); L. A. Abduragimova, P. A. Rebinder, and N. N. Serbina, Colloid J., 17, No. 3, 184 (1955); P. Rebinder, Faraday Society, Discussion on Coagulation and flocculation, No. 18, 1954.

THE EFFECT OF SURFACE-ACTIVE SUBSTANCES ON THE SPECIFIC VISCOSITY OF GELATION SOLUTIONS

S. M. Levi

Deryagin, Levi, and Koltsov [1] put forward the view, which was experimentally confirmed, that the observed sharp change in the viscosity of gelatin solutions under the influence of small amounts of surface-active substances – the colored components – is explained by "adsorption" of the latter, leading to a change in the shape of the gelatin molecule (elongation). This process is represented by the following equation:

$$\frac{1}{c}\ln\frac{\eta}{\eta_0} = f(\Gamma), \tag{1}$$

where c is the concentration of the gelatin solution; η_0 is the viscosity of the gelatin solution before introduction of the surface-active substance; Γ is a quantitative measure of the "adsorption "; f (Γ) is a certain function of Γ. Since in this instance (gelatin solutions) the magnitude of the adsorbing surface is not known, and even the concept of the gelatin particle – dispersion medium interface is somewhat conventional, we take Γ to mean the adsorption (more correctly, sorption) of surface-active substance (wetting agent) in grams per 1 g gelatin.

In the investigation cited [1], we studied the viscosity change as a function of the ratio of the gelatin concentration c to the colored component c_1, i. e.,

$$\frac{1}{c}\ln\frac{\eta}{\eta_0} = f\left(\frac{c_1}{c}\right), \tag{2}$$

assuming that

$$K = f\left(\frac{c_1}{c}\right) = f(\Gamma), \tag{3}$$

where K is the asymmetry coefficient of the particles, equal, according to Einstein, to 2.5 for spherical particles, and having large values, determined by the Simha equation [2], for particles of other shapes.

In our subsequent experiments an attempt was made to determine the value of f (Γ) directly by adsorption measurements. The magnitude of adsorption was found from measurements of the surface tension isotherms in aqueous and gelatin solutions of wetting agents. The adsorption was calculated graphically by means of the Gibbs equation and the Langmuir adsorption isotherm [3]. The following assumption was made: the difference between the adsorption (Γ_W) of the wetting agent in aqueous solution and the adsorption (Γ_g) in gelatin solution is a measure of the "adsorption " of the wetting agent by gelatin, which is the cause of the viscosity change, and therefore

$$K = f(\Gamma_W - \Gamma_g), \tag{4}$$

and it follows from Equation (4) that

$$\frac{1}{c}\ln\frac{\eta}{\eta_0} = f(\Gamma_W - \Gamma_g). \tag{5}$$

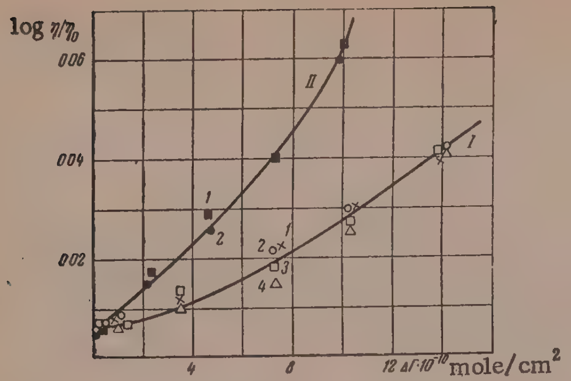

Fig. 1. Effect of adsorption of wetting agent by gelatin on its specific viscosity. I) Wetting agent 2: 1) 4% solution of 30°; 2) ditto, at 35°; 3) 6% solution at 35°; 4) ditto, at 40°; II) wetting agent 3: 1) 4% solution at 35°; 2) 6% solution at 35°.

Equation (5) was tested for the following wetting agents: Dismulgan and octo- and dodecanoglycerides of alkenylsuccinic acids, having the formulas:

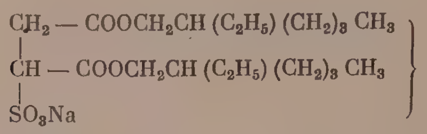

$$\left.\begin{array}{l} CH_2-COOCH_2CH(C_2H_5)(CH_2)_3CH_3 \\ | \\ CH-COOCH_2CH(C_2H_5)(CH_2)_3CH_3 \\ | \\ SO_3Na \end{array}\right\}$$

Wetting agent 1

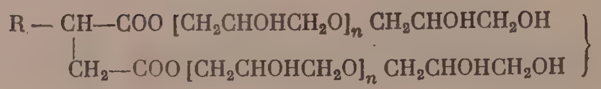

$$\left.\begin{array}{l} R-CH-COO\,[CH_2CHOHCH_2O]_n\,CH_2CHOHCH_2OH \\ \quad\;\, | \\ \quad\;\, CH_2-COO\,[CH_2CHOHCH_2O]_n\,CH_2CHOHCH_2OH \end{array}\right\}$$

Wetting agent 2 with 2n = 6

Wetting agent 3 with 2n = 10

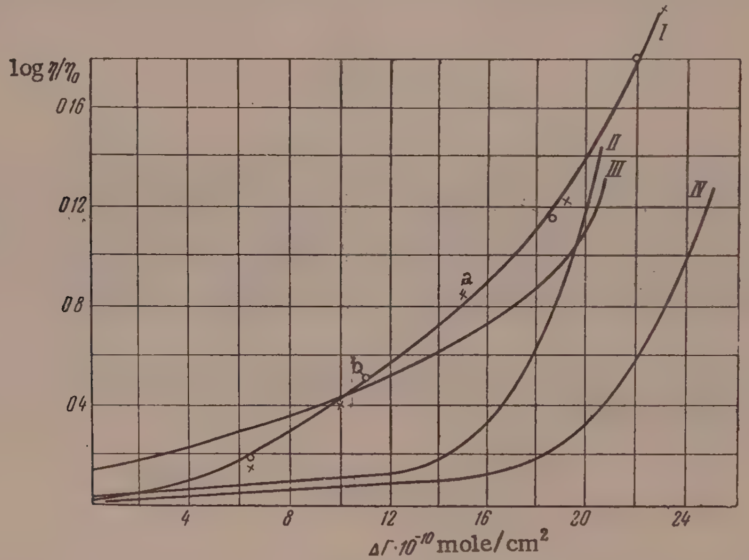

Fig. 2. Effect of adsorption of wetting agent 1 by gelatin on its specific viscosity: 1) 4% (a) and 6% (b) gelatin solutions; II) gelatin I; III) gelatin 2; IV) gelatin

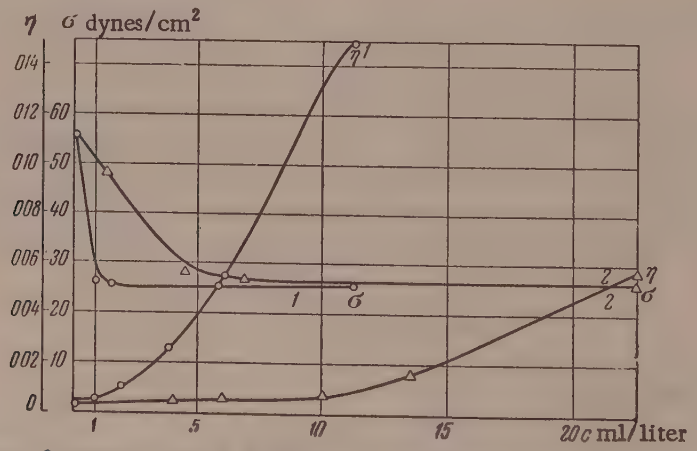

Fig. 3. Effect of additions of wetting agent in different concentrations on the viscosity η (poises) and surface tension σ (dynes/cm) of gelatin solutions; I) wetting agent 1; II) wetting agent 2.

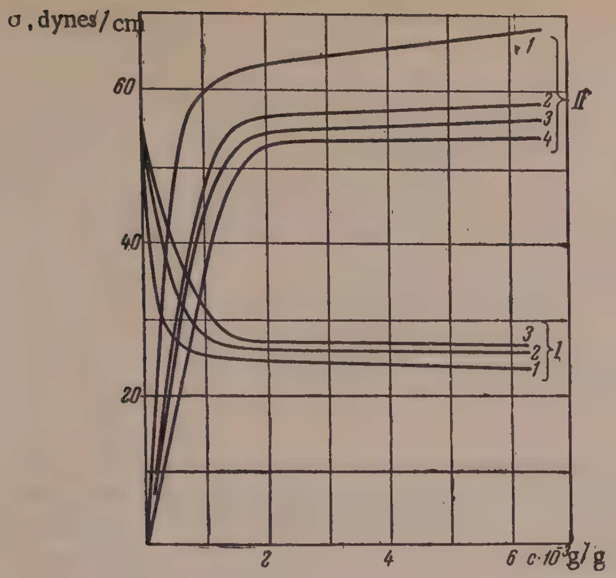

Fig. 4. Surface tension (I) and adsorption (II) isotherms for wetting agent 1 with different gelatin samples (1, 2, 3, and 4).

The Relationship (5) was found from the experimental data given in Figs. 1 and 2 (Curve 1). These figures show that the points for different gelatin concentrations coincided, thus confirming the views put forward. Figure 3 shows the course of the viscosity and surface tension variations with wetting agent concentration. It follows from Fig. 3 that an initial increase of wetting agent concentration produces a considerable decrease of surface tension and a slight change of viscosity. Subsequently, this relationship is reversed, i. e., the surface tension remains almost constant while the viscosity increases considerably. The reason is that initially adsorption occurs mainly at the air interface, and only later at the solvent interface.

Further evidence for the change of viscosity as the result of adsorption is provided by the data in Figs. 2 and 4. Figure 4 shows isotherms for the adsorption and the surface tension σ of wetting agent 1 for aqueous and gelatin solutions (three different gelatins), samples 1, 2, and 3. These results show that the adsorption of the wetting agent by each of the gelatins is different. In Fig. 2 (Curves II, III, and IV), the Relationship (5) is shown for these gelatins; this indicates that the different adsorption by each of the gelatin samples leads to a corresponding change of molecular configuration.

The above data provide direct experimental proof, based on adsorption measurements, of the validity of the views advanced earlier concerning the adsorption mechanism of the influence of surface-active substances on the viscosity of gelatin solutions.

SUMMARY

1. The view is confirmed that the increased viscosity of gelatin solutions on addition of surface-active substances is the result of adsorption of the latter, leading to changes in the shape of the gelatin molecules.

2. A relationship between the change in the specific viscosity of gelatin solutions and the adsorption of surface-active substances is derived and experimentally verified.

Scientific Research Institute for Cinephotography,
Moscow

Received December 29, 1955

LITERATURE CITED

[1] B. V. Deryagin, S. M. Levi, and V. S. Koltsov, Proc. Acad. Sci. USSR 79, 283 (1951).

[2] R. Simha, J. Phys. Chem. 44, 25 (1940).

[3] I. I. Zhukov, Colloid Chemistry, Leningrad State Univ. Press (1952).

EFFECT OF HYDROPHILIC PLASTICIZER ADDITIONS ON THE PROPERTIES OF CONCENTRATED CEMENT SUSPENSIONS

O. I. Lukyanova, E. E. Segalova, and P. A. Rebinder

The disperse structure of the hardened cement in concrete largely determines the mechanical properties and durability of concrete constructions. The formation of this structure in all its stages of origin and development involves colloidochemical processes. The course of hydration reactions of the cement clinker minerals in multiphase systems depends on the extent and qualitative composition of the cement particle surface and also on changes in the specific surface of the cement in the course of hydration.

New phases of the cement hydration products pass through the colloidal state as crystallization nuclei of the most rapidly crystallizing components, such as hydroaluminates and calcium hydroxide, or as slowly crystallizing calcium hydrosilicates, existing for a long time in a submicrocrystalline state.

The formation of a disperse structure as such in the hydration products, including various proportions of still nonhydrated cement grains, is due to bond formation between individual elements of the structure. These bonds may be of the nature of weak coagulation bonds or of crystal coalescence, according to the formation conditions and age of the structure.

It is important for pratical purposes to obtain hardened cement with a compact, monolithic structure, with a low susceptibility to the corrosive effects of the surroundings and a high mechanical strength. This goal is approached by decreasing the total porosity, especially the open (filtering) porosity, caused by evaporation of free water. Effective condensation of the structure is achieved by the combined use of various mechanical and physicochemical methods. Among the substances added to cement pastes and concrete mixes for increasing their density, a special position is held by organic surface-active substances which render the cement particle surfaces hydrophilic. Lignosulfonates in sulfite alcohol wastes (SSB) are most often used for this purpose.

The effects of hydrophilizing plasticizers on cements, caused by the properties of their adsorbed layers, are extremely varied, and are not confined to condensation of the hardened cement structure. It was discovered as early as 1937 [1] that additives of this type have a stabilizing effect on cement suspensions, retard cement hydration, and modify the crystallization rate of the hydration products.

The stabilizing and peptizing effects of SSB on cement suspensions have been discovered in numerous experimental investigations by Soviet [2-6] and foreign [7-9] scientists. The effects of SSB additions on the rate of chemical reaction between cement and water [2, 10], and on modification of the crystallization of cement hydration products and of the individual minerals of cement clinker [11-13] have also been studied. The influence of this plasticizer on the physical structure and mechanical properties of hardened cement has been investigated in detail [2-8].

In the present investigation we have studied some aspects of the influence of SSB lignosulfonates on structure formation in concentrated aqueous suspensions (pastes) of ground Portland cement clinkers during the initial stages of their interaction with water. The materials studied were factory Portland cement clinkers with different tricalcium aluminate contents, as it is known that the principal reactions in the initial period of interaction between Portland cement and water are hydration of the aluminate of the clinker and their interaction with the other cement components [2, 14]. The mineralogical composition of the clinker, calculated from chemical analysis data, is given in the table.

TABLE

Composition of the Portland Cement Clinkers Studied

Factories	Mineralogical composition, %			
	$3CaO\cdot Al_2O_3$	$3CaO\cdot SiO_2$	$2CaO\cdot SiO_2$	$4CaO\cdot Al_2O_3\cdot Fe_2O_3$
Komsomolets (K)	5	58	18	16
Novorossiyski (N)	8	56	22	13
Gigant (G)	9	53	20	14
Chernovechensky (C)	11	51	22	11

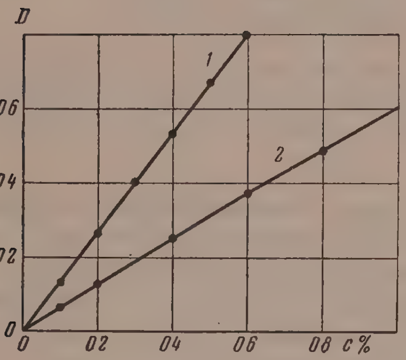

Fig. 1. Optical density of SSB lignosulfonate solutions; 1) pH 6.0; 2) pH < 3.0.

The SSB plasticizer used in our experiments consisted mainly of calcium lignosulfonates, and had a total solids content of 52.32%, including 3.62% calcium and 4.61% reducing substances, inclusive of 2.80% sugars. The small sugar content does not affect the properties of SSB as a cement plasticizer.

The action of calcium lignosulfonates on cement paste, suspensions, or concrete mixes depends largely on their adsorbability on the cement particles. It was therefore necessary to study the behavior of SSB lignosulfonates in cement suspensions during the initial period of interaction between the cement and water. The colorimetric method was used for determining lignosulfonate concentration in aqueous solutions after definite times of contact with the cement. The colorimetric method of lignosulfonate determination is free from error caused by different adsorbability of the lignosulfonates occurring is SSB plasticizers. The same method has been used by Shestoperov and others [2, 9].

In the pH range from 3 to 9 the color intensity of lignosulfonate solutions greatly depends on the acidity of the medium. This is important in relation to cement suspensions, in which large pH variations in the direction of increased alkalinity are possible. Our determinations showed that the optical density (D) of lignosulfonates, measured by the photoelectric colorimeter, greatly diminished with increasing acidity (Fig. 1), reaching a limiting value which does not change on further decrease of pH. Solutions of maximum acidity were therefore used for determinations of the concentration of lignosulfonate solutions. Despite the decreased sensitivity, the accuracy of the determinations is increased by acidification because the aqueous extracts of the cement suspensions do not become turbid in air.

Our experiments showed that adsorption of SSB lignosulfonates in cement suspensions is irreversible over a wide range of additions of SSB to the cement, including adsorbed layers containing 40-50 mg of lignosulfonates per 1 g cement, formed when the system contains more than 5% SSB on the weight of the cement. The adsorption becomes partially reversible at higher lignosulfonate contents in the cement suspensions. When such suspensions are mixed with water, some of the adsorbed substance can pass back into solution.

The irreversibility of the adsorption can be attributed to formation of surface compounds between the lignosulfonates and the clinker minerals, or peculiar denaturation of the former in the surface layers. This latter hypothesis is quite probable, as graphite, which is chemically inert to lignosulfonates, also adsorbs them irreversibly [15].

The formation of adsorbed layers of SSB lignosulfonates is a rapid process, completed within a few minutes. However, the amount of bound lignosulfonates may continue to increase, although at a much lower rate, owing to changes occurring in the system as the result of interaction between the cement and water. The initial adsorption, determined after 5 minutes of contact between the cement and water, or found by extrapolation of the kinetic curves for the binding of the lignosulfonates, comprises the main part of the adsorbed substance, and is a characteristic value. The initial adsorption (a_0) is linearly related to the SSB content of the system (Fig. 2). The linear relationship is also valid for very large additions of SSB, beyond the limits of those used in practice, 8-10% on the cement content. If systems are compared at equal lignosulfate concentrations in the solutions, the results are not independent of the amount of adsorbent (Curves 1,2 and 3,4, Fig. 2). If, however, the basis of comparison is the SSB content of the system relative to the cement content, the values for the adsorption are similar (practically identical) even for systems with an 8-fold difference of the water – cement (w/c) ratio (Curves 5,6, Fig. 2). Therefore, in studying the effects of adsorbed lignosulfonate layers on structure formation in cement suspensions, the SSB concentration in the system should be expressed as a percentage of the cement content.

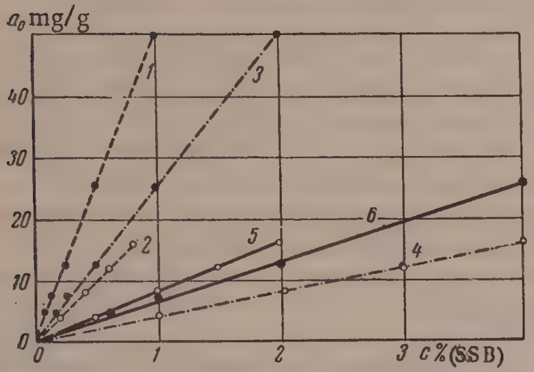

Fig. 2. Initial adsorption of SSB lignosulfonates in cement suspensions: 1, 3, 6 w/c ratio 4.0; 2, 4, 5) w/c ratio 0.5): 1,2) percentage concentration of SSB in solution after adsorption; 3,4) ditto, before adsorption; 5,6) SSB addition as percentage of the cement.

The peculiar character of lignosulfonate adsorption in cement suspensions is probably related to the gel-like nature of the adsorbed layers. The gel-like nature and the stabilizing action of adsorbed lignosulfonate layers in cement suspensions are confirmed, for example, by measurements of the volume of deposits formed in suspensions containing added SSB. The relative volume of the deposit (V) in a stabilized suspension greatly decreases with increasing amounts of lignosulfonates adsorbed by the cement particles, as Fig. 3 shows. This corresponds to increased stabilization of the suspension, i. e., increasingly complete prevention of coagulative structure formation. Complete stabilization of cements ground to medium fineness (with specific surface of 0.2-0.4 m^2/g is reached with additions of 0.5 to 1.0% SSB, on the weight of cement. The initial adsorption (a_0) is 3-5 mg per 1 g cement. The further increase of the volume of the deposit with increasing SSB content in the system is explained by the formation of thick gel-like lignosulfonate layers on the cement particles.

The stabilizing action of SSB on cement suspensions could not be applied in practice for increasing the density of hardened cement if the lignosulfonates did not, in addition, retard processes of cement hydration and crystallization of the newly formed materials. In presence of SSB, a cement suspension remains in its initial stabilized state for a considerable time, which depends on the amount added. The period during which the cement suspension remains in the retarded state may be termed the induction period of structure formation or of hydration.

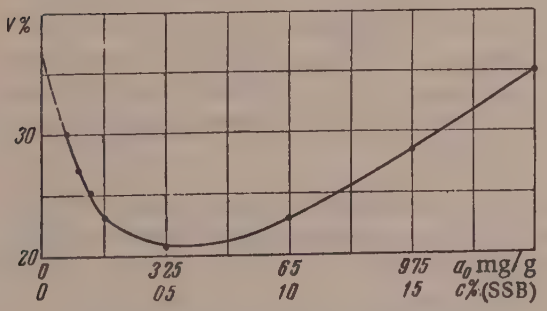

Fig. 3. Relative volume of deposits in cement suspensions stabilized by additions of SSB: $V=v/v_0 \times 100$ where v and v_0 are the volume of the deposit and the total volume of the suspension. Clinker G; S=0.35 m^2/g; w/c= 4.0.

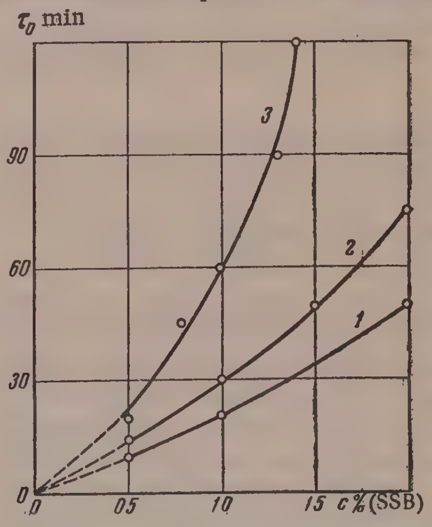

Fig. 4. Duration of the structure formation and hydration induction period (w/c = 0.5) : 1) clinker G; S = 0.5 m^2/g; 2) clinker C; S = 0.35 m^2/g; 3) clinker K; S = 0.5 m^2/g.

The variations in the mechanical properties of cement pastes during the induction period are very slight. The end of the induction period is easily established by the rapid acceleration of structure formation in cement paste, accompanied by an increase of its plastic strength.

The variation of the induction period (τ_0) with the amount of SSB added, for clinkers with different degrees of dispersion and tricalcium aluminate contents is shown in Fig. 4. A comparison of Curves 1 and 3 shows that the clinker with the higher tricalcium aluminate content has the shorter induction period for the same nominal specific surface and with equal amounts of SSB. Curves 1 and 2 represent clinkers with similar tricalcium aluminate contents but differing in specific surface. Comparison of Curves 1 and 2 shows that the clinker with the smaller specific surface has the longer induction period. The duration of the induction period also depends on the concentration of the cement suspension, decreasing with increase of the latter. For example, for the high-aluminate clinker "G", with S = 0.5 m^2/g (retarded by addition of 0.5% SSB), the induction period is increased approximately five-fold as the water – cement ratio increases from 0.4 to 4.0.

During the induction period, concealed processes occur in cement paste stabilized and retarded by additions of SSB, which have almost no effect on the mechanical properties during this stage, but which subsequently lead to the start of structure formation, the setting of the cement paste. Colorimetric measurements showed that the lignosulfonate content of the aqueous phase of the cement suspension does not remain constant, but gradually decreases with time. The sorption of lignosulfonates from solution by the cement occurs at a considerably lower rate than the initial adsorption. Fig. 5 shows the kinetics of sorption of lignosulfonates from aqueous solution by cement, for a cement paste made from clinkers with high and low aluminate contents. It is seen that SSB lignosulfonates are completely taken up from solution by cement paste in the course of time, and that this process is completed earlier in the high-aluminate cement.

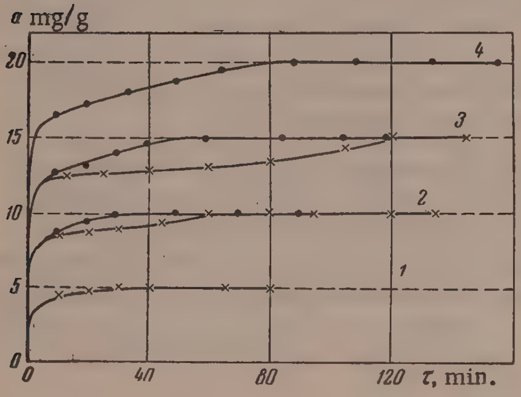

Fig. 5. Kinetics of SSB lignosulfonate adsorption by cement pastes (w/c = 0.5);• – clinker C; S = 0.35 m^2/g; x – clinker K; S = 0.5 m^2/g; 1) 0.5% SSB; 2) 1.0% SSB; 3) 1.5% SSB; 4) 2.0% SSB.

This effect is explained [16, 17] by adsorption of lignosulfonates on the clinker hydration products, the formation of which is greatly retarded in presence of lignosulfonates. Tricalcium aluminate, as the softest and most hydrophilic mineral in cement clinker, undergoes especially strong dispersing action of the adsorbed layers, and is at the same time the most rapidly hydrated mineral in the clinker.

The end of SSB sorption from the aqueous phase of the cement paste coincides with the end of the induction period, and with sharp acceleration of hydration and structure formation in the system. This is seen in Fig. 6, which shows the results of parallel determinations of the kinetics of lignosulfonate adsorption and of structure formation in cement pastes. The end of the induction period and complete sorption of the lignosulfonates from the solution may be somewhat delayed by prolonged stirring of the cement paste. Possibly this is the consequence of a more uniform distribution of SSB in the system. The free lignosulfonates in the solution adsorptively retard the development of new phase nuclei and thus delay the formation of a crystallization structure.

The induction period is followed by a sharp rise of the plastic strength of the cement paste, due to the formation of a crystallization structure in the hydroaluminate [14]. The structural strength in systems with moderate additions is found to be higher than in systems without additions. This effect is especially pronounced in high-aluminate clinkers. Figure 7 shows the kinetics of structure formation in cement pastes made from high-aluminate clinkers (without gypsum) with additions of SSB. Clinker N (Fig. 7, b), with additions of 0.1-0.5% SSB, and clinker G (Fig. 7, a), even with 1 and 2% SSB, show considerably greater increases in the strength of the hydroaluminate structure after the end of the induction period than systems without additions.

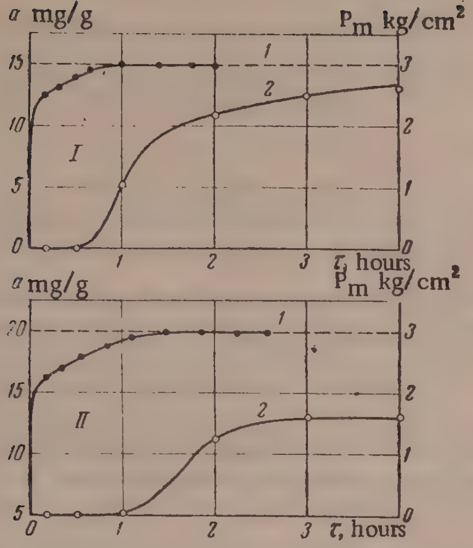

Fig. 6. Kinetics of structure formation and lignosulfonate adsorption in cement pastes (I) 1.5% SSB; II) 2.0% SSB); 1) lignosulfonate adsorption; 2) plastic strength of the cement paste (P_m).

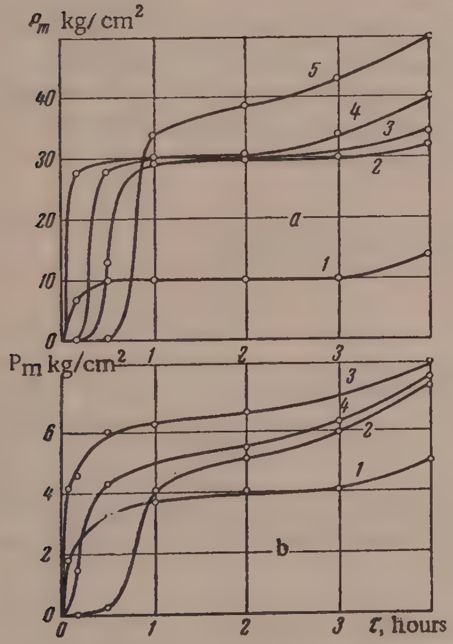

Fig. 7. Kinetics of structure formation in cement pastes made from high-aluminate clinkers (a) clinker G; S = 0.5 m²/g; w/c = 0.25; b) clinker N; S = 0.2 m²/g; w/c = 0.4): 1) without SSB; 2) 0.25% SSB; 3) 0.5% SSB; 4) 1.0% SSB; 5) 2.0% SSB.

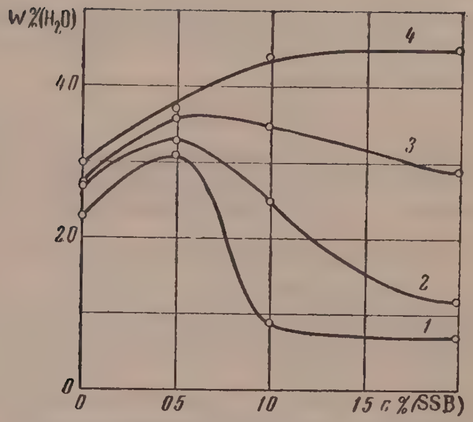

Fig. 8. Contents of chemically bound water (clinker C; S = 0.35 m²/g; w/c = 0.26): 1) 30 minutes after mixing; 2) 1 hour; 3) 3 hours; 4) 7 hours.

The increase of the strength of the structure may be caused by adsorptive dispersion of tricalcium aluminate in the clinker, resulting in an increase of its effective surface and increasing its rate of hydration (solution and therefore crystallization of the hydrate) in presence of SSB additions; this, in turn, results in a more rapid increase of the plastic strength. However, at very high SSB contents structure formation is retarded and the plastic strength of the cement paste is decreased, as can be seen, for example, in Fig. 7,b. This is probably caused by adsorptional blocking of the contacts in the crystallization structure of the hydroaluminate.

Acceleration of the hydration of high-aluminate cements in presence of small amounts of SSB may be observed by means of direct determinations of the kinetics of the chemical binding of water by cement pastes. Figure 8 shows the contents of chemically bound water (W) in cement paste made from high-aluminate clinker C with additions of 0 to 2% SSB, 30 minutes, 1, 3, and 7 hours after mixing of the cement paste. For these determinations the cement paste was treated with alcohol and ether; the resultant powder was dried in a vacuum dessicator and then heated at 1000° to constant weight. A correction for the lignosulfonates, burnt at this temperature, was introduced into the calcination loss values.

It is seen from Fig. 8 that additions of SSB favor an acceleration of chemical action between water and cement clinker, or largely the tricalcium aluminate in it. This acceleration occurs after the end of the induction period, during which very little water is combined. Therefore,in presence of small amount of SSB, acceleration of the hydration is already noticeable 30 minutes after mixing (Curve 1, Fig. 8), while with 1-2% SSB the amount of bound water becomes greater than in the system without added SSB only after several hours (Curves 3,4, Fig. 8).

SUMMARY

1. The adsorption of SSB lignosulfonates by cement suspensions has been studied by means of an improved technique for the colorimetric determination of lignosulfonates in solution.

2. It is shown that the initial adsorption of lignosulfonates increases linearly with increasing SSB content in the cement suspensions, up to 8-10% SSB on the cement. The adsorption is independent of the cement content of the suspension if the SSB concentration is expressed as a percentage of the cement weight; this is a consequence of the irreversible character of the adsorption.

3. The stabilizing effect of SSB lignosulfonates on cement suspensions increases with increasing adsorption and reaches a maximum when the adsorption reaches 3-5 mg/g for cements of moderate fineness (0.2-0.4 m^2/g).

4. The effect of the amount of SSB added on the duration of the induction period of structure formation and hydration has been studied in clinkers of different mineralogical compositions and degrees of dispersion. With equal amounts of SSB the length of the induction period decreases with increasing fineness and tricalcium aluminate content in the clinker, and also with decreasing water content in the suspension. Increase of the amount of SSB added to the suspension lengthens the induction period.

5. The content of SSB lignosulfonates in the liquid phase of the suspension was found to decrease during the induction period; this is caused by binding of the lignosulfonates in the formation of new surfaces during adsorptive dispersion of tricalcium aluminate and in the initial stage of crystallization of the hydroaluminate.

6. It is shown that the strength of the crystallization structure of the hydroaluminate increases and passes through a maximum with increasing amounts of added SSB in the cement suspensions. The amount of chemically bound water increases continuously in the process. This is probably explained by adsorptive dispersion of the tricalcium aluminate, eventually leading to accelerated hydration and structure formation in the suspension. The decreased strength of the structure at very high SSB contents is due to adsorptive blocking of the contact points in the crystallization structure of the hydroaluminate.

The M. V. Lomonosov State University, Moscow
Chair of Colloid Chemistry

Received October 5, 1956

LITERATURE CITED

[1] P. A. Rebinder, Bull. Acad. Sci. USSR, Div. Tech. Sci., No. 4 (1937).

[2] S. V. Shestoperov, . M. Ivanov, A. N. Zashchepin, and T. Yu. F. Lyubimova, Cement Concrete With Plasticizing Additions, Road Construction Press, Moscow (1952).

[3] V. I. Soroker, Bull. Building Technol., No. 10 (1947); Plasticizers for Cement Pastes and Concretes, Moscow, Coal Tech. Press (1951); Plasticized Concretes and Pastes, Moscow-Leningrad, State Building and Architecture Press (1953).

[4] Ts. G. Ginzburg, Hydrotech. Construct., No. 4 (1949); Plasticizing Additions to Hydrotechnical Concrete, Moscow-Leningrad, Hydroelectric Power Press (1956).

[5] B. D. Trinker, Use of Plasticized Cement and of Plasticizing Additions to Concrete, State Construction Press (1952).

[6] Yu. M. Butt and T. M. Berkovich, Cements with Surface-Active Additions (1953).

[7] E. W. Scripture, Eng. News Record, 127, No. 23, (1941;) Pit and Quarry 36, No. 2 (1943).

[8] T. C. Powers, J. Am. Concr. Inst.17, No. 2 (1945).

[9] F. M. Ernsberger, N. G. France, Ind. Eng. Chem. 37, No. 6, (1945).

[10] B. Ya. Yampolsky and E. S. Solovyeva, Trans. III All-Union Conf. Colloid Chem., 42, Acad. Sci. USSR Press, Moscow-Leningrad (1956).

[11] V. V. Stolnikov, Proc. Acad. Sci. USSR, 71, No. 2 (1950); J. Appl. Chem., 23, No. 7 (1950).*

[12] A. B. Shekhter, N. N. Serb-Serbina, and P. A. Rebinder, Proc. Acad. Sci. USSR, 89, No. 21 (1953).

[13] V. A. Tikhonov and L. A. Tikhomirova, J. Appl. Chem., 28, No. 10 (1954).*

[14] P. A. Rebinder, Trans. Conf. on Cement Chemistry, 125, Industrial Construction Press, Moscow (1956); E. E. Segalova and E. S. Solovyeva, ibid., 138.

[15] L. V. Lyutin and G. V. Zakharova, J. Phys. Chem., 4, No. 3 (1933); Colloid J., 4, No. 2-3 (1938).

[16] P. A. Rebinder and E. E. Segalova, Nature, No. 12 (1952).

[17] E. E. Segalova, P. A. Rebinder, and O. I. Lukyanova, Bull. Moscow State Univ., No. 2 (1954); Trans. III All-Union Conf. Colloid Chem., 26, Acad. Sci. USSR Press, Moscow-Leningrad (1956).

---

* Original Russian pagination. See C. B. translation.

PREPARATION OF FERRIC AND ZIRCONIUM HYDROXIDE ORGANOSOLS

V. N. Maslov

The transfer of colloid particles from one dispersion medium to another was observed long ago [1], and has been termed "the Wikkelblech phenomenon" and "pseudoextraction"[2]. The partial coagulation at the interface and within the liquid phases which occurs in the process is now explained [3] by lyophobization of the colloid particle surfaces with respect to both dispersion media.

The preparation of organosols from the corresponding hydrosols by transfer from one medium to another is very rarely used. A definite combination of dehydrating and lyophilizing factors is required for the formation of organosols by this method. For example, by the use of a third liquid which is distributed between the first two, as an auxiliary dehydrator, it proved possible to transfer selectively certain soil colloids from an aqueous into an organic phase [4]. This method has been studied in detail in relation to gold hydrosols and various organic systems [5]. It has also been shown that dissolved electrolytes influence the distribution of colloidal gold between liquid phases [6]. American patents [7] describe the production of organosols by multistage operations, with consecutive introduction of intermediate dispersion media, and including the removal of water by distillation. By replacing water in W, Mo, and Zr coagulates by acetone, and the latter by various hydrocarbon media, it proved possible to obtain organosols of these metals in presence of surface-active stabilizers and rubber [8].

Definite interest attaches to determination of the conditions in which colloidal hydroxides of heavy metals, having great affinity for water, may be transferred into an organic liquid in a single step, without preliminary dehydration of the system.

Colloidal solutions of ferric and zirconium hydroxides, prepared hydrolytically from $FeCl_3$ and $Zr(SO_4)_2$ [9], were used in our work. The iron contents of the aqueous and organic phases were determined by means of radioactive tracers. Benzene and toluene were used as the nonpolar liquids. The following methods were used for intermediate dehydration: 1) separation of the particles at the aqueous solution – air interface; 2) preliminary saturation of the air with vapor of the corresponding organic liquid; and 3) addition of a third liquid (acetone), distributed between the phases. The organosols were stabilized by additions of rubber and oxidized kerosene to benzene or toluene.

The simple apparatus shown in the diagram was used for preparation of the organosols. Each experiment lasted 30 minutes. The volumes of the aqueous phase and organic liquid were 115 ml and 25 ml respectively. Bubbles of air, 3-5 mm in diameter, were bubbled consecutively through the two liquid phases. Only the colloid particles which had been at the aqueous solution – air interface and were thus prepared for transfer into the other phase generally came into contact with the organic liquid. To prevent the ascent of bubbles near the walls, a directing ring was used; its performance was improved considerably by hydrophobizing treatment of its surface in diethyldichlorosilane or phenyltrichlorosilane vapor for 20 minutes [10].

It was found that when air, both with and without organic vapors in it, is bubbled through, no transfer of colloidal ferric and zirconium hydroxide into pure benzene or toluene occurs at all, and the film at the interphase boundary remains very thin and transparent. Additions of up to 4% (on the weight of the organic phase) of oxidized kerosene result in the transfer of accidentally present fine particles (dust, etc.) into the organic phase, and at the end of the bubbling a silvery opalescent film is seen at the interphase boundary. However, no transfer of the colloidal hydroxide occurs in this case either, or on addition of 0.005% rubber. The result is not changed by the presence of up to 4% acetone in the toluene, if rubber or oxidized kerosene are absent.

Simultaneous addition of 1% oxidized kerosene, 0.005% rubber, and 4% acetone, and the bubbling of air saturated with benzene or toluene vapor, results in appreciable transfer of the hydroxides into the organic phase. Ferric and zirconium hydroxide organosols are quite transparent, but the former has a brownish color. A material balance shows that from 25 to 60% of the colloid taken remains in the films at the separation boundary. It is very helpful to dissolve part of the acetone in water first. In this case up to 40% of the ferric hydroxide was extracted into the toluene, from an initial hydrosol with a concentration of 0.02 g Fe/liter. The ratio of the concentrations of the organosols to the concentrations of the residual hydrosols reached 4-5. The resultant ferric and zirconium hydroxide organosols in benzene and toluene are quite stable to light, heating, and keeping, and may be concentrated by evaporation.

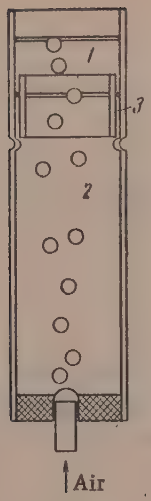

Apparatus for preparation of organosols by means of interphase air bubbling:
1) organic liquid; 2) original hydrosol;
3) directing ring.

SUMMARY

1. To facilitate the direct transfer of colloid particles from an aqueous into an organic phase, in addition to the usual methods, interphase bubbling of air saturated with vapor of the corresponding organic liquid was used.

2. The resultant organosols of ferric and zirconium hydroxides in benzene and toluene are stable on keeping and may be concentrated by evaporation.

The Mendeleev Institute of Chemical Technology
Moscow

Received April 14, 1956

LITERATURE CITED

[1] K. Wikkelblech, Z. angew. Chem. 19, 1953, (1906).

[2] K. Kharichkov, J. Russ. Chem. Soc., Chem. Section, 52, No. 1-2-3, 96 (1920).

[3] E. M. Natanson, Colloid J., 9, 428 (1947).

[4] N. K. Krupsky, Trans. 3-rd Intern. Congr. Soil Sci., Oxford 1, 46, (1953).

[5] A. Janek, A. Schmidt, Koll.-Z. 66, 296, (1936).

[6] T. R. Bolam, J. Bowden, Rec. trav. chim. 58, 1109, 1939; C. A. 34, 3560^8.

[7] C. A. 42, P2064 h.

[8] E. M. Natanson, Proc. Acad. Sci. USSR, New Series, 64, No. 6, 831 (1949).

[9] H. B. Weiser, Inorganic colloid chemistry, v. 2, New York, 1935.

[10] I. P. Alimarin and M. N. Petrikova, J. Anal. Chem., 10, No. 4, 251 (1955).

EXPERIMENTAL INVESTIGATIONS OF LAMINAR SYSTEMS

23. KINETICS OF THE FORMATION OF HYDROXIDE FILMS ON THE SURFACE OF CUPRIC AMMINE SOLUTIONS

S. G. Mokrushin and G. A. Kitaev

The spontaneous formation of hydroxide films on the surfaces of solutions of complex ammines of copper and nickel has been studied by one of the authors [1, 2]. The nature of the effect is that when such a solution is left to stand, hydrolysis of the complex salt accompanied by formation of colloidally dispersed hydroxide commences in its surface layers. The hydroxide particles become fixed in the solution surface, forming a very thin invisible film. The thickness of the film increases with time, it acquires interference colors and becomes visible.

The aim of the present investigation was to study the kinetic relationships in the formation and thickness increase of copper hydroxide films on the surface of cupric ammine solutions.

The copper hydroxide films were prepared by the improved technique described by Mokrushin [1], in which air is blown over the surface of a solution contained in a watch glass. In the present investigation a glass thermostat was used instead of the watch glass, while the air blown over the solution surface was heated and saturated with water vapor, so that the temperature of the solution was kept constant both throughout its volume and at the surface, and evaporation was prevented. The glass thermostat was heated by water by means of a Hoeppler circulation thermostat. The cup of the glass thermostat was cleaned by chromic acid mixture and then washed thoroughly with tap and distilled water. To prevent flow of surface-active substances onto the solution surface, a paraffin wax ring was made around the outer wall of the thermostat cup. The ammine solutions were made from copper sulfate solution and poured into the thermostat cup from a buret.

Experiments showed that a copper hydroxide film is not formed on a clean surface of ammine solution. If a monolayer of a nonvolatile surface-active substance is applied to the solution surface, a uniform lustrous hydroxide film is formed, exhibiting interference colors. It was found that a hydroxide film of more uniform thickness is formed on application of a substance which forms a liquid monolayer, such as oleic acid, to the surface of the solution. Substances which form solid films, such as palmitic acid, cetyl alcohol, and cellulose, also assist the formation of hydroxide films, but less uniform in thickness.

In the present communication the results of a study of the kinetics of copper hydroxide film formation on the surface of ammine solutions under a monolayer of oleic acid are discussed. Oleic acid was applied to the solution surface in a quantity sufficient to give a monomolecular layer. Ammoniacal solutions of copper sulfate of the following concentrations were studied: 0.025; 0.05; 0.10 and 0.15 mole/liter, at 10; 20; 30; 40; 50° with air blown at 0.5 and 1.0 liter/minute.

Figure 1 shows the growth of the thickness of hydroxide films on cupric ammine solutions. The thickness of the hydroxide films was determined by comparison of the interference colors of the films with the colors of Newton's rings in an air layer. The refractive index of the films was taken to be $n = 1.66$ [1].

Curve 1 (Fig. 1) represents the growth of a hydroxide film on a solution containing a slight excess of ammonia, while Curves 2 and 3 refer to solutions with ammonia in considerable excess. Comparison of the slopes of Curves 1 and 2 shows that excess ammonia in the solution has practically no effect on the rate of growth of the film thickness, but only affects the time interval before film formation begins. Variation of the rate of air blowing in the range 0.5-1.0 liter/minute has a similar effect. The character of Curves 2 and 3 is explained as follows. During the first 20-25 minutes the air blown over the solution surface removes excess ammonia. When the ammonia content of the solution has decreased enough for hydrolysis of cupric ammine to be possible, formation of the hydroxide film begins. At first isolated islets of the film are formed and the solution surface remains mobile. Gradually the islets become more numerous and finally they fill the whole surface of the solution, coalescing into a continuous immobile colorless film. The thickness of the film then begins to increase. It is easily seen that from 600 A the growth of film thickness is described by a linear equation. The rate of film growth is given by the tangent of the angle this line forms with the time axis.

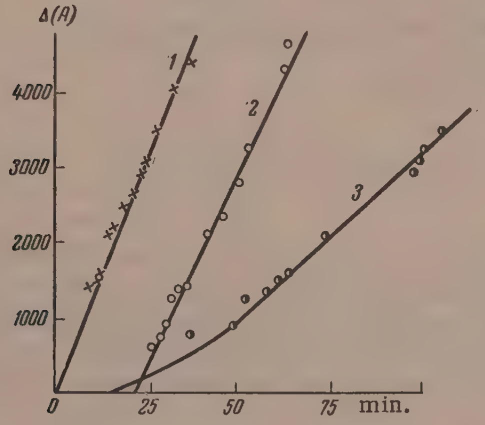

Fig. 1. Growth of the thickness of hydroxide films on cupric ammine solutions with concentration of 0.10 mole/liter (1 and 2) at 30° and 0.024 mole/liter (3) at 20°; air flow rate 0.5 liter/minute.

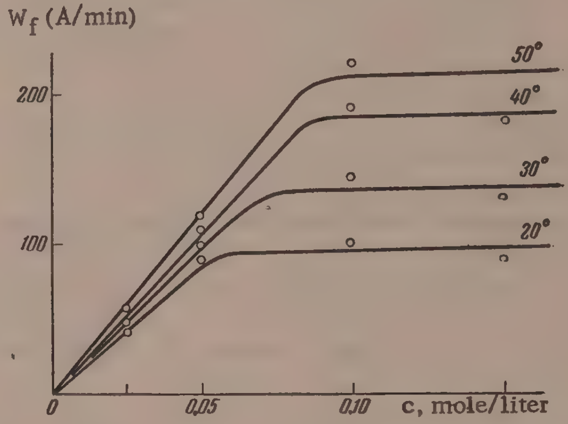

Fig. 2. Variation of the rate of growth of film thickness with concentration of cupric ammine solution at 20, 30, 40, and 50°.

Figure 2 shows the variation of the rate of growth of the film thickness (W) with concentration of the cupric ammine solution (c). The linear character of the initial portions of the curves indicates that the growth of films from solutions up to 0.1 mole/liter in concentration is determined by a process the kinetics of which can be represented by the equation for a monomolecular reaction.

The formation and growth of the film may be divided into several stages. In the first stage the rate of growth is determined by the rate of the reaction of ammine hydrolysis, i. e., by the formation rate of copper hydroxide, the material from which the film is formed. The hydrolysis reaction, for example of the complex ion $[Cu(NH_3)_2]^{2+}$, may be represented by the equation:

$$[Cu(NH_3)_2]^{2+} + 2H_2O = Cu(OH)_2 + 2NH_3 + 2H^+ .$$

Since the hydrolysis is accompanied by liberation of ammonia, the hydrolysis rate is determined by the rate at which ammonia is removed from the reaction zone.

In the second stage, the hydroxide particles become fixed on the solution surface. We regard this as a surface coagulation process, the kinetics of which may be represented by an equation for a reaction of the second order. It is probable that for solutions with a concentration of 1 mole/liter the surface coagulation process does not determine the rate of the aggregate process of hydroxide film growth. Conversely, in solutions of higher concentrations the rate of film growth is determined by the coagulation rate of the primary colloidally dispersed particles of copper hydroxide.

In order to find the rate-determining step, both the kinetics of ammonia evaporation and the kinetics of the hydrolysis reaction were studied. The kinetics of both processes can be described by an equation for a reaction of the first order, of the form

$$\frac{dx}{d\tau} = k(a - x),$$

where k is the reaction rate constant; a is the initial amount of ammonia or ammine complex; x is the amount of ammonia evaporated or ammine reacted in time τ.

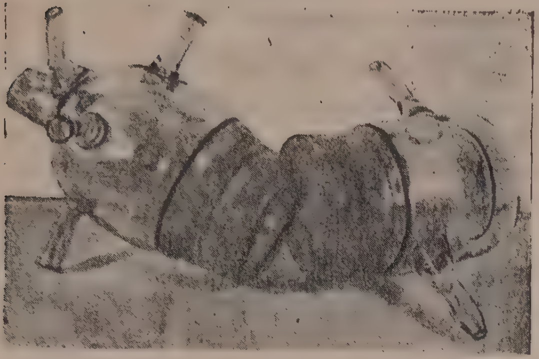

Fig. 3. Thermostat for studying the kinetics of ammonia evaporation and of the hydrolysis reaction (explanation in text).

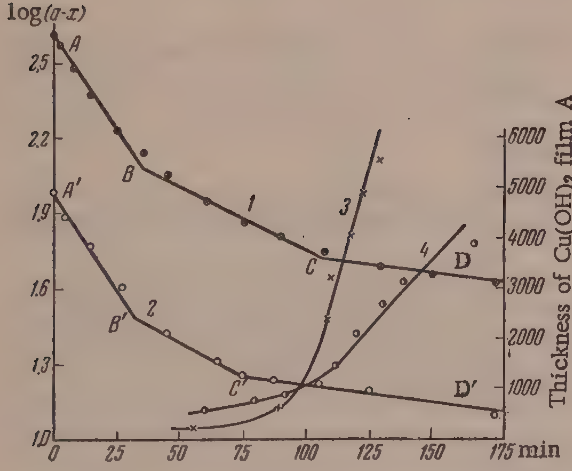

Fig. 4. Rate of ammonia evaporation (1,2) and growth of film thickness (3,4) for cupric ammine solutions with concentrations of 0.15 mole/liter (1) and 0.05 mole/liter (2,4) at 40°.

The glass thermostat shown in Fig. 3 was used for studying the kinetics of these processes. 10 ml of cupric ammine solution with an accurately known ammonia content was put into the lower part 1 of the thermostat. Heated air saturated with water vapor was fed through the central tube 2 of the upper part of the thermostat, and then passed into wash bottles containing sulfuric acid. Ammonia was absorbed in the first wash bottle, containing 50 ml of 0.2 N H_2SO_4; the second contained 50 ml water, to which was added two drops of 0.2 N H_2SO_4 and two or three drops of bromocresol purple or phenolphthalein. The amount of ammonia absorbed was determined by back titration of excess acid by caustic soda solution. The second wash bottle served to check the complete absorption of ammonia in the first. The growth of the film was observed (by the alternation of its interference colors) through the thermostat wall.

The kinetics of ammine hydrolysis was studied in the same thermostat by a potentiometric method with the use of a cathode voltmeter, whereby it was possible to observe continuously variations in the concentration (activity) of the copper ions in solution. A saturated calomel electrode was used as the reference electrode. A copper-plated platinum electrode and an electrolytic switch were introduced through the two side tubes 3 of the glass thermostat (Fig. 3) and securely sealed. In this way it was possible to observe the film growth, variation of Cu^{2+} ion activity, and removal of ammonia from the solution simultaneously.

Figure 4 shows the experimental data for the kinetics of ammonia evaporation and growth of the film thickness at 40°.

The ammonia contents in 10 ml of cupric ammine solutions corresponding to the inflection points B and B' were found to be 120 and 30 mg, and corresponding to the points C and C', 53 and 18 mg. These amounts of ammonia correspond to the calculated amounts necessary for the formation of complex ions: 102 and 34 mg for $[Cu(NH_3)_4]^{2+}$ and 51 and 17 mg for $[Cu(NH_3)_2 \cdot (H_2O)_2]^{2+}$.

The agreement between the calculated and experimental data leads to the following explanation of the process of formation and growth of copper hydroxide films. First, ammonia in excess of the amount stoichiometrically required for formation of the $[Cu(NH_3)_4](OH)_2$ complex and binding of the sulfate ions of the copper is removed. A comparison of the slopes of the regions AB and A'B' of Curves 1 and 2 shows that the rate of ammonia removal does not depend on the amount of it added to the solution. At the instants corresponding to points B and B', hydrolysis of the copper tetrammine complex begins according to the equation

$$[Cu(NH_3)_4](OH)_2 + 2H_2O = [Cu(NH_3)_2(H_2O)_2](OH)_2 + 2NH_3.$$

The rate of ammonia evaporation decreases, and is determined at this stage by the hydrolysis rate of the ammine. Thus, the regions BC and B'C' represent evaporation of the ammonia formed by hydrolysis of the copper tetrammine complex. It should be noted that no film is formed at this stage.

At the points C and C' the ammonia contents of the solution are 53 and 18 mg (the theoretical amounts are 51 and 17 mg). Hydrolysis of the diammine-diaquo complex commences at this point, with formation of copper hydroxide according to the equation:

$$[Cu(NH_3)_2(H_2O)_2](OH)_2 = Cu(OH)_2 + 2NH_3 + 2H_2O.$$

Fig. 4 shows that rapid growth of the hydroxide film commences at the same time. This confirms that the regions CD and C'D' represent evaporation of the ammonia formed by hydrolysis of the diammine-diaquo complex.

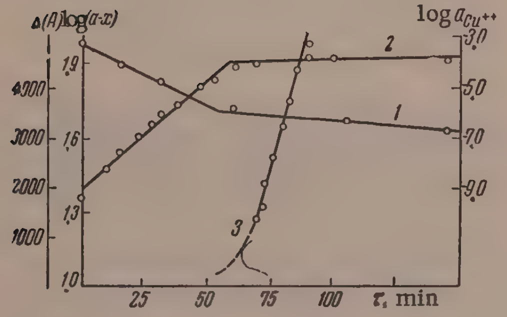

Fig. 5. Rate of ammonia evaporation (1), variation of the activity of copper ions with time (2), and growth of film thickness (3) for cupric ammine solutions at a concentration of 0.15 mole/liter, 40° and air blowing rate of 0.5 liter/minute.

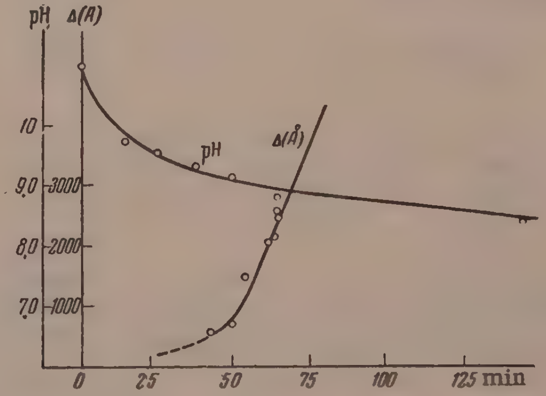

Fig. 6. Dependence of the growth of film thickness on the variation of pH with time for cupric ammine solution of c = 0.15 mole/liter.

Investigation of the kinetics of the hydrolysis of the cupric ammine complex by the potentiometric method, with simultaneous absorption of the liberated ammonia and observations of the growth rate of the hydroxide film, confirmed the mechanism of the process postulated above. As an example, Fig. 5 gives data for cupric ammine solution. The inflection point on Curve 1 corresponds to 52 mg ammonia in the solution, which corresponds to the amount necessary for formation of the diammine-diaquo complex. The inflection on the curve for the variation of cupric ion activity with time (2) coincides in time with the inflection on the ammonia evaporation curve (1). Formation and thickness increase of the film begins at the same time, which indicates the start of hydrolysis of $[Cu(NH_3)_2(H_2O)_2]^{2+}$ and formation of copper hydroxide.

The cupric ion activity at the start of film formation (inflection point on Curve 2, Fig. 5) is $a_{Cu^{2+}} = 10^{-3.9}$ Assuming that his is equal to the concentration, and using the value of the decomposition constant of the diammine complex

$$K = \frac{[Cu^{2+}]\cdot[NH_3]^2}{[Cu(NH_3)_2^{2+}]} = 1.05\cdot10^{-8},$$

When the ammonia concentration in the solution has been determined, it is possible to calculate the solution pH at which hydrolysis of the $[Cu(NH_3)_2]^{2+}$ ion occurs. The ionization constant of NH_4OH is $10^{-4.75}$ [4], and the ionic product for water at 40° is $10^{-13.42}$. Hence the pH is 9.73.

TABLE

Calculated Values of m_1 and m_2 in mg/min for Cupric Ammine Solution at 40° and Air Blowing Rate of 0.5 liter/min

Solution concentration in mole/liter	$m_2 \cdot 10^{-3}$	$m_1 \cdot 10^{-3}$
0.025	34	34
0.05	68	64,5
0.10	136	97
0.15	204	90

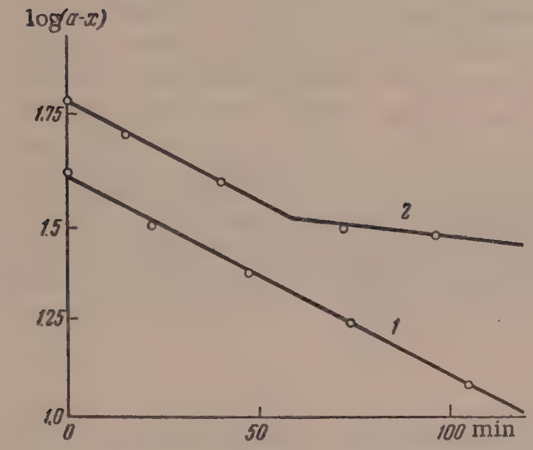

Fig. 7. Rate of evaporation of ammonia from solutions with a clean surface (1) and with surface covered with a monolayer of oleic acid (2).

The results of our simultaneous observations of variations of solution pH and film thickness, given in Fig. 6, confirm this approximate calculation. Film growth does in fact occur at pH 9.0. In our opinion, therefore, it may be concluded from the foregoing that rapid film growth coincides with the start of hydrolysis of the diammine-diaquo complex, accompanied by formation of copper hydroxide.

To decide whether ammonia evaporation or hydrolysis of the cupric ammine complex is the rate-determining step, a study was made of the evaporation of ammonia from a solution with a clean surface, i. e., in conditions in which a hydroxide film is not formed. The results of one such experiment are shown in Fig. 7. Hydroxide film begins to form at the point of inflection on Curve 2. The course of Curves 1 and 2 shows that evaporation of ammonia through the hydroxide film is the determining step in the growth of the copper hydroxide film.

The foregoing experimental results indicate that film formation coincides with the start of hydrolysis of the diammine-diaquo complex, and the rate of growth of the hydroxide film is determined by the rate of ammonia evaporation through this film.

Satisfactory agreement may be demonstrated between data for the evaporation of ammonia from the solution and the rate of film growth for solutions of concentrations ≤ 0.1 mole/liter. The film area in our experiments was $S = 15.95\ cm^2$, the density of copper hydroxide $d = 3.37$ g/cc [4]; in one minute the film thickness increases by an amount which numerically corresponds to the film growth rate W in A/minute. Hence the weight increase m_1 of the film in unit time, i. e., the amount of copper oxide passing into the film, is $m_1 = SWd \cdot 10^3$ mg/minute. On the other hand, it is also possible to calculate the amount of copper hydroxide formed in the surface layers of solution in unit time from the rate of evaporation of the ammonia formed by hydrolysis of the complex ion $[Cu(NH_3)_2(H_2O)_2]^{2+}$.

The rate constant for the evaporation of ammonia through the hydroxide film is $K = 1.39 \cdot 10^{-3}\ min^{-1}$, and the evaporation rate is evidently Kc_{NH_3} where $c_{NH_3} = a - x$. In accordance with the equation for the hydrolysis of the $[Cu(NH_3)_2(H_2O)_2]^{2+}$ ion, the hydrolysis rate is equal to half the rate of ammonia evaporation, and can be calculated from the expression:

$$m_2 = \frac{1}{2} \cdot \frac{98}{17} k (a - x).$$

An examination of the tabulated values of m_1 and m_2 shows that for solutions with concentrations of 0.025, 0.05, and to some extent 0.5 mole/liter the amount of hydroxide passing into the film is equal to the amount formed in solution ($m_1 \sim m_2$).

For solutions the concentration of which is > 0.1 mole/liter, m_1 differs considerably from m_2, which indicates that at these concentrations the evaporation rate of ammonia does not determine film growth. We believe that in this instance coagulation of the colloidally dispersed copper hydroxide may be taken as the rate-determining step. Evidence for this is provided by electron microscope investigations of copper hydroxide films, carried out by Mokrushin, Kitaev, and Shabalina [5], who showed that copper hydroxide films are formed from colloid particles the size of which lies in the range 100-200 A. Larger particles cannot act as structural elements in the films.

In the formation of films on the surface of solutions with concentrations greater than 0.10 mole/liter, the coagulation rate of the originally formed copper hydroxide particles probably increases owing to an increase in the concentration of the surface sol. Consequently the number of particles of optimum size decreases, and as a result the rate of film thickness growth decreases also. The horizontal regions of the curves in Fig. 2 for solutions of high concentrations may be attributed to surface coagulation effects.

SUMMARY

1. A study has been made of the kinetics of growth of hydroxide films on the surface of cupric ammine solutions in relation to the concentration, temperature, and air blowing rate.

2. It is shown that $Cu(OH)_2$ films are not formed on clean solution surfaces. The presence of a monolayer of a surface-active substance is a necessary condition for film formation.

3. It is shown that the rate of film growth increases with increasing solution concentration and temperature and does not depend on the air flow rate.

4. On the basis of experimental data on the kinetics of ammonia evaporation and the hydrolysis of the cupric ammine, the process has been divided into the following steps: evaporation of excess ammonia, hydrolysis of the cupric tetrammine, hydrolysis of the diammine-diaquo complex, fixation of the colloidal copper hydroxide particles on the solution surface to form the film.

5. It is shown that for solutions with concentrations < 0.10 mole/liter the step which determines the growth rate of the $Cu(OH)_2$ film is evaporation of ammonia formed by hydrolysis of the diammine-diaquo complex, while for solutions of higher concentrations the rate-determining step is fixation of the hydroxide particles in the solution surface.

The S. M. Kirov Polytechnic Institute, Urals

Received May 28, 1956

LITERATURE CITED

[1] S. G. Mokrushin and P. S. Konyaev, J. Phys. Chem., 6, 1, 95 (1935).

[2] S. G. Mokrushin, J. Phys. Chem., 5, 8, 1082 (1934); Colloid J., 10, 4, 305 (1948).

[3] I. M. Kolthoff and J. J. Lingane, Polarography, State Chem. Press, Moscow-Leningrad, p. 185 (1948).

[4] Chemist's Reference Book, vol. 2, State Chem. Press, Moscow-Leningrad (1951).

[5] S. G. Mokrushin, G. A. Kitaev, and O. K. Shabalina, Proc. Acad. Sci. USSR, 1946, 1109 (1954).

THE RELATIONSHIP BETWEEN THE AFFINITY AND STRUCTURE OF DIRECT DYES

P. V. Moryganov and B. N. Melnikov

It has now been established that the selective takeup of direct dyes by cellulose fibers depends on such factors as linearity and plane structure of their molecules, the presence in the molecules of long chains of conjugated double bonds and groups capable of forming hydrogen bonds, and also a number of other less important factors. In Schirm's view [1], lengthening of the chain of conjugated double bonds between the outside auxochrome groups in the dye molecule leads to an increase in the residual valence forces at the ends of such a chain, and therefore increases the affinity of the dye for cellulose fibers. This readily explains why dyes derived from J acid have greater substantivity than dyes which are derivatives of γ or H acid.

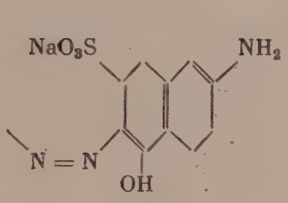

J-acid

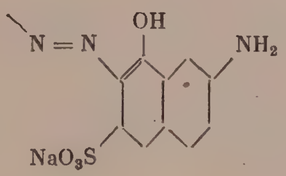

γ-acid

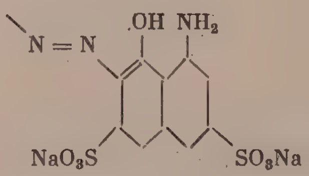

H-acid

The above formulas clearly show that the molecule of J acid has the longest chain of conjugated double bonds. According to Schirm, a dye molecule must contain a chain of not less than eight conjugated double bonds to ensure substantivity for cellulose fibers. Later work [2] has shown that this is not always true, a chain of five double bonds being sometimes quite sufficient. However, the lack of an exact definition of the concept of the affinity of a dye for a fiber delayed further detailed development of the theory of substantivity, as its value has frequently been determined under arbitrarily chosen conditions, making interpretation of the results difficult. Determinations of the affinity of direct dyes for cellulose fibers on a thermodynamic basis reported in a series of publications [3, 4] make it possible to verify and to extend considerably the views advanced earlier.

Accordingly, the purpose of the present work was determination of the thermodynamic affinity of a number of direct dyes of the same type with different lengths of conjugated double bond chains, and also a study of the effect of disrupted conjugation and of benzoylation of the free amino groups of the dyes on the affinity.

The affinity of a dye for the fiber was calculated from the formula:

$$-\frac{\Delta\mu^{\circ}}{RT} = \ln [D]_{\varphi}\cdot[\mathrm{Na}]_{\varphi}^{z} - \ln [D]_{\sigma}\cdot[\mathrm{Na}]_{\sigma}^{z} - (z+1)\ln V, \tag{1}$$

where $[D]_\phi$ and $[Na]_\phi$ are the concentrations of dye and sodium ions in the fiber in gram-ions per kilogram of absolutely dry fiber $[D]_\sigma$ and $[Na]_\sigma$ are the concentrations of the same ions in solution in gram-ions per liter; V is the effective volume of the cellulose phase in liters per kilogram of the absolutely dry fiber; $\underline{z}$ is the valence of the dye anion.

The theoretical derivation of this formula and a detailed description of the equilibrium dyeing method were given in a number of our earlier papers [4-6].

The equilibrium dyeing experiments were performed at 80 and 100° with the following dyes:

Direct Sky Blue K (C. I. 406)

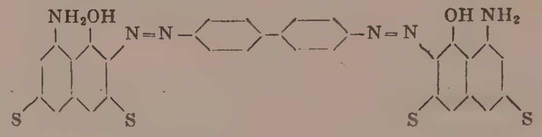

Direct Diazo Black O (C.I.395)

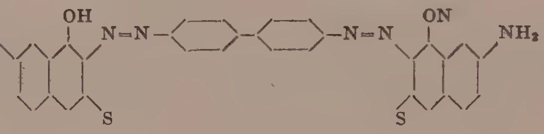

Analog of Direct Sky Blue K

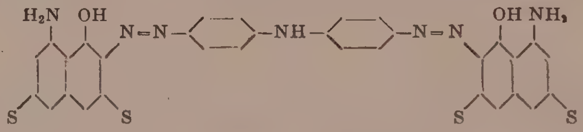

Benzoylated analog of Direct Sky Blue K

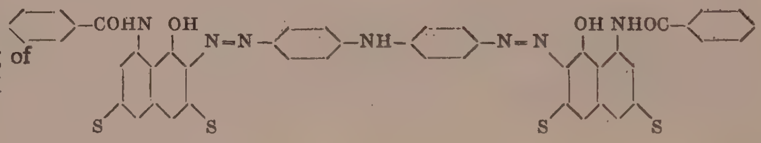

Analog of Direct Diazo Black O

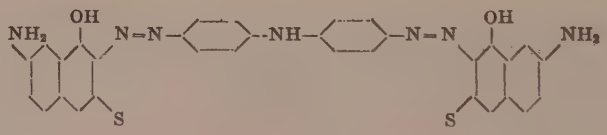

Benzoylated Analog of Direct Diazo Black O

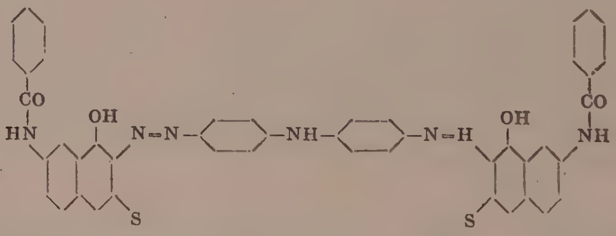

The results of determinations of the affinity of these dyes for cotton fabric are given in the table.

A comparison of the structure and affinities of the dyes studied shows that an increase of the number of sulfo groups in the dye molecule decreases affinity for cotton fiber. A particularly interesting feature is the sharp decrease of affinity in dyes derived from 4,4'-diamino-diphenylamine (analogs of Direct Sky Blue K and Direct Diazo Black O); this is probably largely explained by disruption of conjugation in the molecules of these dyes, and also partly by the fact that the azo groups in these dyes, in contrast to the corresponding dyes derived from benzidine, are separated by a distance greater than the repeat period of the cellulose macromolecule.

Dye	Experimental values in cal./mole		Calculated values in cal./mole	
	$-\Delta\mu^\circ_{373}$	$-\Delta\mu^\circ_{353}$	$-\Delta\mu^\circ_{373}$	$-\Delta\mu^\circ_{353}$
Direct Diazo Black O	5.40	6.06	—	—
Direct Sky Blue K	3.73	4.45	—	—
Analog of Direct Sky Blue K	2.34	2.56	—	—
Benzoylated analog of Direct Sky Blue K	3.77	4.38	3.85	4.07
Analog of Direct Diazo Black O	3.75	4.12	—	—
Benzoylated analog of Direct Diazo Black O	5.41	6.09	5.26	5.63

Replacement of hydrogen by the benzoyl residue in the amino groups increases the affinity of the dyes for cellulose in both cases owing to formation of carbamide groups, which confer high substantivity.

The higher affinity of benzoylated direct dyes in comparison with the same dyes before benzoylation may be attributed to an increase of the hydrocarbon—water interface by introduction of additional benzene rings into the dye molecule. This viewpoint has recently been developed extensively by Derbyshire and Peters [7].

In the formation of aqueous solutions of dyes, the large hydrophobic surfaces of their molecules cause the separation of water molecules against the action of intermolecular forces. This becomes possible only when the energy liberated in solvation of the sulfo groups present in the dye molecule completely compensates the absorption of energy in the formation of new hydrocarbon—water interfaces. Removal of dye from the solution by fixation in the fiber, and the consequent disappearance of hydrocarbon—water interfaces, results in a return of this energy, which appears in the form of free energy of dyeing. It is assumed that the dye is attached to the fiber by nonpolar van der Waals forces between the cellulose surface and the hydrophobic surface of the dye molecule. The solvated sulfo groups of the dye still remain solvated after the dye has become attached to the cellulose surface, at least until the dyed fiber has been removed from the dye bath and dried. Accordingly, introduction into the dye molecule of additional hydrophobic surfaces, with the same content of groups capable of strong hydration in them, leads to increase in the hydrocarbon—water interfaces, and consequently to decreased solubility on the one hand [8], and an increase of the free energy of dyeing on the other.

The decrease of the absolute value of the free energy of solvation, and therefore the increase of the free energy of dyeing, can be calculated from the formula:

$$-\Delta F = N\sigma\Delta S, \tag{2}$$

where ΔS is the increase in the molecular surface on introduction of the hydrophobic group R; σ is the free energy per unit R . . . solv. surface; N is the Avogadro number.

Yatsimirsky [8] showed that Equation (2) provides a route to quantitative evaluation of the influence of various groups on the solubilities of organic compounds. Hartley [9] and later Meggy [10], gave the value $\sigma = 30\,\mathrm{erg/cm^2}$ for the C—H . . . H_2O interface; Equation (2) can accordingly be written as:

$$-\Delta F = 0.043\,\Delta S. \tag{3}$$

In this equation ΔS is in A^2 and ΔF is in kilocalories. Equation (3) would be valid on the condition that all interaction between the separated water molecules ceases when the organic molecules are introduced into the solution. In reality the molecules do not become separated by infinitely large distances, interaction between them continues, and its value, according to Meggy [10], is about a half of the total free energy. Consequently, the free energy decrease resulting from introduction of the hydrocarbon residue into the aqueous solution is

$$-\Delta F = 0.021\,\Delta S. \tag{4}$$

The surface area of an individual molecule can be estimated from known values for different bond lengths; according to our data, the value for the benzene nucleus is 36 A^2. This value, which represents the increase of the hydrophobic surface of a benzoylated direct dye over that of the nonbenzoylated dye, makes it possible to calculate the expected increase in the affinity of the former dyes in comparison with the latter. The corresponding calculated values for the affinities of benzoylated dyes are shown in the table above.

The reasonably good agreement between the experimental and calculated values suggests that the increased affinity of benzoylated dyes may be attributed not only to the strong substantivizing influence of the carabamide groups, but also to the considerably greater hydrophobic surface of these dyes. Good confirmation of this is also provided by the azotol series; they each contain a single carbamide group in the molecule, but differ very greatly in fiber affinity; this may be explained by the increase of the hydrophobic surface of the azotols with increasing molecular complexity.

SUMMARY

1. The length of the conjugated double bond chain is shown to have a strong influence on the affinity of direct dyes for cotton fiber. Disruption of this chain results in a sharp decrease of affinity, while replacement of one of the hydrogen atoms in the amino group by a benzoyl residue compensates for this decrease, and raises the affinity to the level of that of a nonbenzoylated dye before disruption of the conjugation.

2. It is shown that quantitative calculation of the increase in the affinity of a dye for fibers by introduction of new hydrocarbon–water interfaces into its molecules is possible in principle.

We express our gratitude to S. N. Solodushenkov for providing the dyes, derived from p,p'-diaminodiphenylamine, synthesized by him.

LITERATURE CITED

[1] E. Schirm, J. Prakt. Chem. 144, 69 (1935).

[2] B. M. Bogaslovsky, Dissertation (1946).

[3] W. J. Marshall and R. H. Peters, J. Soc. Dyers Col. 63, 446 (1947).

[4] P. V. Moryganov and B. N. Melnikov, Trans. Ivanovo Inst. Chem. Technol. 5, 121 (1955).

[5] P. V. Moryganov and B. N. Melnikov, Textile Ind. No. 8, 33 (1955).

[6] P. V. Moryganov and B. N. Melnikov, Colloid J. 18, 49 (1956).

[7] A. N. Derbyshire and R. H. Peters, J. Soc. Dyers Col. 71, 530 (1955).

[8] K. B. Yatsimirsky, J. Anal. Chem. 8, 5, 314 (1953).

[9] G. S.Hartley, Koll.-Z. 88, 22 (1938).

[10] A. R. Meggy, J. Soc. Dyers Col. 66, 510 (1950).

Received February 12, 1956

Ivanovo Institute of Chemical Technology

STRUCTURE OF HIGH POLYMERS

COMMUNICATION 18. STRENGTHENING OF THE MOLECULAR STRUCTURE OF TIRE YARN

A. B. Pakshver, L. S. Gerasimova, and Kh. N. Kozlovskaya

Tire yarns made from artificial fibers have high heat endurance (viscose yarn) or high tensile strength (capron). Nevertheless, these fibers, especially capron, have a serious defect: the fibers are very extensible under low loads, and as a result the tires are deformed by the action of small loads (i. e., the tires " swell "). This effect can be explained by the low value of the modulus M.* We have shown [1] that the magnitude of the modulus M depends on intermolecular interaction, which is determined by the existence of dipole bonds between the polar groups of the macromolecules, and it may increase or decrease within wide limits according to the methods for the production and subsequent processing of the fibers. When fibers are stretched, especially in the heated or swollen state, the molecular structure is strengthened considerably; this is manifested in an increase of the modulus M, a decrease of the sorption capacity [1] and rate of sorption of various polar substances [2], retardation of variation of fiber length during swelling [3], and decrease of the heat of solution [4]. It is known [5] that when fibers, especially thermoplastic, are stretched, the strengthening of the molecular structure is accompanied by increase in the heat endurance of the fibers.

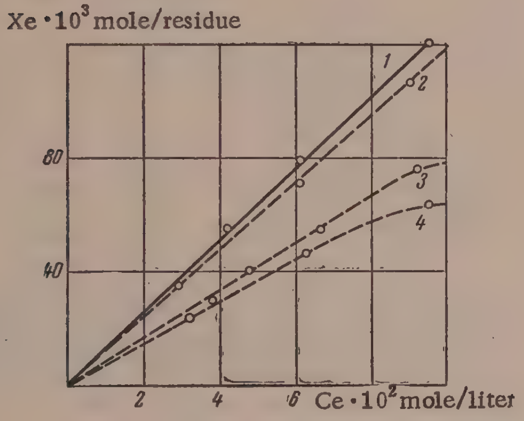

Fig. 1. Sorption of phenol by capron yarn. 1) Original yarn at 17°; 2) heat-stretched at p = 500 g, 17°; 3) ditto, 55°; 4) ditto, 100° .

The stretching of fibers in the heated or swollen state is accompanied by weakening of intermolecular bonds and slipping of the macromolecules in the direction of the stretch. If the cause of the weakening of the intermolecular bonds is then removed, then the intermolecular forces may either increase, or decrease as the result of increasing flexibility of the macromolecules, depending on whether the fibers are cooled or washed in the stretched or relaxed state. In the former case the "rigidity" of the fiber is increased and the modulus M increases considerably; in the latter, the modulus M decreases and the fiber becomes softer. In tire cord production it is particularly valuable to increase the modulus M, by processing the fibers in the stretched state.

To determine the effects of stretching on the physicochemical and physicomechanical properties (values of K_e , D, and M) of viscose and capron tire yarn, experiments were carried out in which the yarns were stretched in the heated state in a laboratory tube, with definite times, temperatures, and extensions* . The methods described previously [1] were also used to determine values of the modulus M at 5% extension (by means of a recording dynamometer), the rate and equilibrium value of the sorption of phenol by capron fiber, and of copper from cuprammonium reagent [6] and of triethylbenzylammonium base (TEB) from its solutions by viscose fiber. The data so obtained were used to calculate the diffusion coefficients D and the sorption equilibrium constants K_e. Tables 1 and 2 give the values found for M, D, and K_e. Sorption isotherms for the original, stretched, and relaxed fibers are also shown in Figs. 1-3. Figures 4-7 show the influence of heating time, load, initial fiber modulus, and temperature on the modulus of capron yarn. Figures 4 and 7 show that under laboratory conditions the maximum value of the modulus M_5 is reached when capron yarn is heated to 150° for 8 seconds, or to 170° for 1.5 seconds at loads up to 500 g per thread, i. e., at 30% of the breaking load. According to the literature [5] treatment of nylon yarn for use in tire cords requires heating to 180-190° for 7 seconds at 50% of the breaking load. The data in Figs. 4-7 show that when the heating time is increased above the optimum, the modulus again decreases rapidly and the fiber loses strength. The optimum value of the modulus M is reached more rapidly at higher temperatures, greater loads, and with higher values for the initial fiber modulus. In presence of lactam the modulus M increases more rapidly, but storage of capron fibers containing lactam for 2 months leads to a sharp deterioration of the heat stretching process and to decreased values of the modulus M for the same temperatures and times of heating. Thus, lactam acts as a typical plasticizer, but in course of time fibers containing lactam become more brittle, age, and are found to be less suitable for heat stretching.

---

* The modulus M is our term for the load on the thread which produces a given extension.

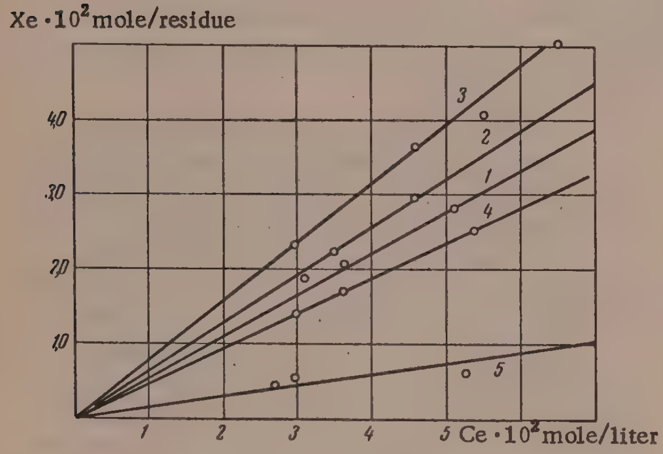

Fig. 2. Sorption of copper from cuprammonium reagent by viscose yarn No. 100: 1) original yarn; 2) treated with 5% NaOH; 3) ditto, 10% NaOH; 4) heated for twenty four hours at 110°; 5) heated for 5 days at 110°;

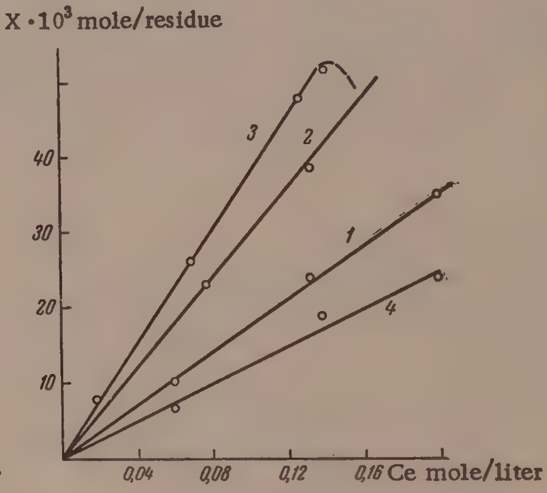

Fig. 3. Sorption of triethylbenzylammonium base (TEB) by viscose yarn No. 100: 1) original yarn; 2) treated with 5% NaOH; 3) ditto, 10% NaOH; 4) heated for twenty four hours at 110°.

Figures 8 and 9 show that the modulus M rises sharply with decreasing rate of diffusion of phenol and decreasing sorption capacity of the fiber. The parameters D and K_e characterize condensation of the molecular structure in heat stretching.

Comparison of the data in Tables 1 and 2 clearly shows the small influence of heat treatment on viscose yarn in comparison with capron. The modulus of viscose yarn is increased by only 10% even by heating under the optimum conditions at 160° for 10 seconds. Similar treatment of capron cord yarn increases the deformation modulus from 280 to 500 g per thread, i. e., by 80%.

---

* The optimum heat treatment conditions vary according to the dimensions of the heating tube; the temperature and duration of heat treatment should increase with increasing size of the equipment used for the treatment.

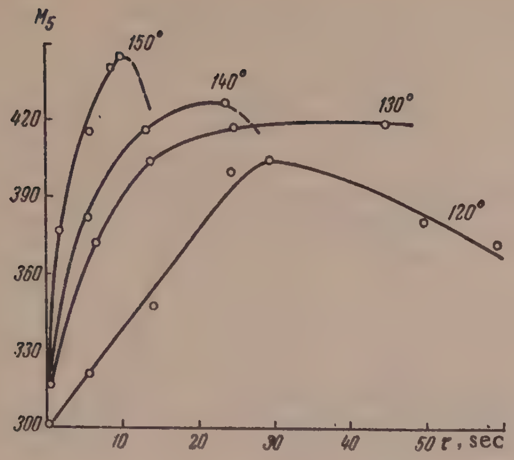

Fig. 4. Effect of heating time on M_5 modulus in heat stretching of capron yarn; load p = 200 g per thread.

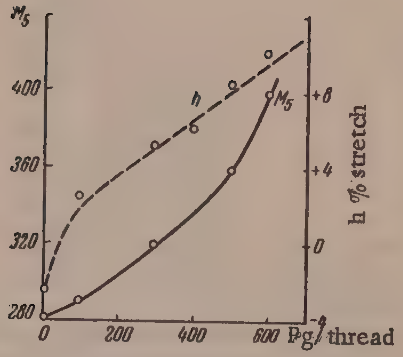

Fig. 5. Effect of load on modulus M_5 and stretch h in percent in heat stretching of capron yarn, heated for 1.5 sec. at 170°.

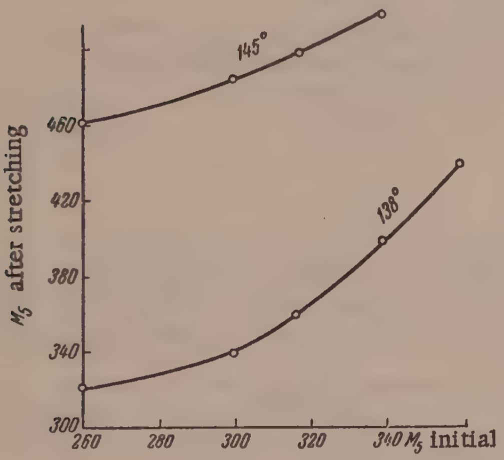

Fig. 6. Effect of initial modulus on increase of M_5 in heat stretching of capron yarn for 10 seconds at p = 200 g per thread.

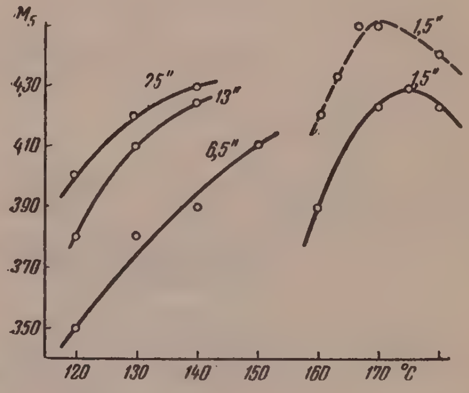

Fig. 7. Effect of temperature on heat stretching of capron yarn at p = 200 g per thread; continuous lines — yarn without lactam; broken line — yarn with lactam.

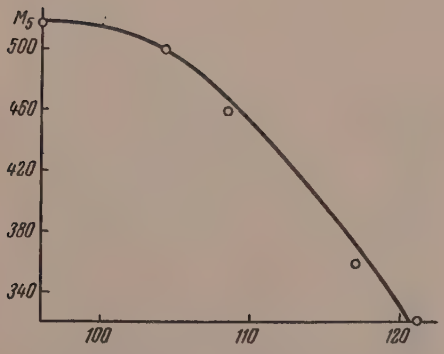

Xe, millimole / residue

Fig. 8. Relationship between sorption of phenol and modulus M; phenol concentration c = 8.5 mole/liter.

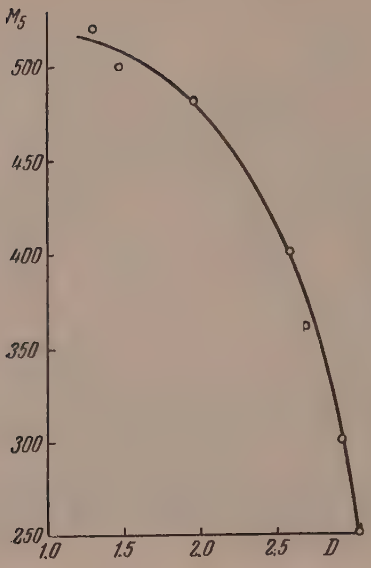

Fig. 9. Relationship between diffusion rate (D × 10^{10}) of phenol and modulus M.

TABLE 1

Effects of Different Treatments of Capron Yarn No. 34

Treatment of capron yarn No. 34		Sorption temperature, °C	K_e	$D \cdot 10^{10}$	M_5 g/thread
duration of preliminary heating, sec.	Heat stretching at 150° under loads in g/thread				
—	—	17	1 35	2 90	280
—	—	55	1 0	—	—
—	—	100	0 6	—	—
—	100	17	—	2 59	—
—	200	17	1 2	1 94	440
—	200	55	0 9	—	—
—	200	100	0 75	—	—
10	200	17	—	1 47	445
8	500	17	—	—	500

TABLE 2

Effects of Different Treatments on Viscose Yarn

Characteristics of viscose fibers studied	Treatment		K_e at 17° for sorption of		Modulus M_s in g per thread
	heating temperature, °C	heating time	cuprammonium base	triethylbenzylammonium base	
Viscose yarn No. 100	—	—	0.038	0.200	100
Ditto, treated (without tension) with 5% NaOH	—	—	0.060	0.300	85
Ditto, 10% NaOH	—	—	0 068	0.360	72
Ditto, heated dry under tension	110	1 hr.	0.018	0.118	90
	160	10 sec.	—	—	110
	170	10 sec.	—	—	95
Ditto, heated in glycerol (without tension)	180	2 hrs.	0.050	0.255	100
Viscose cord No. 7.3	—	—	0.068	0.267	560
Ditto, heated under tension	160	10 sec.	0.060	0.210	600

SUMMARY

1. Heat stretching increases the modulus M of viscose yarn by 10%, and almost doubles that of capron yarn. The increase of the modulus is accompanied by decreases in the rate and magnitude of sorption, i. e., in the physicochemical data which characterize the strength of the intermolecular structure.

2. Above certain optimum values of temperature, heating time, and load, the quality of the yarn deteriorates.

3. Free swelling of viscose yarn in alkali solution (shrinkage) results in increased softness, decrease of the modulus M, and increased sorption of bases.

4. Lactam acts as a plasticizer in the heat stretching of capron.

LITERATURE CITED

[1] A. B. Pakshver, E. E. Natan and I. F. Katushkina, Colloid J., 19, 109 (1957).*

[2] E. K. Mankash and A. B. Pakshver, Colloid J., 16,451 (1954); V. D. Tetyushkina, A. B. Pakshver, and S. S. Frolov, Colloid J., 17,120 (1955).*

[3] E. K. Mankash and A. B. Pakshver, J. Appl. Chem., 26, 835 (1953).*

[4] E. K. Mankash, Trans. Ivanovo Inst. Chem. Technol., 109 (1954).

[5] Litzler., Mod. Text. Mag. 35, No. 2, 32, (1954).

[6] B. D. Tukhlov, S. S. Frolov, and A. B. Pakshver, J. Appl. Chem., 27, No. 8, 907 (1954).*

Ivanovo Institute of Chemical Technology

Received October 19, 1955

---

* Original Russian pagination. See C. B. translation.

MOLECULAR STRUCTURE OF HIGH POLYMERS

COMMUNICATION 17. INVESTIGATION OF THE INTERMOLECULAR STRUCTURE OF THERMOPLASTIC FIBERS

A. B. Pakshver, E. E. Natan, and I. F. Katushkina

It has been shown in the case of capron fiber that as the intermolecular structure is strengthened by stretching or heat treatment of the fiber, sorption of phenol [1] and hydrochloric acid [2] is retarded, the equilibrium amounts of sorbed phenols are decreased [3], the dyeing rate is diminished [4], and changes of fiber length during swelling are retarded [5]. The decreased coefficients of diffusion of various substances into the fiber, decreased equilibrium amounts of bound phenols or acids, and retardation of shrinkage processes during swelling, characterize the strengthening of intermolecular dipole bonds between the amide groups of the macromolecules. Stretching of polyamide fibers, especially in the heated state, increases the energy of intermolecular interaction and the deformation modulus. Brief heating or swelling of the fibers in the unstretched state, on the other hand, weakens the intermolecular bonds, causing increased sorption of phenols and a decrease of the deformation modulus.

These effects are characteristic for all thermoplastic fibers, in which intermolecular dipole bonds are rapidly weakened by increase of temperature. The most characteristic thermoplastic fibers are fibers made from polyvinyl polymers, such as "khlorin" fibers from chlorinated polyvinyl chloride and "nitron" from polyacrylonitrile, and also acetate fiber. Data on the rate and magnitude of phenol sorption by nitron yarn and on the magnitude of acetone sorption by khlorin and acetate fibers are given below. Phenol was determined by the bromide – bromate method [1], and acetone iodometrically [6]. The diffusion coefficients were calculated by the same method as before. The equilibrium constant K_e was calculated from the sorption isotherms by the formula

$$K_e = \frac{x}{(1-x)\,c_e},$$

where x is the amount of sorbed substance in mole/mole; c_e is the equilibrium concentration in solution of the substance being absorbed, in mole/liter.

For the linear portions of the isotherms this equation simplifies to $K_e = \frac{x}{c_e}$. Figs. 1 – 3 show isotherms for the sorption of acetone by acetate and khlorin yarn, and of phenol by nitron yarn. The table gives calculated values of the equilibrium constant K_e and of the deformation modulus M, in kg/mm². Figures 4 and 5 show the effects of temperature, load, and stretching time on the deformation modulus M and give the optimum conditions for the production of fibers with maximum modulus.

The data in the table and Figs. 1-5 show that stretching of thermoplastic fibers increases the modulus of deformation and decreases the equilibrium constant K_e and the diffusion coefficient D. Thus, stretching of these fibers intensifies intermolecular interaction, decreases the sorption capacity of the fibers for substances which solvate the polar groups of the polymers, and makes the fibers more rigid.

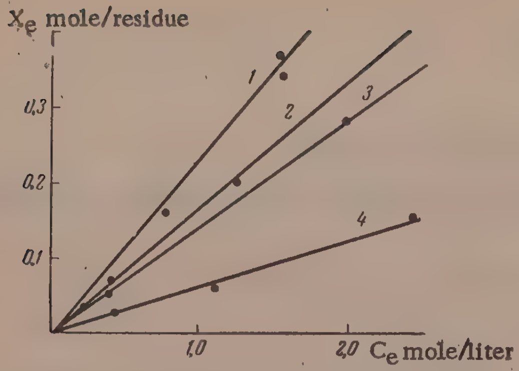

Fig. 1. Sorption of acetone by khlorin: 1) resin; 2) unstretched yarns; 3) yarn after 4-fold stretching; 4) yarn after 4-fold stretching and additional 22% stretch at 60°.

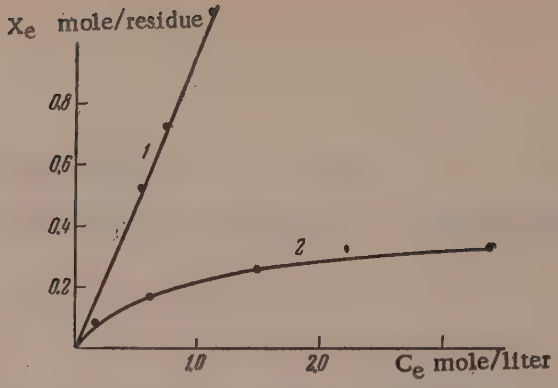

Fig. 2. Sorption of acetone by acetate yarn: 1) original yarn; 2) yarn stretched by 21% at 135°.

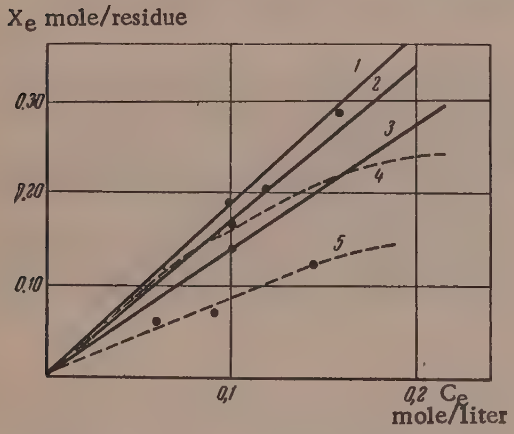

Fig. 3. Sorption of phenol by nitron yarn and resin: 1) nitron resin at 17°; 2) ditto, at 47°; 3) ditto, at 100°; 4) nitron yarn at 17°; 5) ditto, at 55°

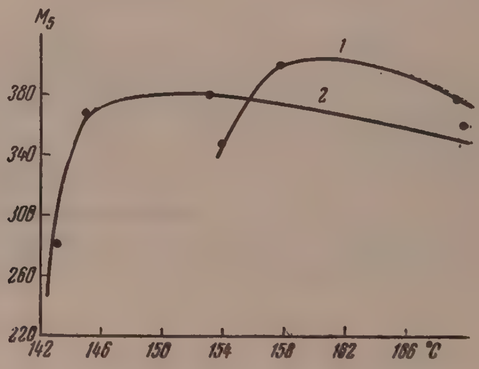

Fig. 4. Heat stretching of nitron yarn: 1) load 25 g per thread, 1.8 sec.; 2) load 10 g per thread, 6 sec.

TABLE

Equilibrium Constants K_e, Diffusion Coefficients D and Deformation Moduli M of Khlorin, Nitron, and Acetate Yarns After Various Treatments.

Type of yarn and treatment	N_m	Sorption temperature, °C	K_e	$D \cdot 10^{11}$	Deformation modulus	
					$M_{1\%}$	$M_{2.5\%}$
Original khlorin resin	10	17	0.200	—	1.13	5.16
Ditto, spun without stretch	32	17	0.165	—	2.26	—
Ditto, yarn stretched 4-fold at 160°	93	17	0.155	—	7.3	—
Ditto, additional 22% stretch at 60°; 3.5 sec.; load 30 g per thread	100	17	0.065	—	8.0	—
Original acetate yarn	90	17	1.02	—	—	3.1
Ditto, 14% stretch at 125°; 3 sec.; load 20 g per thread	118	17	0.33	—	—	7.16
Ditto, 21% stretch at 135°; 2.5 sec.; load 25 g per thread	134	17	0.19	—	—	11.36
Original nitron resin	—	18	0.205	—	—	—
	—	47	0.177	—	—	—
	—	100	0.133	—	—	—
Ditto, after heating at 160°, 60 min.	—	18	0.113	—	—	—
Original nitron yarn	100	18	0.147	14.6	—	—
	100	53	0.118	—	—	—
	100	95	0.079	—	—	—
Ditto, 10-fold stretch in spinning	100	18	0.254	—	—	—
Ditto, 15-fold stretch	100	18	0.197	—	—	—
Ditto, 20-fold stretch	100	18	0.147	—	—	—
Ditto, 15-fold stretch and additional 13% stretch at 155°	115	18	0.149	7.7	—	—

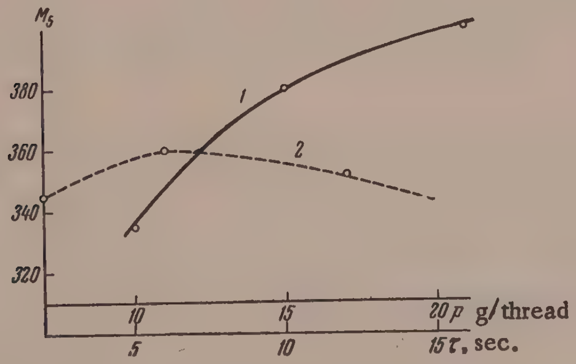

Fig. 5. Heat stretching of nitron yarn: 1) effect of load at 155°, 1.8 sec.; 2) effect of heating time at 155°, load 15 g per thread.

SUMMARY

1. Sorption of phenol by nitron yarn and of acetone by acetate and khlorin yarns decreases with increasing stretch of the fibers.

2. The sorption decreases with increase of temperature, which is characteristic for processes occuring with a decrease of enthalpy.

3. Stretching of acetate, khlorin, and nitron yarns results in decrease of the equilibrium constant K_e, increase of the modulus of deformation M, and decrease of the diffusion coefficient D. All this definitely indicates strengthening of the intermolecular structure.

Ivanovo Institute of Chemical Technology

Received October 19, 1955.

LITERATURE CITED

[1] E. K. Mankash and A. B. Pakshver, Colloid J., 16, No. 6, 451 (1954). *

[2] V. A. Myagkov and A. B. Pakshver, Colloid J., 17, No. 2, 120 (1955).*

[3] V. D. Tetyushkina, A. B. Pakshver, and S. S. Frolov, Colloid J., 17, No. 1, 63 (1955).*

[4] E. K. Mankash and A. B. Pakshver, J. Appl. Chem., 26, No. 9, 976, and No. 11, 1200 (1953).*

[5] E. K. Mankash and A. B. Pakshver, J. Appl. Chem., 26, No. 8, 835 (1953).

[6] A. N. Akhreyanova, K. N. Vanyushina, and B. E. Geller, Factory Labs., No. 12, 1431 (1951).

---

* Original Russian pagination. See C. B. translation.

~~THE~~ ELECTROCHEMISTRY OF HIGH-POLYMER DISPERSIONS

3. EFFECT OF pH ON THE ELECTROKINETIC POTENTIAL OF GLOBULES IN SYNTHETIC LATEXES

R. M. Panich and S. S. Voyutsky

The effect of pH on the electrokinetic potential (zeta potential) of natural latex particles has been studied by several workers [1-3]. It has been established that the zeta potential of natural latex globules first increases with pH, and then remains constant or even decreases. The increase of zeta potential with increasing pH of the latex is probably caused by the greater ionization of the stabilizer molecules in an alkaline medium. The subsequent fall of zeta potential is probably caused by desorption of proteins, readily soluble in alkaline media, from the globule surfaces, by cation adsorption, and also by increase of the ionic strength of the medium as the result of addition of alkali.

Decrease of pH results in charge reversal in natural latex globules, and the latex passes through the isoelectric point at which it coagulates if special steps are not taken.

Maron and Bowler [4], and also Voyutsky and his associates [5-7] showed that the zeta potential of synthetic latexes changes similarly to that of natural latex with increased pH. Coagulation was observed by all foreign workers in synthetic latexes with decrease of pH. However, in 1950 the present authors showed for the first time that if the latex is sufficiently dilute (not more than 3-4% solids content) and the required amount of acid is added rapidly, the pH can be decreased to 2.5 and less. Qualitative experiments on determination of the charge of the particles in latex acidified with hydrochloric acid showed that in this case the globules are positively charged.

The isoelectric point of undialyzed synthetic latexes was also found, and the nature of the variations of the zeta potential in the region below this point was studied; it was found that the potential first increased and then decreased as acid was added to the latex.

In the present investigation the effect of pH on the zeta potential of globules in dialyzed synthetic latexes at constant known ionic strength was studied. In this way it is possible to take into account the influence of a number of complicating factors in determinations of electrophoretic mobility, and therefore to obtain more correct values for the zeta potential.

Materials studied and methods for determination of electrokinetic potential. Two latexes were studied: latex A, consisting of a dispersion of vinyl chloride – divinyl copolymer in ammonium oleate solution, and latex B, which was a dispersion of a polar polymer in ammonium naphthenate solution. Both latexes were used in the form of dialyzates, denoted by AD2 and BD1 respectively. Fuller details of the original latexes and their dialyzates are given in earlier publications [8, 9].

The zeta potential was determined by means of macroelectrophoresis by a method described previously [9]. In this method the dialyzed latexes were diluted with a buffer mixture of known composition. A suitably diluted buffer mixture was also used as the auxiliary liquid in electrophoresis. Since the electrolyte contents of dialyzed latexes are very low in comparison with those of buffer solutions, it may be assumed that in this instance the ionic strengths of the latex and auxiliary liquid are practically equal. This method had a number of advantages, including the fact that it enabled us to make corrections for electrophoretic lag and electrical relaxation. The determinations themselves were performed in the Rabinovich and Fodiman apparatus [10].

The buffer mixtures used were solutions containing univalent ions only, of different pH values, but with the same ionic strength of 0.02. Buffer mixtures of higher ionic strength caused coagulation of the latexes at low pH values.

Effect of pH on the electrokinetic potential of latex globules. Latex AD2 was diluted with distilled water before the determinations to approximately 1% solids content, and then diluted twofold with buffer mixture. Thus, the values given below for the zeta potential refer to globules in latex with ~ 0.5% solids content. The numerical coefficient in the Henry formula used to calculate the zeta potential was chosen on the basis of the facts that the ionic strength of the final solution was 0.01, the buffer solution contained univalent ions only, and the particle radius of AD2 latex was 210 A [8].

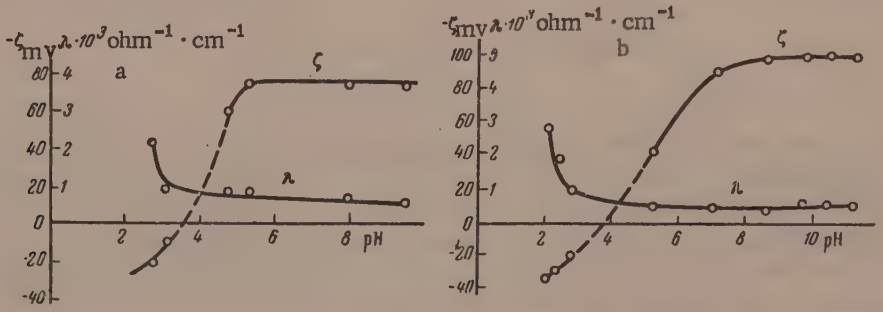

Fig. 1. Variations of the electrokinetic potential (ζ) of the globules, and of the specific conductance (λ_0) of latex AD2 (a) and BD1 (b) with pH.

The results of the experiments on AD2 latex are shown graphically in Fig. 1, a. It is seen in Fig. 1, a that the zeta potential remains unchanged as the pH varies between 10 and 5.3, and then falls sharply with further increase of hydrogen ion concentration, becoming zero at pH of about 3,7, and finally reaching increasing positive values.

The specific conductance, variations of which are also shown in Fig. 1 a, is more or less constant at pH > 3 and increases appreciably only in strongly acid media. This increase must evidently be attributed to the exceptionally high mobility of the hydrogen ion.

The results of experiments on latex BD1 are shown in Fig. 1, b. It is seen that the general character of the variation of zeta potential with hydrogen ion concentration is the same as for latex AD2, but the curve begins to descend at pH 7.

Effect of pH on the aggregative and sorptional stability of synthetic latexes. To determine the effect of pH on the aggregative stability of synthetic latexes, an investigation was made of the change in the particle size in diluted AD2 latex after twofold dilution by buffer mixtures of various pH., but with the same ionic strength of 0.02. The degree of dispersion was determined nephelometrically [11] half an hour, and 25 days after dilution of the latex. The sorptional stability of the resultant systems toward cotton wool was determined at the same time. For this, 20 ml of the latex diluted by the buffer was placed in contact with 0.5 g cotton wool, and after 30 minutes the latex was poured off and its rubber content was determined nephelometrically.

The results of the experiments are given in the table.

It is seen from the table that latexes with 0.375% solids content have considerable aggregative stability at pH above 6.2 — their particle size remains practically unchanged for 25 days, which is quite consistent with the high negative values of their zeta potential.

The particle size does not increase upon reversal of charge when the latex pH is taken to 2.7; however, the resultant latex has low aggregative stability and in the course of 25 days its particle size is increased by about a half. If during the charge reversal the pH is taken to only 3.1, the latex particles increase in size during the process; the size increase continues in the reversed latex and the latex coagulates in twenty four hours. At the isoelectric point, pH 3.9, a stable latex cannot be obtained.

TABLE

Particle Size and Sorptional Stability of Diluted AD2 Latex at Various pH Values

pH	in mv	Particle diameter after dilution, in A		Latex concentration, % solids		Sorption, %
		after ½ hour	after 25 days	before sorption	after sorption	
8.3	—72	510	520	0.375	0,334	10.9
6,2	—72	513	520	0.375	0.328	12.5
3.9	(—8)	Coagulation occurred on dilution of the latex by the buffer				
3.1*	+11.4	575	—	0.375	0.093	75.5
2.7	+20.6	486	725	0.375	0.225	40

---

* The latex coagulated after 24 hours.

The table also shows that positively charged latex particles are sorbed much more rapidly than negatively charged particles by cotton fibers.

DISCUSSION OF RESULTS

It has hitherto been believed that reversal of the charge on the globules on acidification is possible only in natural latexes, stabilized by natural proteins, the molecules of which have two functional groups: the amino group, causing the positive charge of the globules in an acid medium, and the carboxyl group, which causes the globules to be negatively charged in an alkaline medium. In the case of synthetic latexes stabilized by soaps,it was considered that in an acid medium the soap is converted into an acid which has no protective properties, and the latex should coagulate.

Our experiments have shown that under certain conditions charge reversal on acidification is also possible in dispersions stabilized by substances which cannot cause a change in the sign of the charge when the reaction of the medium is changed. The cause of this evidently lies in the fact that the latex remains stable at low pH values owing to adsorption of positively charged hydrogen ions by the globules. The hydrogen ion has high adsorbability and in many instances can act as a stabilizer. There are indications in the literature of the possibility of charge reversal, by means of hydrogen ions, of particles in certain colloids and emulsions, including rubber globules, originally stabilized by hydroxyl ions [1].

The graph shows that when the pH is decreased by addition of acid the absolute values of the zeta potential of the globules in AD2 and BD1 latexes first remain constant over a certain pH range, and then begin to decrease after pH 5.3-7 has been reached. This form of the zeta potential – pH curve is in good agreement with the general relationship established by Jordan [2] for natural latex. The decrease of the zeta potential after sufficient acidification is probably the result of conversion of the strongly ionized soap into a weakly ionized acid. Although the latter is adsorbed on the globules, it does not form a protective ionic layer characterized by the zeta potential. Maron and Bowler's explanation [4] of the weaker stabilizing action of acids as being due to lower adsorption by the globules is not, in our opinion, satisfactory. A fatty acid, being less soluble, will always be adsorbed better than soap on rubber globules. The known fact that the surface tension of latexes is decreased on acidification is explained, not by passage of the fatty acid particles formed from the soap into the solution, but by the fact that the acid has higher surface activity than the soap.

If the medium is sufficiently acid, all the soap is converted into an acid devoid of protective properties. This corresponds to the isoelectric state of the system. In accordance with the values found for the isoelectric points, the stabilizers – ammonium oleate and naphthenate soap – present in latexes AD2 and BD1 are evidently converted into the corresponding acids at pH 3.7-3.9. Upon further acidification, hydrogen ions are adsorbed on the polymer globules and confer a positive charge on them. As the pH decreases the adsorption of hydrogen ions increases and the positive zeta potential rises. Nevertheless, the absolute value of the positive potential in an acid medium is considerably lower than the value in an alkaline medium. This is certainly associated with the nature of the stabilizing ion.

The aggregative stability of the latexes also increases with increasing absolute values of the zeta potential. The increase of latex stability with increasing absolute values of the negative zeta potential on addition of alkali is common knowledge. However, we see that this is also true for latexes with positively charged globules. The connection between zeta potential and stability is also confirmed by the fact that latexes with negatively charged particles with high zeta potentials are much more stable than latexes with positively charged particles and relatively low zeta potentials.

The zeta potential – pH curve for undialyzed latexes, determined by us earlier [7] had maxima in the acid and alkaline regions.

The explanation for these maxima should be sought in the fact that while the experiments with dialyzed latexes were performed with solutions of strictly constant ionic strength, this was not the case in the experiments with undialyzed latexes. In the latter case the pH was increased by addition of alkali to the latex, which resulted in an increase of ionic strength, and consequently to compression of the electric double layer and a decrease of the absolute value of the negative zeta potential. In this same way, considerable decreases of pH in this case were produced by additions of large amounts of acid to the latex, which also increased the ionic strength and decreased the value of the positive zeta potential. Similar effects have been reported earlier for dilute mineral oil emulsions [12].

SUMMARY

1. Latex particles stabilized by anion-active soaps can undergo charge reversal on acidification. An essential condition for charge reversal is low latex concentraion and rapid addition of the acid, so that the sign of the particle charge can be reversed before any appreciable coagulation occurs.

2. The zeta potential of latex globules remains constant on acidification over a certain pH range, then decreases as the result of the conversion of soap into undissociated acid, reaches zero (isoelectric point), and then becomes positive in acid media, probably as the result of adsorption of hydrogen ions.

3. When the zeta potential of the globules is close to zero, the latexes completely lose their aggregative stability. It has been found that the isoelectric point of latexes stabilized by soaps is at pH 3.7-3.9.

4. The zeta potential – pH curves for undialyzed latexes have maxima at high and low pH values. The presence of these maxima is probably caused by the increase of ionic strength as the result of addition of large amounts of alkali or acid to confer high or low pH values on the solution.

5. Latexes with reversely charged particles are much less stable than the original latexes; this is due to the lower absolute values of the zeta potential of the particles of such latexes in comparison with the original.

6. The positively charged particles of reversed latexes are actively sorbed by cotton fibers and can therefore be successfully used for impregnating paper, cardboard, and for similar purposes.

The M. V. Lomonosov Institute of Fine Chemical Technology
Moscow

Received February 12, 1956

LITERATURE CITED

[1] A. R. Kemp, D. F. Twiss, Rubb. Chem. Techn. 9, 551 (1936).

[2] H. F. Jordan, Proceedings of the Rubber Technol. Conference, 1938, p. 111.

[3] W. W. Bowler , Ind. Eng. Chem., 45, 1790 (1953).

[4] S. H. Maron, W. W. Bowler, J. Am. Chem. Soc. 70, 3893 (1948).

[5] S. S. Voyutsky, Yu. A. Smetkin, R. M. Panich, and K. A. Kalyanova, Proc. Acad. Sci. USSR, 70, 1013 (1950).

[6] S. S. Voyutsky, R. M. Panich, and K. A. Kalyanova, Collected Papers of the Central Sci. Res. Inst. for Leather Substitutes on the Theory and Practice of Impregnation, State Light Ind. Press, p. 90 (1952).

[7] S. S. Voyutsky, R. M. Panich, and K. A. Kalyanova, Trans. Lomonosov Inst. Fine Chem. Technol., Moscow, No. 5, State Chem. Press, p. 30 (1953).

[8] R. M. Panich and S. S. Voyutsky, Colloid J., 18, 326 (1956).

[9] S. S. Voyutsky and R. M. Panich, Colloid J., 18, 647 (1956).

[10] A. I. Rabinovich and E. F. Fodiman, J. Phys. Chem., 2, 336 (1931); 3, 8(1932).

[11] P. Debye, J. Phys. Coll. Chem., 51, 18, (1947).

[12] R. Ellis, Z. Phys. Chem. 78, 321, (1912).

THE FRACTIONAL COMPOSITION OF FINE CELLULOSE FIBERS

S. L. Talmud, A. N. Turzhetskaya, and A. A. Kuleshova

It has been shown by one of the present authors and co-workers [1] that cellulose may be refined by size fractionation of sulfite cellulose fibers; for this, fine cellulose fibers must be removed. For a correct evaluation of the role of fine cellulose fibers and of the possibilities of utilizing them rationally, it was necessary to determine the chemical composition of this fine fraction, and to study the molecular heterogeneity of its constituent cellulose.

The cellulose was fractionated by consecutive solution in phosphoric acid solutions of known concentrations [2, 3]. Akim and Kilkki [4] used this method to show that a definite relationship exists between the fractional composition and the reactivity of sulfite viscose cellulose. According to these authors, a viscose cellulose with good reactivity has a low content of low molecular fractions with degree of polymerization up to 200, and is completely free from high molecular fractions with degree of polymerization above 1200. Thus, consecutive solution of cellulose in phosphoric acid solutions is a convenient method for comparative determinations of the degree of polymerization of different technical cellulose fractions.

We have studied the fine cellulose fibers obtained from sulfite pulp waste waters (fibers present in pitch settling tank effluents). The quantitative proportions of different fractions (by fiber length) were determined by means of a microscope with a micrometer eyepiece, by fiber counts in several fields. The results of the microscopical analysis are given in Table 1.

TABLE 1

Microscopical Analysis of Fine Cellulose Fibers

Fiber length, mm	Content of fraction, as % of total fibers	Fiber length, mm	Content of fraction, as % of total fibers
1.0	2.5	0.3	9.4
0.7	–	0.2	21.0
0.5	2.7	0.1	34.2
0.4	–	0.05	30.2

Table 1 shows that most of the fine fibers, 84.4%, were from 0.05 to 0.2 mm long.

The fine cellulose fibers contained 4% moisture, 1.45% ash, and 16.2% resins and fats (soluble in dichloroethane).

For fractionation of the fine cellulose fibers by molecular weight, it was first necessary to extract resins and fats. However, after thorough extraction of the fine cellulose fibers by dichloroethane, or by ethyl ether and ethyl alcohol, successful fractionation could not be achieved, as phosphoric acid solution had practically no solvent action on the cellulose.

It was noticed that the contents of resins and fats, determined by extractions by the above solvents, steadily decreased during storage of the fine cellulose fibers. Evidently the resins were oxidized and the oxidation products were not extracted by the solvents. In a discussion of this problem, S. S. Malevskaya reported that she had observed similar effects, and that when resins and fats are extracted from cellulose by ethyl ether and acetone, oxidized resin is also extracted.* The content of resins and fats, soluble in ethyl ether and acetone, in the fine cellulose fibers was found to be 18.2%. It proved possible to fractionate the cellulose after extracting the fine cellulose fibers with ethyl ether and acetone to remove unoxidized and oxidized resins and fats.

---

* We are deeply grateful to S. S. Malevskaya for this communication [6, 7].

The results of the fractionation of extracted fine cellulose fibers are given in Table 2. Table 2 gives the average results of at least two parallel determinations for each experiment. If the discrepancies were considerable, the number of parallel determinations was increased to 3-5.

TABLE 2

Molecular Heterogeneity of Extracted Fine Cellulose Fibers

Degree of polymerization of cellulose	Amounts of fractions, wt. %					
	I	II	III	IV	V	mean
Up to 10	3.0	3.8	3.9	2.8	3.4	3.4
10 — 200	2.7	2.8	0.9	3.7	2.5	2.5
200 — 300	2.7	6.7	2.5	0.7	3.0	3.1
300 — 420	31.4	28.5	33.3	34.8	27.9	31.2
420 — 600	0.0	0.0	0.0	1.8	6.3	1.6
600 — 1200	2.9	0.0	0.7	0.0	0.0	0.7
Over 1200 (by difference)	57.3	58.2	58.7	56.2	56.9	57.5

Table 2 shows that extracted fine cellulose fibers contain on the average only 42.5 wt. % of cellulose with degree of polymerization up to 1200; most of the cellulose (57.5%) is insoluble in phosphoric acid and has degree of polymerization above 1200.

The lignin content of the extracted fine cellulose fibers, determined by the sulfuric acid method, was 5.62%.

Analysis of the fine cellulose fibers gave the following results, calculated on the absolutely dry material (in wt. %):

	wt. %
(1) Resins and fats	19.0
(2) Lignin	7.2
(3) Ash	1.5
(4) Cellulose	72.3
(5) Including cellulose with degree of polymerization up to 1200	30.7
(6) above 1200	41.6

This low quality of the cellulose fines is probably due to the morphological structure. These results confirm the possibility and advisability of refining cellulose by removal of the low quality portion, the fine fibers [1].

Cases are known when viscose cellulose, which confirms to various technical specifications, proves to be insufficiently reactive, and the viscose has poor filterability. In our opinion, this may be the result of incomplete removal of the fine cellulose fibers, for example, during bleaching.

The extracted fine cellulose fibers proved to be quite unreactive (with 110% CS_2 and 11% NaOH).

The advantages of cellulose fractionation by fiber length [1] have been confirmed by the work of

Perila [5], who reported that after removal of 12.6% of short fiber material the reactivity of the cellulose is raised and the filterability of viscose solutions is improved.

SUMMARY

1. The chemical composition of fine cellulose fibers (a short fiber fraction of sulfite cellulose) has been determined and the constituent cellulose has been fractionated by molecular weight.

2. It is shown that fine cellulose fibers contain, calculated on the absolutely dry substance: 19.0% resins and fats (soluble in ethyl alcohol and acetone), 7.2% lignin, 1.5% ash, and only 72.3% cellulose. Most of the cellulose (45.8%) in the fine fibers has degrees of polymerization below 200 and above 1200, and only 26.5% of the fine fiber material, with degrees of polymerization between 200 and 1200, is suitable for chemical processing. This low quality of the fine cellulose fiber fraction is probably due to its morphological structure.

3. The results indicate the possibility and suitability of cellulose refining by removal of the low grade portion, the fine fiber fraction.

The V. M. Molotov Technological Institute
Leningrad
Chair of Physical and Colloid Chemistry

Received April 14, 1956

LITERATURE CITED

[1] S. L. Talmud, A. M. Ivanyushkina, L. A. Popova, and L. P. Yanzuvalova, Proc. Acad. Sci. USSR, 92, 2, 397 (1953).

[2] N. I. Nikitin, Chemistry of Wood, Acad. Sci. USSR Press, p. 96 (1951).

[3] Ekenstam, Svensk Papperstidning 45, 61, (1942).

[4] L. E. Akim and V. E. Kilkki, Paper Ind., 10, 5(1953).

[5] O. Perila, Paperi ja Puu, 35, 4a, 139 (1953).

[6] S. S. Malevskaya, V. D. Karnaukhova, and S. D. Kharad, Paper Ind., 9, 14(1955).

[7] S. S. Malevskaya and V. D. Karnaukhova, J. Appl. Chem., 29, 401(1956).

DISCUSSION

CHARACTERIZATION OF THE STATE OF HIGH-POLYMER GELS

A. V. Nikolaev, R. E. Neĭman, and O. V. Neĭman

The question of the nature of the gelation process has repeatedly been discussed in the literature. This is not surprising, since formation of gels from high-polymer solutions is met fairly frequently and in a number of cases is of definite practical importance.

One cannot fail to agree with Lipatov and Meerson [1] that in a number of cases (dyes and purified polymers) gels have all the signs of thermodynamic instability, and that gelation is merely an intermediate stage on the way to complete separation of the system into two phases. We are therefore dealing with phenomena occurring in systems with limited mutual solubility (limited swelling of the polymer) over a definite temperature range; on heating, this passes into complete miscibility. When such homogenized systems are cooled, their behavior may differ:

a) In some cases phase separation occurs and a state of equilibrium is reached fairly rapidly. One of the phases formed is a partially swollen polymer, i. e., an equilibrium gel of a constant composition for a given temperature, and the other is a solution of polymer in low molecular liquid.

b) In other cases the separation is delayed for indefinite periods. A nonequilibrium, continuous, one-phase gel is formed. The persistence of this nonequilibrium state is aided, as is known, by inhomogeneity of the polymer and presence of impurities in it. Thus, solutions of ordinary gelatin on cooling are converted into gels which do not separate into phases for indefinitely long periods. Nevertheless, as was shown by Tager and Kargin [2], when solutions of highly purified gelatin are cooled they separate fairly rapidly into two layers.

In our opinion the study of nonequilibrium gels is not only of specialized but also of very general interest, since the equilibrium state is in many cases reached through this intermediate stage.

1. The formation of gels directly by cooling solutions of a number of polymers, i. e., case "b" above, was studied by us thermographically [3, 4]. We were not able to detect any heat effect on gelation. We must again stress that this refers to the formation of a gel from the solution, and not to its subsequent phase separation.

Lipatov and Meerson [1], in referring to these studies, regard the result of our thermographic investigation as failure on our part. They see the reason for this failure in the fact that we used nonfractionated materials. However, the data of Lipatov and Feldman [5] can be used to show that this view is incorrect. Indeed, these authors used nonfractionated gelatin and agar, individual fractions of these, mixtures of such fractions, and in a number of cases they also added various electrolytes. In all these cases differential thermograms of the same type were obtained; in the authors' view, these provided evidence for the existence of a heat effect of gelation. The values of these effects varied somewhat with variations of the experiments, but remained of the same order of magnitude. Therefore it is necessary to seek some other cause of the diametrically opposite results obtained in our investigations [3, 4], by Lipatov and Feldman [5], and by Lipatov and Meerson [6].

We must point out that, in numerous repetitions of the thermographic experiments and with careful attention to all the precautions necessary in obtaining differential thermograms, we were never able to detect—within the limits of the fairly high sensitivity of our determinations — any appreciable heat effects on gelation. It is also necessary to bear in mind that these thermographic results of ours are in any event in agreement with the results of our highly sensitive dilatometric determinations [3, 7], in which we did not detect any volume changes in the formation of gels from solutions. Thus, two independent methods gave results which were similar in principle.

We therefore continue to regard our thermographic and dilatometric data as quite reliable.

2. The absence of a heat effect of gelation contradicts, in our opinion, the data of Lipatov and Meerson [8] on the temperature dependence of the heat of solution of polymers. These authors showed that the magnitude of this heat effect decreases in a certain temperature range; in their opinion, this is due to an endothermic process of bond rupture between the polymer chains. This intermediate region is regarded by them as a region of phase transition, completed after rupture of the interchain bonds and solution of the polymer.

The transition from an equilibrium heterogeneous system (partially swollen polymer in excess liquid), on heating, to a homogeneous solution, from the latter on cooling to a nonequilibrium gel, and finally the return to the initial state on phase separation of the gel, may be represented in the form of an energy diagram (Fig. 1).

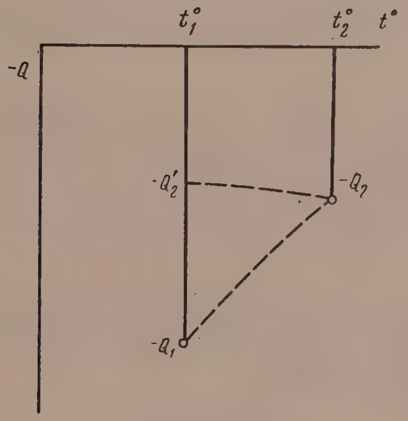

Fig. 1. Energy diagram for the transitions: equilibrium heterogeneous system ($-Q_1$) – homogeneous solution ($-Q_2$) – nonequilibrium gel (Q_2').

At the lower temperature t_1° a heterogeneous system is formed when the polymer is mixed with the liquid. This process is characterized by the heat effect $-Q_1$. In agreement with Lipatov and Meerson's data [8], the complete solution of the polymer at a higher temperature t_2° to give a homogeneous solution should correspond to a smaller heat effect $-Q_2$.

The difference $[Q_1 - Q_2]$ determines the heat of phase transition, corresponding to the region of phase transition on Lipatov and Meerson's $Q = f(t^\circ)$ curve.

If, when the homogeneous solution is cooled from temperature t_2° to t_1°, a continuous nonequilibrium gel is formed; this means that phase separation is delayed. The system does not return to the initial state in which it was found before it was homogenized by heating. Thus gelation may not be phase transition. Therefore the heat effect corresponding to such transition is absent. The difference between $-Q_2'$ for the nonequilibrium gel and $-Q_2$ for the homogeneous solution is determined only by the temperature term of the heat content. Only on subsequent slow phase separation of the nonequilibrium gel can we expect to find a heat effect corresponding to the difference $-[Q_1 - Q_2']$. Here transition to a state of equilibrium occurs, and one of the two phases formed is an equilibrium gel of definite composition.

3. Transition of a polymer solution into a nonequilibrium gel without a heat effect or volume change is not a new phenomenon. It has long been known for the melt – glass system. To illustrate this, we give a heating curve, of interest from our point of view, obtained by one of us [9] for a series of borate glasses. When a borate glass is heated (branch $\underline{a}$ of Curve $\underline{t}$ in Fig. 2) at a definite reproducible temperature the molecules become mobile and the glass passes into crystals with evolution of heat (effect 1 on the Curve Δt), and the crystals melt at once with absorption of heat (effect 2). The heat effects 1 and 2, are, of course, of equal magnitude. When the resultant melt is cooled (branch $\underline{b}$), neither absorption nor evolution of heat can be detected by the most sensitive differential recording, although the melt is completely converted into glass. The glass so obtained can be heated again, and the whole cycle can be reproduced repeatedly.

We must emphasize that the analogy between glass and a nonequilibrium gel relates to energy only. The mechanism by which the nonequilibrium state is produced may differ for gels and glasses, but for our purpose (energy analogy) this is immaterial.

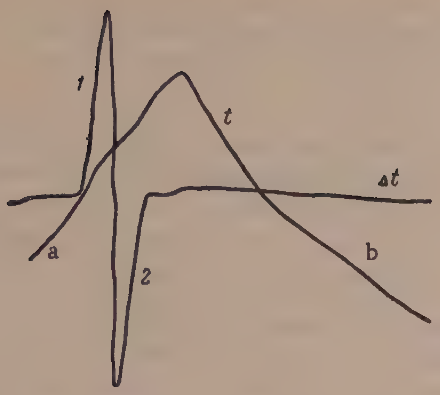

Fig. 2. Heating curve for borate glasses (explanation in text).

4. Our theoretically important modification of the Lipatov and Meerson scheme, like the scheme as a whole in its new form, may be illustrated with the aid of data published a relatively long time ago by one of the present authors [10]. In fact, phenomena occur in the gel which are very similar to phase transitions in their nature and in the accompanying effects, such as the volume effect. Thus, the contraction of a gel on coagulation is accompanied by a volume effect comparable to that for the formation of a gel from a true solution at a low concentration of coagulant. When a 4% solution of ferric chloride is mixed with an equal volume of caustic soda solution, equivalent quantities give a volume increase of + 0.874 cc per 1 g of the ferric hydroxide formed. If the same reaction, with the same amounts and concentrations of ferric chloride and caustic soda, is carried out in 10% or 20% solutions of common salt, the corresponding volume changes will be +0.559 cc (− 35.3%) and +0.487 cc (− 45%).

In other words, the contraction of a gel by the action of a coagulant is accompanied by a volume effect comparable in magnitude (being 35-45% of the latter) with the effect in such an evident phase transition as the formation of a precipitate in solution.

In the same investigation the volume effect of the transition of a sol into an uncontracted gel was also studied for 4% ferric chloride solution; its value was $^1/_2$ of the value for the phase transition.* This volume effect diminishes with decreasing concentration of the coagulant (concentrations of the solutions being mixed), tending to zero or a very small value at infinite dilution, in the following way:

Volume effect in the sol − gel transition as % of the volume effect in the formation of a sol from a true solution**	−2,43	−3.40	−5,0	−9.6
Concentration of original ferric chloride solution, %	1.0	2.0	3.0	4.0

This variation of the volume effect with concentration must attributed wholly to changes of the gel volume, as the volume effect of sol formation from true solution depends very little on the concentration. The values of this effect without corrections for dilution are:

Concentration of ferric chloride solution, %	2	3	4
Volume effect of sol formation in cc per 1 g $Fe(OH)_3$	0.681	0.687	0.690

Therefore there is no doubt that the volume effect of the sol − gel transition depends very much on the state of the gel: in absence of a coagulant it is equal or close to zero, *** while in the shrinkage of a gel by the action of a coagulant (analogously to syneresis) it may be comparable with the effect in phase transition.

---

* As small as $^1/_{49}$ for 2% solution.

** Without the dilution effect on mixing being taken into account; if this factor is taken into account, the values diminish still further, for example, −9.6% for 4% ferric chloride solution becomes − 8.5% after the correction is applied (see above).

*** This is in good agreement with the thixotropy of a given gel.

We have thus confirmed the validity of our scheme (Fig. 1), but instead of heat effects we used their equivalent volume effects, and instead of syneresis, we considered gel shrinkage by coagulation .

5. In our energy scheme (see Fig. 1) the nonequilibrium gel which has not separated into layers should not have a structural network. Formation of such a network should then be the essential cause of a heat effect in the phase separation of a nonequilibrium gel. However, another hypothesis probably cannot be excluded.

The formation of a structural network in a nonequilibrium gel, while unconnected with phase transition, would nevertheless correspond to formation of a definite number of local bonds between the polymer macromolecules. This process, in its turn, should be accompanied by heat and volume effects. What is the reason that this effect cannot be detected by highly sensitive differential thermograms ? We tentatively suggest that mutual compensation of two opposite heat effects may occur in the formation of a structural gel network .

The polar groups of the macromolecules in solution are solvated by the solvent molecules. At the same time, there is a definite degree of macromolecular association, which depends on the temperature, in the solution . Thus, fluctuating processes of solvate and aggregate formation and destruction develop in the solution, with definite statistical average period of their existence corresponding to each given temperature . As the solution is cooled, a definite number of bonds becomes fixed between the most polar groups of the macromolecules and finally the structural gel network is formed. Since, in solution, the polar groups of the macromolecules are blocked by solvating molecules of solvent, it may be assumed that preliminary desolvation is a condition for bond formation between them. Therefore, in the formation of the structural network in the gel, two heat effects opposite in sign and similar but not equal in magnitude may be mutually compensated.

Of the total number of polar groups contained in a macromolecule, only a relatively small part is involved in the formation of the structural gel network. The molar concentrations of polymers in solutions are, however, very low . Thus, for gelatin with molecular weight $5 \cdot 10^4$, a 25% solution corresponds to a concentration of $\sim 5.10^{-3}$ mole/liter . It may be that because of the compensation of the opposite effects and because the number of local contacts is very small, the heat of formation of intermolecular bonds in the structural gel network becomes vanishingly small.

In phase separation of a nonequilibrium gel the number of intermolecular bonds rises sharply, and the small energy difference relative to hydration bonds is then manifested quite clearly in the form of heat and volume effects .

Institute of General and Inorganic Chemistry
Acad. Sci. USSR, Moscow
Voronezh State University
Engineering and Building Institute, Voronezh

Received May 21, 1956

LITERATURE CITED

[1] S. M. Lipatov and S. I. Meerson, Colloid J., 17, 230 (1955).*

[2] A. A. Tager and V. A. Kargin, J. Phys. Chem., 15, 1029 (1941).

[3] A. V. Nikolaev, G. I. Golub, and P. Osetrov, Colloid J., 8, 345 (1946).

[4] R. E. Neiman and O. V. Neiman, Colloid J., 9, 203 (1947) .

[5] S. M. Lipatov, N. V. Stepanova, and R. I. Feldman, Colloid J., 3, 703 (1937); R. I. Feldman, Colloid J., 6, 753, 875 (1940); S. M. Lipatov and R. I. Feldman, Colloid J., 6, 805 (1940).

[6] S. M. Lipatov and S. I. Meerson, Trans. Moscow Sci. - Res. Textile Inst., 13, 74 (1954).

[7] R. E. Neiman, Colloid J., 14, 107 (1952); 16, 201(1954).*

[8] S. M. Lipatov and S. I. Meerson, Colloid J., 8, 143 (1946).

[9] L. G. Berg, A. V. Nikolaev, and E. Ya. Rode, Thermography, Acad. Sci. USSR Press (1944).

[10] A. V. Nikolaev and A. G. Kurnakova, Symposium, Protective Films on Salts, Acad. Sci. USSR Press, p. 138 (1944).

---

* Original Russian pagination. See C. B. translation.

LETTER TO THE EDITOR

COAGULATION OF ATMOSPHERIC CONDENSATION NUCLEI ON DUST PARTICLES

M. L. Mikhelson

As was shown earlier [1], one of the main problems which arises in development of the condensation method for the removal of flying dust is the influence of atmospheric condensation nuclei on the growth of the droplets formed on the dust particles.

Critical supersaturation values for some soluble nuclei may be of the same order as for dust particles $\sim 1\mu$ in size. Therefore in some cases atmospheric nuclei may act as competitors which take up a considerable amount of the condensing moisture, thereby decreasing the residual supersaturation. Moreover, being present in air in tens and hundreds of times as high as the usual dust content of mine air, atmospheric nuclei are capable of increasing, in roughly the same proportions, the amounts of energy required to bring about supersaturation in a condensation type dust filter. In this connection, the coagulation of atmospheric condensation nuclei on dust particles which we have discovered is a very favorable factor in the condensation method and is worthy of investigation.

In our experiments, the atmospheric nuclei were detected directly in the condensation filter when air was passed between parallel moist surfaces with different temperatures [2]. The experiments were carried out as follows. The Deryagin – Vlasenko flow ultramicroscope [3] was used to determine the concentration of atmospheric nuclei formed in the apparatus (Fig. 1) before introduction of dust into the dust chamber; its value was $3 \cdot 10^5$/cc. After introduction of coarse dust ($r \sim 10 - 100\mu$) into the dust chamber to a concentration $n_0 = 10^4$/cc, no atmospheric nuclei at all could be detected after 20 minutes under the same conditions, i. e., conditions determining supersaturation in the apparatus (temperatures of the hot and cold moist surfaces, the distance between them, length of the channel, flow rate). The distance between the moist surfaces $\underline{d}$ was 7 cm. the channel length $\underline{l}$ was 150 cm; the air flow rate $\underline{v}$ was 5 m/second. The same apparatus was then used to determine the concentration of atmospheric nuclei as a function of time (Fig. 2). In order to avoid changes of dust concentration during the experiment by precipitation of the dust particles, the dust used had average particle size $R \sim 1\ \mu$. As Fig. 2 shows, the concentration of the atmospheric nuclei fell, which may be attributed to coagulation of the atmospheric nuclei on the dust particles. In this experiment the initial concentration of the atmospheric nuclei was $N_0 = 7.5 \cdot 10^5$/cc, and the dust concentration $n_0 = 6 \cdot 10^4$/cc.

The coagulation of atmospheric nuclei on the dust particles is probably mainly due to their Brownian movement. The coagulation rate is easily calculated by means of the Smoluchowski equation applied to one absorbing particle of radius R

$$Q = -4\pi DRN, \quad D = kTB, \tag{1}$$

where Q is the number of atmospheric nuclei absorbed in unit time; N is the concentration of the atmospheric nuclei; D is the coefficient of diffusion corresponding to an atmospheric nucleus of radium $\underline{r}$; $\underline{k}$ is the Boltzmann constant; T is the absolute temperature; B is the mobility of the atmospheric nuclei calculated from Formula (8.6) [4, p. 39].

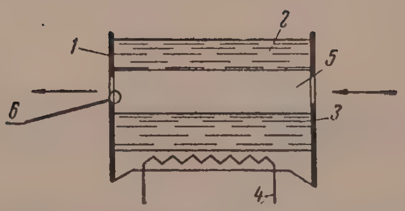

Fig. 1. Apparatus for measurement of the concentration of atmospheric nuclei: 1) body of the apparatus; 2) running water with t = 16°; 3) water with t = 65°; 4) heater; 5) vapor – air channel; 6) branch tube for sampling, by the flow ultramicroscope, from the center of the stream.

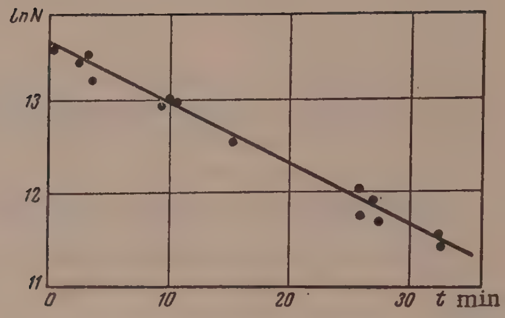

Fig. 2. Variation of the concentration of atmospheric nuclei with time.

If the dust concentration is n_0 and n_0 absorbing nuclei are therefore present, then

$$\frac{dN}{dt} = -4\pi DRNn_0 , \qquad (2)$$

or, in integral form

$$\ln N = \ln N_0 - 4\pi DRn_0 t . \qquad (3)$$

In our experiment $N_0 = 7.5 \cdot 10^5/\text{cc}$, $n_0 = 6 \cdot 10^4/\text{cc}$, $R \sim 1\mu$. To plot the line $\ln N = f(t)$ it is necessary to know the size of the atmospheric nuclei.

The straight line calculated from Formula (3) coincides with the experimental plot at $r = 3.0 \cdot 10^{-6}$ cm. According to Nolan and Guerrini [5]. the radius of the atmospheric nuclei $r = 2.85 \cdot 10^{-6}$ cm; the maximum on the size distribution curve for atmospheric nuclei, reported by Kumai [6], corresponds to $2.5 \cdot 10^{-6}$ cm. Thus, the foregoing considerations are confirmed by the linear character of the $\ln N = f(t)$ relationship and the satisfactory agreement of our value for the radius of the atmospheric nuclei with results obtained by other authors.

Coagulation of atmospheric nuclei should probably also occur rapidly on mist droplets, which is very significant in relation to studies of precipitation conditions. In such cases the coagulation process will probably be accelerated or retarded depending on whether the mist droplets undergo condensational growth or evaporation [7].

SUMMARY

1. The effect of coagulation of atmospheric nuclei which has been detected is of meteorological interest in relation to studies of precipitation, and is also important in relation to the condensation method of dust removal. For example, it seems likely that, because of prolonged contact with dusty air, atmospheric nuclei will be totally absent in mine air.

2. The calculated values for the size of atmospheric nuclei, based on experimental results, are in agreement with the data of other authors.

The Scientific Research Mining Institute
Krivoi Rog

Received April 14, 1956

LITERATURE CITED

[1] B. V. Deryagin, S. S. Dukhin, M. L. Mikhelson, and V. M. Kaganer, Silicosis Prevention, Symposium, vol. 2, Acad. Sci. USSR Press, p. 22 (1955).

[2] S. S. Dukhin, B. V. Deryagin, and M. L. Mikhelson, Proc. Acad. Sci. USSR, 105, No. 6 (1955).

[3] B. V. Deryagin and G. Ya. Vlasenko, New Ideas in the Study of Aerosols, Symposium edited by B. V. Deryagin, Acad. Sci. USSR Press (1949); Proc. Acad. Sci. USSR, 63, No. 2 (1948).

[4] N. A. Fuks, Mechanics of Aerosols, Acad. Sci. USSR Press (1955).

[5] J. Nolan, N. Guerrini, Trans. Faraday Soc. 32, 1175, (1936).

[6] M. Kumai, J. Met. 8, No. 3, 151 (1951).

[7] B. V. Deryagin and S. S. Dukhin, Proc. Acad. Sci. USSR, 106, No. 5 (1956).

THE SEVENTIETH ANNIVERSARY OF THE BIRTH AND FIFTY YEARS OF THE SCIENTIFIC ACTIVITY OF GRIGORY SEMENOVICH PETROV

October 27, 1956 was noted by the scientific community as the seventieth birthday and the end of fifty years of scientific activity of Professor Grigory Semenovich Petrov, Doctor of Technical Sciences — an eminent scientist, widely known in the USSR and abroad. From 1904 G. S. Petrov carried out a wide series of investigations on the decomposition of fats, and invented his famous "kontakt," obtained by treatment of various petroleum distillates with fuming sulfuric acid or sulfuric anhydride. Kontakt is still widely used in the USSR and abroad, mainly in the fat industry for splitting of fats and in the textile industry as a detergent in place of soap or alizarin oil, etc. In 1911-1914 G. S. Petrov and his associates laid the foundations of the national plastics industry. Being the first to organize the production of phenolic resins in Russia, he is rightly acknowledged to be the founder of the large plastics factory "Karbolit." After the October Socialist Revolution Petrov directed extensive work on the synthesis of carboxylic acids by oxidation of liquid petroleum distillates, carried out in the Karpov Institute. A carboxylic acid plant was installed at the Vakhitov factory as the result of this work.

The main direction of G. S. Petrov's scientific activity, however, has been the synthesis and study of various high polymers obtained by condensation. He has synthesized a large number of high polymers based on various phenols and aldehydes, urea, melamine, and aldehydes, glycols and carboxylic acids, etc. In particular, he determined the differences in the behavior of various substances at high temperatures in relation to the "coke number," and was first to observe that the heat stability of high polymers is increased by introduction of benzene nuclei in the chain. He therefore attached great importance to the condensation products of phenols and aldehydes for the production of plastics used in high-temperature conditions. G. S. Petrov made detailed studies of the formation of high polymers in condensation reactions in relation to the reaction conditions and the use of various catalysts. His work on the compatibility of numerous condensation polymers with polymers having high elasticity, such as rubber, has proved particularly valuable.

Long before the publication of work on block and graft polymers, G. S. Petrov indicated the possibility of, and predicted an important future for, the formation of chemical bonds between various polymeric products. In recent years he has been engaged in extensive work on the oxidation of high polymers, and in particular of phenol—aldehyde condensation products. He has established that oxidized condensation products have increased hardening rates.

G. S. Petrov has written 13 books on the technology of plastics, fats, and petroleum; he has published 85 papers, and has been awarded more than 200 author's certificates for inventions. Many of the inventions have been adopted in industry.

Jointly with Professor I. P. Losev, G. S. Petrov organized the Department of Plastics in the Mendeleev Institute of Chemical Technology, Moscow.

G. S. Petrov is an eminent research worker and teacher, and has trained many pupils who are now working in scientific institutions, factories, and teaching establishments.

M. S. Akutin

COLLOID JOURNAL OF THE U.S.S.R. IN ENGLISH TRANSLATION

January-February, 1957

TABLE OF CONTENTS

	Page	Russ. Page
1. Calculation of the Limiting Shear Stress (Yield Value) of Disperse Systems in Experiments with the Cone Plastometer. N. N. Agranat and M. P. Volarovich.	1	3
2. Theory of the Cone Immersion Method for Determination of the Yield Values of Disperse Systems. N. N. Agranat and M. F. Shirokov.	9	9
3. An Electron Microscope Study of Structure Formation in Loess. 1. Influence of the Dispersion Medium. E. Aripov, Z. Ya. Berestneva and V. A. Kargin	15	14
4. An Electron Microscope Studv of Structure Formation in Loess. 2. Influence of Loess Components on Structure Formation. E. Aripov, Z. Ya. Berestneva and V. A. Kargin	19	17
5. The Effect of Air Ionization on the Disperse Phase of Aerocolloids. I. I. Belyaeva, A. E. Mikirov and N. S. Smirnov.	25	24
6. Intermolecular Structure of High Polymers. Communication 22. Modification of the Molecular Structure of High Polymers by the Inclusion Method. A. N. Bykov and A. B. Pakshver.	29	27
7. Equilibrium of a Viscoplastic Disperse System on a Rotating Disk. A. M. Gutkin.	33	31
8. Investigation of the Structure and Properties of Carbon Chain Polymers in Dulute Solutions. 2. Solutions of Vinyl Chloride – Acrylonitrile Copolymer. S. G. Zelikman and N. V. Mikhailov.	37	35
9. Distribution of a Weak Electrolyte in the Double Layer. I. G. Ivanter.	43	41
10. Compatibility of Nitrocellulose with Butadiene – Acrylonitrile Copolymers. 3. Dependence of the Glass Transition Temperature and Flow of Nitrocellulose Films on their Contents of Various Butadiene – Acrylonitrile Copolymers. L. E. Kalinina, V. I. Alekseenko and S. S. Voyutsky	57	51
11. Thixotropic Structure Formation and Elasticoplasticoviscous Properties of Askangel Suspensions. E. I. Kobakhidze and M. E. Shishniashvili	65	59
12. Gelatinized Emulsions. 13.O/W Type Emulsions of Maximum Concentration with a Thixotropic Dispersion Medium. L. Ya. Kremnev.	75	68
13. Investigation of Structurized Suspensions. E. F. Kurgaev.	79	72
14. The Effect of Surface-Active Substances on the Specific Viscosity of Gelatin Solutions. S. M. Levi.	85	78
15. Effect of Hydrophilic Plasticizer Additions on the Properties of Concentrated Cement Suspensions. O. I. Lukyanova, E. E. Segalova and P. A. Rebinder	89	82
16. Preparation of Ferric and Zirconium Hydroxide Organosols. V. N. Maslov	97	90

COLLOID JOURNAL OF THE U.S.S.R. IN ENGLISH TRANSLATION

January-February, 1957

TABLE OF CONTENTS (Continued)

		Page	Russ. Page
17.	Experimental Investigations of Laminar Systems. 23. Kinetics of the Formation of Hydroxide Films on the Surface of Cupric Ammine Solutions. S. G. Mokrushin and G. A. Kitaev	99	93
18.	The Relationship Between the Affinity and Structure of Direct Dyes. P. V. Moryganov and B. N. Melnikov	105	100
19.	Structure of High Polymers. Communication 18. Strengthening of the Molecular Structure of Tire Yarn. A. B. Pakshver, L. S. Gerasimova and Kh. N. Kozlovskaya	109	104
20.	Molecular Structure of High Polymers. Communication 17. Investigation of the Intermolecular Structure of Thermoplastic Fibers. A. B. Pakshver, E. E. Natan and I. F. Katushkina	115	109
21.	The Electrochemistry of High-Polymer Dispersions. 3. Effect of pH on the Electrokinetic Potential of Globules in Synthetic Latexes. R. M. Panich and S. S. Voyutsky	119	113
22.	The Fractional Composition of Fine Cellulose Fibers. S. L. Talmud, A. N. Turzhetskaya and A. A. Kuleshova	125	118

Discussion

		Page	Russ. Page
23.	Characterization of the State of High-Polymer Gels. A. V. Nikolaev, R. E. Neiman and O. V. Neiman	129	121

Letter to the Editor

		Page	Russ. Page
24.	Coagulation of Atmospheric Condensation Nuclei on Dust Particles. M. L. Mikhelson	133	125

Tribute

		Page	Russ. Page
25.	The Seventieth Anniversary of the Birth and Fifty Years of the Scientific Activity of Grigory Semenovich Petrov. M. S. Akutin	137	127

APPLIED PHYSICS

APPLIED PHYSICS Sections
of the
PROCEEDINGS OF THE ACADEMY OF SCIENCES
OF THE USSR (DOKLADY)

including all reports on:

- Biophysics
- Crystallography
- Electrotechnics
- Hydraulics
- Hydromechanics
- Mechanics
- Mineralogy
- Theory of Elasticity

and related subjects.

As in all sections of the Proceedings, the papers are by leading Russian scientists. 36 issues to be published in six issues annually. Translation began with the 1957 volume. Translation by C. B. bilingual scientists, in the regular convenient C. B. format.

Annual subscription	$200.00
Single issues	40.00
Individual articles	5.00

As in all Consultants Bureau publications the translations are complete and accurate including all figures, diagrams, and tabular material integral with the text; clearly reproduced by the multilith process; books are staple bound. Sample Tables of Contents on request.

CONSULTANTS BUREAU, INC.
227 West 17th Street, New York, N.Y.

SOVIET RESEARCH
in
CATALYSIS

Chemistry Collection No. 3. Covers all aspects of catalysis; papers selected from all Soviet chemical journals translated by Consultants Bureau, 1949-1955.

Sections may be purchased separately as follows:

I.	Theoretical and Sundry Associated Effects	262 pages	**$50.-**	
IIa.	General	250 pages	**50.-**	**$125.-**
IIb.	General	250 pages	**50.-**	
IIc.	General: Reduction-Oxidation and Fischer-Tropsch	214 pages	**50.-**	
III.	Hydrogenation Dehydrogenation Cracking	294 pages	**50.-**	
IV.	Isomerization Alkylation Dehydration	274 pages		**$50.-**
V.	Polymerization Friedel-Crafts Zeigler	128 pages		**30.-**

The Collection, comprising 1,672 pages, 262 papers may be purchased as a unit for **$200.00**

Individual papers are available separately — Table of Contents on request.

CONSULTANTS BUREAU, INC.

227 WEST 17TH STREET, NEW YORK 11, N. Y.